Redundancy Evaluation of Steel-Concrete Composite Twin I-Girder Bridges

October 2017

Heang LAM

Redundancy Evaluation of Steel-Concrete Composite Twin I-Girder Bridges

October 2017

Waseda University
Graduate School of Creative Science and Engineering
Department of Civil and Environmental Engineering,
Research on Structural Mechanics

Heang LAM

Acknowledgement

After several years of research at Waseda University, my life as a doctoral student finally came to an end with the publishing of this dissertation. During this period, I received the help from many people who walked me through all the difficulties I encountered. Without the people mentioned below, it would not have been possible for me to finish this doctoral dissertation.

Firstly, I would like to express my deepest gratitude to my research advisor, Prof. Teruhiko YODA, for his priceless advice, guidance, and contribution throughout my research. He was always there whenever I needed him, providing me unwavering support, suggestions, and comments to my research as well as during my time in Japan. As a mentor, his kindness and patience given during our countless hours of discussion, have given me not only invaluable knowledge in my research career but also many precious lessons in my life, especially on how to be a wise man.

Secondly, I would like to express my great appreciation to my dissertation advisor, Prof. Kiyoshi ONO, for his numerous valuable suggestions and corrections to this dissertation. Despite knowing him for a brief period, Prof. Ono has spent many hours carefully checking this dissertation. On top of that, he provided me with useful resources and guidance to finish this doctoral dissertation.

I also want to express my appreciation to the members of my dissertation committee including Prof. Atsushi KOIZUMI, Prof. Osamu KIYOMIYA, and Prof. Mitsuyoshi AKIYAMA, for providing valuable feedback that helped shape the quality of this dissertation.

Special thanks to Dr. Weiwei LIN and Dr. Hideyuki KASANO for their helpful suggestions, comments, and discussions concerning my research. In addition, I want to thank all the members of Yoda Laboratory for the generous assistance in the experimental program and for making my life at Waseda University enjoyable. Special thanks to all the members of Ono laboratory who made my time at Waseda University full of joy.

Furthermore, I want to thank Waseda University for providing the financial support under the “Asia Special Scholarship Program” that enabled me to pursue the doctoral degree at Waseda University.

Lastly, despite being thousands of miles away, I want to thank my parents for their support, encouragement, and the love they provided which walk me throw many difficult moments. I also want to thank my grandparents for their endless love and prayers for my success. Special thanks to my brothers and my friends who always encourage me.

Abstract

The large number of old bridges and rapid increase in traffic have led to concerns over bridge safety in Japan as well as the other parts of the world. In Japan, it has been reported that around 10,000 bridges on the national highway and major expressways have been in service for over 50 years as of 2016, and this number is expected to be double in the next five years (Fujino, 2006). Meanwhile, in the United States, 503 bridge collapse cases were confirmed between 1989 and 2000, among which 18.3% were caused by overload, deterioration, and fatigue of steel members (Wardhana et al., 2003; Deng et al., 2016). Owing to the large number of old steel bridges, member fracture emerged as a major reason of bridge damage critically affects the load-carrying capacity and safety of the bridges. For this reason, the redundancy level in the post-fracture condition of such structures needs to be investigated to ensure their survivability in fracture damage condition.

Steel-concrete composite twin I-girder bridges are commonly used as highway bridges in Europe, Asia, and the other parts of the world owing to their low-cost, high span-to-depth ratio, and simple construction procedure compared to other types of bridges. Particularly in Japan, the number of twin I-girder bridges has been increasing significantly in comparison with other bridge types over the last 20 years. Such bridges are rarely used in the United States because all two-girder bridges are classified as non-redundant and fracture-critical (AASHTO, 2012). A fracture-critical bridge is a bridge having one or more members whose single failure would lead to the collapse of the entire bridge system. However, in several cases, it has been found that composite twin I-girder bridge systems do not collapse even after the severe fracture occurs in one of the main girder sections (Daniels et al., 1988). In fact, it has been reported that many bridges have not collapsed despite suffering from a full-depth fracture of the main girder, owing to the alternative load-carrying mechanism of the deck under large rotations at the fracture (Connor et al., 2005). Thus far, very limited research has been conducted to evaluate the redundancy and to compare the pre- and post-fracture mechanical behavior and safety of composite twin I-girder bridges. With this background, the present study, involving both experimental and numerical studies, is carried out to investigate the redundancy evaluation and performance of a composite twin I-girder bridge system in critical fracture condition.

The content of this dissertation can be classified into three main parts. The first main part is focusing on the literature review on existing redundancy evaluation method of the bridge structure which is currently considered as inadequate in the design stage. The second main part presents the redundancy evaluation and mechanical behavior of the simply supported

composite twin I-girder bridge systems including the experimental and numerical analyses. The third main part discusses the effects of the bracing systems and degree of continuity on the redundancy evaluation of the composite twin I-girder bridge systems including full-scale composite twin I-girder bridge models. Base on the objectives of the present study, this dissertation is divided into six chapters.

Chapter 1 gives an introductory explanation to the topic of this study including the research topic background and the motivation toward the research trend. The application of composite twin I-girder bridges in highway bridge design has been seen rapidly increasing in Japan and the other part of the world due to their low cost and high span-to-depth ratio. Meanwhile, concerned over the safety of this kind of bridges has been rising since it is currently considered as non-redundant and fracture critical according to the AASHTO Specification. However, several past experiences have shown that composite twin I-girder bridge systems do not collapse even after the severe fracture occurs on one of the main girders section which indicated that this bridge system can be classified as redundant. Arguments still exist among bridge researchers, designers, and engineers on redundancy classification on both composite and non-composite twin I-girder bridge systems. With this background driven by these reasons, it is essential to evaluate the redundancy level of the composite twin I-girder bridge system. The research motivation, research objectives, research methodology, and the dissertation outline are detailed in this chapter.

Chapter 2 presents the literature review on the redundancy evaluation of bridge structures. Several famous historical bridge collapse events led to the research in relation to redundancy. The criteria concerning redundancy analyses including fracture critical members, quantitative measure, qualitative measure, and probability measure of redundancy are discussed. From the extensive literature review concerning bridge redundancy, although uniform redundancy evaluation criteria are currently not exist, it has been widely recognized by structural engineering community that redundancy is an important criterion which guarantees the survival of the bridge in critical damaged condition. In the current design specifications in Japan, Europe, United States and many others, only general prescriptions and very limited guidelines are provided to prevent system collapse from single member failure during the design and maintenance processes. In current research and design practice of bridge redundancy, the method based on reliability analyses is becoming more and more acceptable from engineering community due to its promising deterministic level of redundancy. From the existing literature to the design practice, a uniform redundancy evaluation should consist of two important

aspects: providing a uniform level of reliability with an objective measure which is independent to design specifications, and engineering practice which is applicable to general bridge designers.

Chapter 3 investigates the redundancy evaluation and mechanical behavior of simply supported composite twin I-girder bridges based on the experimental results. Two specimens including an intact and a damaged specimen were tested under one-point load at mid-span section. The damaged specimen, which consists of fracture of whole web and bottom flange on one of the main girder at mid-span section, is the typical critical damaged cases found on existing I-girder bridges. Vertical deflection, relative slip between steel and concrete slab, shear strain and bending strain on the shear studs, strain of the steel, concrete and reinforcing bar were measured during the loading test. Results of the damaged specimen and intact specimens, including yield strength and ultimate strength, are compared to evaluate the redundancy level of the bridge system. The experimental results indicated that the damage assumed in this study significantly increase the shear strain on the studs near the middle section, thus reducing the strength and lifespan of the shear studs against fatigue failure. However, the damaged specimen in this study can sustain the damage without significant deformation under self-weight and manage to carry some imposed live load, which yields the present system as the redundant bridge system.

Chapter 4 investigates the redundancy evaluation and mechanical behavior of the composite twin I-girder bridge system by using Finite Element Method. Numerical models were built to simulate the behavior of the composite twin I-girder bridge model. Nonlinear analyses are carried out to investigate the performance of the composite twin I-girder bridges under different fracture locations. Load-deflection curves and load-strain curves from experimental results were used for verifying the validity of the numerical models. Then, parametric studies were performed to investigate the effects of structural indeterminacy and the effect of concrete slab on the safety of the composite twin I-girder bridges in the fracture condition. Results show that composite twin I-girder bridges generally have an adequate level of redundancy and can be classified as non-fracture critical bridge system. Furthermore, the concrete slab is found to be the key element for load redistribution in the fracture condition for composite twin I-girder bridge systems. In addition, the use of a continuous span instead of a simple span for the composite twin I-girder bridge system can significantly increase the load ratio between the damaged and intact structures which results in high redundant bridge system. It is recommended to employ a continuous girder bridge with strong and thick concrete slab to

achieve a high level of redundancy.

Chapter 5 investigates the effect of bracing systems on the redundancy analyses of continuous composite twin I-girder bridge system based on numerical analyses. The effectiveness of bracing systems was evaluated transverse beams and bottom lateral cross bracing system. The three-dimensional numerical model is validated based on the experimental results from a small scale three-span continuous composite twin I-girder bridge model. The bottom X-type lateral bracings with the transverse beam are found to be effective in increasing the redundancy factors and the load carrying capacity of the small scale three span composite twin I-girder bridge model. It was found that the bottom X-type cross bracing is effective for the experimental models. To validate the application of this X-type bracing in the design of the actual bridge, a full scale five spans composite twin I-girder highway bridge model is analyzed in this section. The location of the fracture critical members is first determined. The numerical results indicated that the bottom X-type lateral bracings are effective in increasing the redundancy level of the composite twin I-girder bridge system. With the existence of transverse beams, this effect can be largely increased. At the same time, it can somehow decrease the deflection of the bridge at the ultimate load and thus reducing its ductility level. Meanwhile, transverse beams can increase the efficiency of the bottom lateral bracing systems to distribute the load in damaged condition.

Chapter 6 summarizes the key findings, potential impact, and future works of the redundancy evaluation of composite twin I-girder bridge systems. To provide detailed results and knowledge concerning the redundancy analyses and mechanical behavior of the steel-concrete composite twin I-girder bridge system in critical damaged condition, the research program based on an extensive literature survey, experimental results, and numerical analyses are presented. Though a unified redundancy evaluation method for bridge structures is currently not existing in the design practice, general aspects of redundancy which provide a uniform level of reliability with an objective measure and engineering practice without requiring nonlinear analyses can be used as a key concept in the research of unifying redundancy evaluation for bridge systems. Despite findings in this dissertation, the outcomes of this research are based on a limited number of experimental and numerical models. More researches are required to develop a unified redundancy evaluation for composite twin I-girder bridge structures as well as for general bridge systems to implement a general method in the design of bridge structures.

Table of Contents

List of Figures

List of Tables

1. Introduction

1.1 Research Background

Steel-concrete composite twin I-girder bridges are commonly used for highway bridges in Europe, Asia, and other parts of the world due to their low cost, higher span-to-depth ratio, and simpler construction procedure comparing to other types of bridges. Particularly in Japan, the number of the twin I-girder bridges has been increasing significantly in comparison with other bridge types in recent twenty years, as shown in **Fig.1.1** (Nagai, 2006). On the other hand, such a bridge is rarely used in the United States because all two girder bridges are classified as non-redundant and fracture critical (AASHTO Specifications, 2012). A fracture critical bridge is a bridge which contains one or more members whose single failure can result in the collapse of the entire bridge system. For example, the failure of one of the gusset plate the collapse of the I-35W truss bridge over Mississippi River in 2007 resulted in a direct economic loss of more than 60 million US dollars (Deng et al., 2015). The scene after the collapse of this bridge is shown in **Fig.1.2**. Investigation report concluded that the collapse of this bridge is triggered by the failure of one of the gusset plate (NTSB, 2007). The report also revealed that some of the gusset plates (including the one that triggers the failure) have inadequate capacity due to the error by the designer which is the main cause of this disaster. The increase of the dead load of the bridge due to some modifications and improper placement of the concentrated construction load on the bridge are also contributed to the failure of the bridge structure. Despite in service for more than 40 years and under many times of inspections and maintenance, the under-design gusset plate was never discovered during its service life. As the bridge system is non-redundant, the total collapse of the bridge triggered right after the failure of one of the gusset plate, leaving no time for the evacuation which resulted in 13 casualties and 145 injuries (NTSB, 2007). For composite twin I-girder bridge system, on the other hand, it has been reported that the full-depth fracture of the main girder did not lead to collapse, usually owing to the alternative load carrying mechanism of the deck under large rotations at the fracture (Connor et al., 2005). With this background, it is essential to evaluate the redundancy level as well as safety level of the composite twin I-girder bridge system in damaged or fractured conditions.

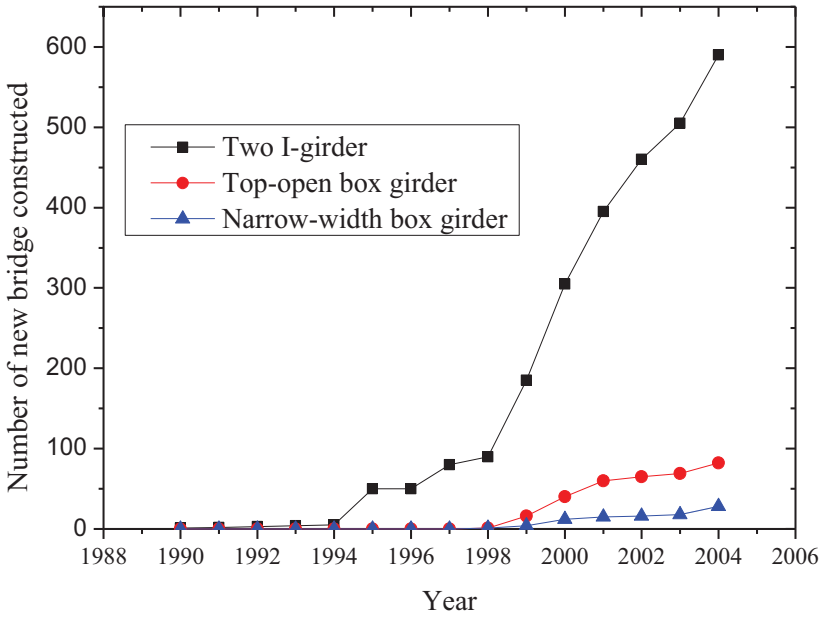

Fig.1.1 Number of bridges constructed in Japan (Nagai, 2006)

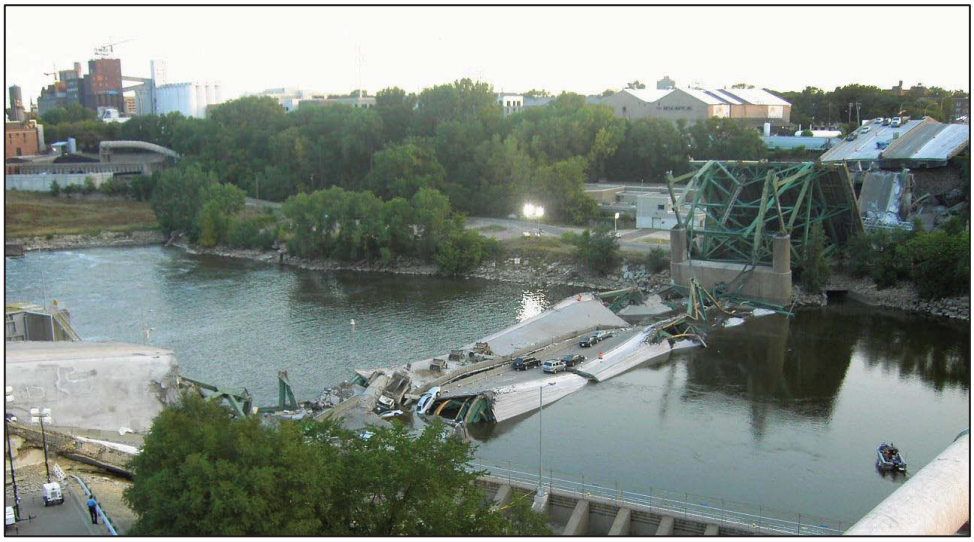

Fig.1.2 Collapse of I-35W Mississippi River Bridge (Mike Wills, 2007)

1.2 Problem Statements

In Japan, it has been reported that 6% of the 150,000 bridges across the country had been in service for over 50 years. This ratio continues to grow rapidly and will increase to around 50% by 2026 (Nagai, 2006). Another report also stated that an estimate of ten thousand bridges was in service for over fifty years by 2016 will be doubled by 2021 (Fujino, 2006). For this reason, the safety consideration for old bridges is becoming more and more important for current bridge infrastructures in Japan. To cope with this problem, perhaps extending the service life of the bridge inventory has become necessary because of the

increased construction costs, environmental impact, and traffic disruptions related to bridge replacement (Lin et al., 2013). In addition, the behavior and response of the bridge after losing or damaged some part of the structural elements is getting more and more attention since several bridge collapse disasters continue to happen all around the world. Bridge collapse normally is unpredictable and often not only causes the damage or collapse of bridge structures itself but also leads to the loss of human lives and affect the traffic condition before the new bridge is built. In the United States alone, 503 bridges collapse cases were reported between 1989 and 2000 (Wardhana and Hadipriono, 2003; Deng et al., 2016). To prevent or minimize the number of the bridge collapse, using redundant bridge system is the most effective way because a redundant bridge system generally resists the collapse caused by overloading or failure of one of its structural members. In other terms, redundancy is the property of the bridge structure itself that guarantees its survival after an incident initiated by partial or full damage on the critical member of the bridge system.

The redundancy level of the bridges is highly depending on the structural system. Generally, determinate structures such as simply supported truss bridges are classified as non-redundant since the structure itself cannot survive the failure of a random single structural element. Multi-girder system generally is considered as redundant when the number of the main girders is greater than three. If one of the main girders fails due to fracture, corrosion, or collision, the loading of the bridge on the damaged girder is expected to be carried by adjacent girders and the collapse of the entire bridge normally can be avoided. For two girders system, on the other hand, the possibility of the adjacent girder to carry the entire load if the other girder subjected to complete failure is hardly achieved from the viewpoint of design consideration. However, in the actual situation, it is highly unlikely that the entire one main girder completely fails by any reasons. In fact, most girder damage cases only take part in the very limited area such as brittle fracture at certain locations or corrosion on some parts of the surface of the girders. In these cases, according to the past experiences, the serviceability of the bridge sometimes can be highly affected; however, collapse is unlikely to happen. Despite these facts, in current design practice, all types of twin girders bridge system are considered as non-redundant (AASHTO, 2012). This classification is based on the unrealistic concepts widely held by bridge engineers, resulting from the oversimplified assumptions normally used in the design, and not on the realistic behavior of the as-built three-dimensional structure (Daniel et al., 1988). The terms oversimplified here is referred to the two-dimensional assumption currently used in the design practices which only consider main girders as the design load path available for transmitting the vertical load like dead load,

live load, and impact load to the substructure. The secondary members, including diaphragms and bottom lateral bracings (if any), are neglected in sharing or resisting the vertical load. Furthermore, the torsional strength of the deck in balancing the live load is also not considered. In the actual three-dimensional environment, the vertical load is less or more shared by all the components of the superstructure especially under the unsymmetrical loading condition. Even in nearly full-depth fracture condition, the composite twin I-girder bridge systems do not necessarily collapse.

Nowadays, arguments still exist among bridge researchers, designers, and engineers on the redundancy classification of composite twin I-girder bridge systems. This is simply due to the lack of concreting research results on the redundancy analyses for composite twin I-girder bridges. In this dissertation, a detailed study was carried out focusing on the redundancy evaluation of composite twin I-girder bridge system. Results from the experimental program and the numerical analyses of composite twin I-girder bridges systems are presented. The main purpose of this research is to study the relation between mechanical behavior and redundancy level of the composite twin I-girder bridge system under overload condition and critical fracture condition.

1.3 Research Motivation, Limitation, and Objectives

The application of composite twin I-girder bridge in highway bridge design is rapidly increasing in Japan due to their low cost comparing to other types of bridges. Considering the huge numbers of applications of composite twin girders bridges systems in Japan and all around the world, the redundancy evaluation method in bridge engineering is a very important aspect that can guarantee the safety level for this kind of bridge during its service life. Approaches which contribute to the optimization between economic aspect and public safety aspect are essential and highly connected to the redundancy analyses of the bridge structures. Driven by these reasons, the research focusing on the redundancy evaluation of composite twin I-girder bridge were carried out in this study. The main purpose of this dissertation is evaluating as well as improving the redundancy level of the composite twin I-girder bridge systems by any means necessary. By focusing on the composite twin I-girder bridge system, this research is limited to the medium span bridge and dealing with only the superstructure. For this reason, only vertical loading condition (dead load and traffic load) is considered in this study. Horizontal loading condition such as strong wind and earthquake, which more likely affects the performance of the substructure, is not in the scope of this study. The research methodology is based on the existing literature, the results of the experimental

program and the numerical analyses. To achieve this goal, objectives were set and presented as below:

- Conducting an extensive research on the existing literature concerning the redundancy evaluation method in bridge engineering as well as in other fields that related to this aspect. Data from past experiences were collected concerning bridges failures as well as bridges damage. The collected data concerning existing bridge redundancy evaluation method and actual bridge damaged scenario are essential in establishing proper experimental and numerical programs that lead to the redundancy evaluation of the composite twin I-girder bridge systems.
- Conducting an experimental program on a simply supported composite twin I-girder bridge system to understand the mechanical behavior of the bridge under overload condition and extreme damage condition. Redundancy evaluation and reliability analyses were carried out at the same time based on experimental results provided by the intact specimen and damaged specimen.
- Conducting numerical analyses on the tested simply supported composite twin I-girder bridge. Numerical analyses based on finite element method and nonlinear analysis were verified based on the existing experimental results. Parametric studies were performed to confirm the key elements that contribute to the redundancy of the composite twin I-girder bridge structure in extreme damage conditions. The numerical model is extended to the continuous span, and redundancy level affecting by the degree of continuity was also confirmed and reported in this study.
- Conducting parametric studies focusing on the effect of the secondary members on the redundancy level of the full-scale continuous composite twin I-girder bridge; the advantages and disadvantages of the bracing systems on the redundancy and safety level of the bridge systems were also reported.

1.4 Research Methodology

The research results presented in this study is based on the experimental program, numerical analyses, as well as background theory concerning redundancy analysis of bridge systems. The theoretical approaches to determine the redundancy level of the bridge structure is mainly based on the existing reliability concept widely used in civil engineering. The experimental approach, which includes simulating the damaged on the actual bridge, is used for studying the performance of the bridge system in pre- and post-damaged condition. The results from the experimental program are also used for verifying the validity of the

numerical models. Numerical study based on Finite Element Method is used for performing parametric studies to investigate the effect of each structural element on the redundancy level of composite twin I-girder bridge system.

1.5 Dissertation Outline

This dissertation is divided into three main parts. The first main part is focusing on existing literature reviews which consist of **Chapter 1** and **Chapter 2**. **Chapter 1** gives an introductory explanation which shows the importance of this studies in current aging infrastructure in Japan and others part of the World. Research background and the objectives of this research are briefly explained. **Chapter 2** is focusing on the literature review on existing redundancy evaluation method of the bridge structure. The existing studies concerning the redundancy evaluation of the composite twin I-girder bridge system were also presented. The second main part presents the redundancy evaluation of the simply supported composite twin I-girder bridge systems. This part consists of **Chapter 3** and **Chapter 4**. **Chapter 3** presents the experimental program conducted on the simply supported composite twin I-girder Bridge. The details of the experimental program including test specimens, instrumentation, testing procedures, and testing conditions were presented. Results obtained from experimental program concerning the redundancy level, safety level, and failure mechanism of the bridge systems were discussed in this chapter. In **Chapter 4**, the numerical models of the test specimens used in the experimental program were built and utilized based on nonlinear analysis and finite element method. Studies were extended to the effect of the loading conditions, the degree of indeterminacy, the fracture location, the concrete slab thickness, and the concrete strength on the redundancy level of the simply supported composite twin I-girder bridge systems. The third main part discusses the effect of the bracing systems on redundancy evaluation of the composite twin I-girder bridge system. This part consists of **Chapter 5** which discusses the effect of bracing systems on a small scale three spans continuous composite twin I-girder bridge system and also its application to a full-scale five spans continuous composite twin I-girder bridge. Finally, conclusions and summary of all the results and the contribution in this research toward redundancy evaluation of composite twin I-girder bridge systems are presented in the last chapter of this dissertation.

References:

AASHTO (American Association of State Highway and Transportation Officials), (2012). "AASHTO "LRFD Bridge Design Specification", 6th edition, Washington, DC.

Connor, R.J., Dexter R., and Mahmoud H. (2005). "Inspection and Management of Bridges with Fracture-Critical Details." NCHRP Synthesis 354, National Cooperative Highway Research Program, Washington, DC.

Fujino, Y. (2006). "Steel Bridges in Japan-Current Circumstances and Future Tasks." Steel Construction Today and Tomorrow, Japanese Society of Steel Construction, No. 15.

Daniels, J. H., Kim, W., and Wilson J.L. (1988). "Recommended Guidelines for Redundancy Design and Rating of Two-Girder Steel Bridges", NCHRP Report 319, National Cooperative Highway Research Program, Washington, DC.

Deng, L., Wang, W., and Yu, Y. (2016). "State-of-the-Art Review on the Causes and Mechanisms of Bridge Collapse" Journal of Performance Construction Facility, ASCE, Vol. 30, No. 2, 04015005.

Lin, W., and Yoda, T. (2013). "Experimental and Numerical Study on Mechanical Behavior of Composite Girders under Hogging Moment." International Journal of Advanced Steel Construction, Vol. 9, No. 4, pp. 309-333.

Nagai, M. (2006). "Steel Bridges in Japan- Rationalized Design Methods in Japan." Japan Society of Steel Construction, No. 15.

National Transportation Safety Board. (2007) "Collapse of I-35W Highway Bridge Minneapolis, Minnesota", Highway Accident Report NTSB. https://www.ntsb.gov/investigations/AccidentReports/Reports/HAR0803.pdf.

Wardhana, K., and Hadipriono, F. (2003). "Analysis of Recent Bridge Failures in the United States." J. Perform. Constr. Facil., 2003, Vol. 17, No. 3, pp. 144-150.

2. Redundancy Evaluation Method of Bridge Structure

2.1 Historical Background

In civil engineering, redundancy can be understood as the property of a structure to survive after one of its members failed to perform its function. The term redundancy has been gained substantial interest in structural design following several failure incidents of bridge systems. In 1967, an eyebar-chained suspension bridge (Silver Bridge) in the United States suddenly collapsed during the rush hour without any prior warning, when the bridge was crowded with heavy traffic load (Lichtenstein, 1993). This collapse resulted in 46 casualties and 9 injuries (Lichtenstein, 1993). The collapse was triggered by the failure of one of the two eyebars. The failed eyebar has been defected after in service for almost 40 years which subjected to the rapid increase of the traffic load that was much higher than the bridge initially designed for. Although overload is concluded as one of the main reason, the collapse without any prior warning, which is mainly due to the insufficient level of redundancy of the bridge system, should not be tolerable in future design practice. The Silver Bridge before and after the collapse is shown **Fig.2.1**. One year later, part of a precast 22-storey building in London names " Ronan Point" collapsed after a gas explosion at its 18 floors as shown in **Fig.2.2** (Pearson, 2000). The collapse is triggered after the failure of the bearing walls due to the gas explosion which causes the top four floors losing its supports. The prefabricated system without considering of alternative load path after the failure of the bearing resulted in a non-redundant structure which prevents the load from transferring to another part of the building. The progressive collapse happened afterward due to the non-redundant structural system is concluded as the main course of this incident (Ellingwood and Dusenberry, 2005). Four lives were lost during this incident and questions rose concerning the public safety of the high rise building that normally requires strict control in both design phase and construction phase. Others notable failures and collapse incidents due to the lack of redundancy including the collapse of Mianus River bridge in 1983 as shown in **Fig.2.3**, which was caused by the corrosion at the connection and hanger; the collapse of the I-35W Mississippi River Bridge in 2007, which resulted from the failure of one of the under-design gusset plate; and the Collapse of I-5 Skagit River Truss Bridge 2013, which resulted from the failure of the secondary member as shown in **Fig.2.4** (CNN, 2013).

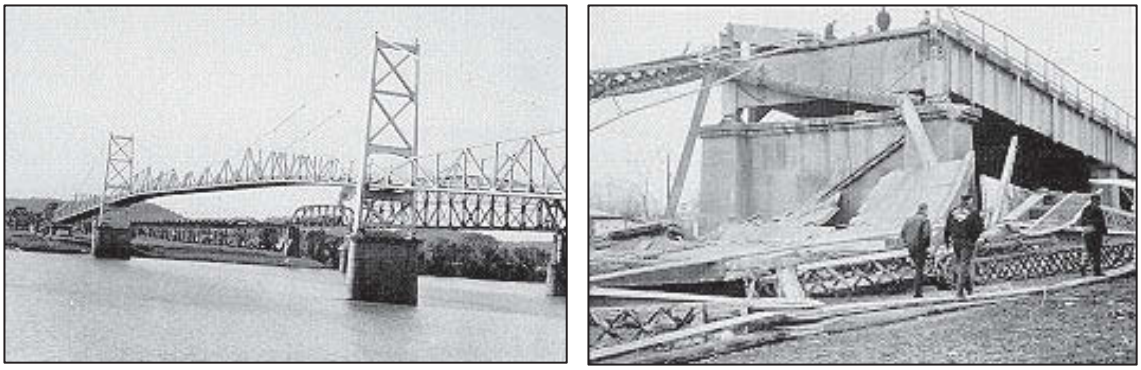

Fig.2.1 Silver Bridge before (left) and after the collapse (right) (FHWA, 1996)

Fig.2.2 Partial Failure of Ronan Point building, London,1968 (Pearson, 1968)

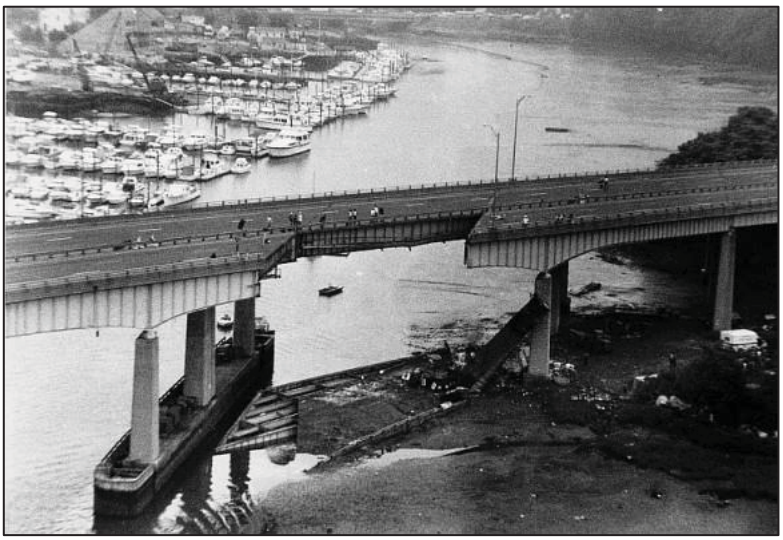

Fig.2.3 The collapse of Mianus River bridge in 1983 (NEWS8, 1983)

Fig.2.4 Collapse of I-5 Skagit River Truss Bridge (CNN, 2013)

Unlike non-redundant structural systems, bridges with the adequate level of redundancy normally do not collapse in critical damaged condition. For example, the Hoan Bridge incident that took place in the year 2000 attracted the civil engineer society to pay more attention to bridges redundancy and its great benefit. The structure consists of 18 side spans of continuous composite three girder bridges and the main unit of three span tied arches crossing the Milwaukee River. The bridge lost its functionality after the occurrence of full depth fracture of two girders at one of the side span as shown in **Fig.2.5** (FHWA, 2000). However, the damaged structures can continue to carry their self-weight that allow repairing process to take place. Not only non-causality consequence was achieved, the loss of economics was also minimized since retrofit works were only needed instead of entire span replacement (an estimate of 33millions dollar were saved).

Besides these incidents, in the United States alone, approximately 11% of the steel bridges are classified as fracture critical (Connor et al., 2005) and 503 bridge collapse cases were confirmed between 1989 and 2000 (Wardhana et al. 2003; Deng et al. 2016). Around 18.3% of the 503 collapse cases that caused by overload, deterioration, and the fatigue of the steel can probably be avoided or predicted if those bridges were designed as redundant. Meanwhile, in Japan, many steel plate girder bridge damages were found on national roads in Japan from the inspections over an approximately ten-year period (Tamakoshi et al., 2006). At the same time, the numbers of the old bridges are expected to increase exponentially in the next five years (Fujino, 2006). The rapid increase in the number of old aged bridges, following by many bridge incidents happened all around the world, highlights the importance of the redundancy evaluation and analyses method for bridge systems.

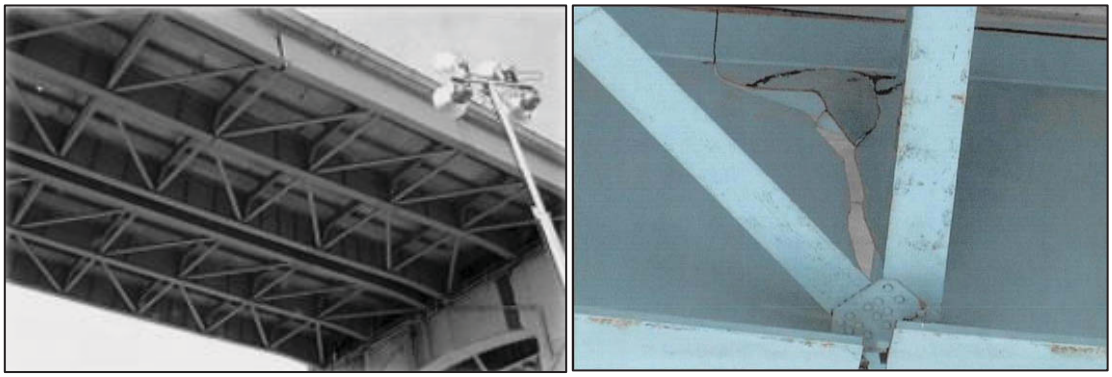

Fig.2.5 Fracture of Hoan Bridge (FHWA, 2000)

2.2 Redundancy Evaluation of Bridge Structure

Research on redundancy rating and evaluation method has been interested since the 1970s when many bridges have been shown to contain alternate load path which can prevent the bridge from collapse in the event of some incidents happened on the bridge members (Csagoly and Jaeger, 1970). Continuous spans bridges are likely to survive in the event of failure or fracture of one main load carrying component or main girders such as Lafayette Street bridge over the Mississippi River, the Interstate I-79 bridge crossing the Ohio River in Pittsburgh, and the Ontario-35 bridges at Meiden (Csagoly and Jaeger, 1970). The terms single load path and multiple load path were introduced to describe and differentiate bridges geometry configurations to evaluate the redundancy level. The initial idea of redundancy of structural system is highly dependent on the degree of indeterminacy that a structure possesses. In this sense, a structure with a higher level of degree of indeterminacy was judged as having a higher level of redundancy. However, some researchers argue that higher level of degree of indeterminacy did not guarantee a higher level of redundancy. Little work had been done on quantifying the degree of redundancy that is needed (ASCE-AASHTO Task Committee, 1985). In current state-of-the-art, very few rating methods are available for civil engineers or structural designers to account for the redundancy in the design stage and during service life stage of bridge systems. The redundancy rating on the bridges structures is still a difficult task even with modern computer software due to the very complicated bridge response after damage or failure of members. Further effort is needed to collect data on bridge loading and behavior, to consistently deal with insufficient knowledge on bridge response, and to implement system reliability-based factors in bridge design and evaluation specifications (Frangopol, 1992). Despite the difficulties in collecting data, redundancy rating method has never been clearly defined in civil engineering practice and a good, concise, universally accepted definition of

redundancy does not currently exist in the bridge design or evaluation specifications (FWHA, 2012b). In the current situation, very limited guidelines are available to evaluate the bridge redundancy level. In Europe, the redundancy approach is still in a more theoretical phase which lacks specific guidelines for bridge engineers, while the US approach concentrates on developing tools and criteria for the numerical evaluation of the capability of a bridge structure to continue to carry the load after the failure of a member (Anitori et al., 2013). Meanwhile, in Japan, it is required for the bridge designer to take into consideration of the probability that some members of the bridge will be damaged, resulting in a collapse or other fatal situation for the bridge (JRA, 2002). Up to now, technical reports were carried out in the United States, Europe, and Japan to account for redundancy in the design stage (Ghosn and Moses,1998; COST, 2011; JSCE, 2014). Despite that, specific measures according to uniform evaluation criteria to prevent such fatal situation do not yet exist in the specifications. More details studies are required to establish an accurate redundancy rating method for the bridge structures in critical damaged condition.

2.3 Fracture Critical Members

In current design practice, single member failure is normally used during the design process. In redundancy analyses, the evaluation process focuses on the performance of the entire structure after single member failure. To this point, during the analyses, one member is assumed to have failed during some accident condition and the performance of the whole structure needs to be checked afterward. If this single member failure has triggered the failure of the entire system under a permitted load afterward, this member is classified as Fracture Critical Members (FCMs). On the other hand, members whose failure would not cause the collapse of the bridge structure is considered as “Redundant Member”. Single element failure is typically not the ultimate state of the structure in redundancy analysis. The spread of the damage after the failure of this element is the key point in redundancy evaluation. Determination of Fracture Critical Members (FCMs) can be considered as one part of the redundancy analyses. The bridge that contains FCMs is not necessary non-redundant if “such members are designed in a way that will not fail before other redundant members or the system itself is expected to be out of service before the failure of such members”. In most of the cases, it is important to show that a bridge can be considered as redundant or non-redundant based on the existent of this type of members. In current state-of-the-arts, FCMs can be defined as steel tension members or steel components of members whose failure would be expected to result in the collapse of the bridge (AASHTO, 2011). United State National Bridge Inspection

Standard (NBIS) also defines FCM as “a steel member in tension, or with a tension element, whose failure would probably cause a portion of or the entire bridge to collapse” (FHWA, 2012a). **Fig.2.6** illustrates the criteria of the fracture critical members based on a four-span continuous beam. In the first damage case, if one of the two end spans has been cut in half, one side of the system is no more in the static condition and the failure of the system is expected as shown in **Fig.2.7**. Thus, the two side spans of this system can be classified as fracture critical members without requiring any calculation. In the second damaged case, as shown in **Fig.2.8**, if one of the two middle spans has been cut in half, it will result in two new static systems. In this case, unlike the damage in case-1, it is not able to judge that the system after the damage is still stable or not without detailed analyses. The safety of the system in Case-2 is depending on both the loading level and the strength of the beam to resist the load after the damage of the bridge. Classification of fracture critical members cannot be predefined and detailed analysis is required in this case, which depends on the strength and the action applied on the system. For the actual bridge, due to the complexity of the structural systems in three-dimensional space, the determination of FCMs normally required detailed analyses which depend on many parameters including the remaining load carrying capacity of the damage system, the applied load, and the deflection level of the bridge etc.

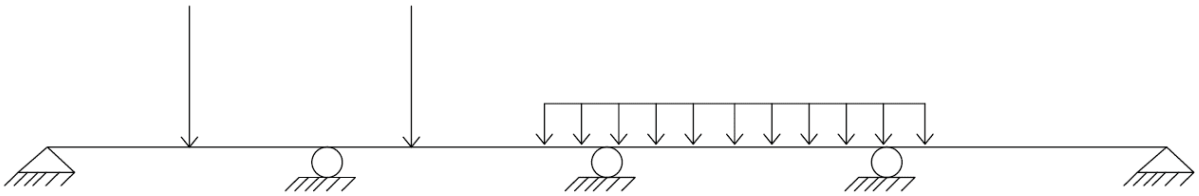

Fig.2.6 Four-span continuous beam

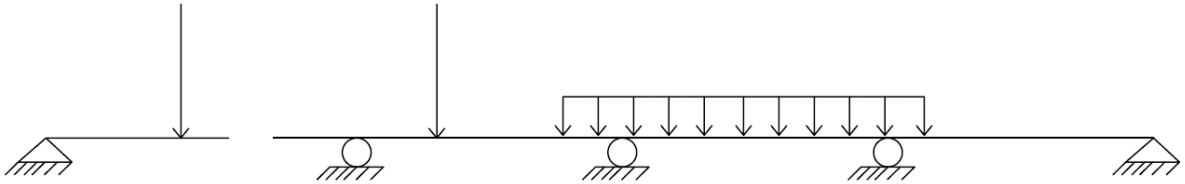

Fig.2.7 Four-span continuous beam (Damage case-1)

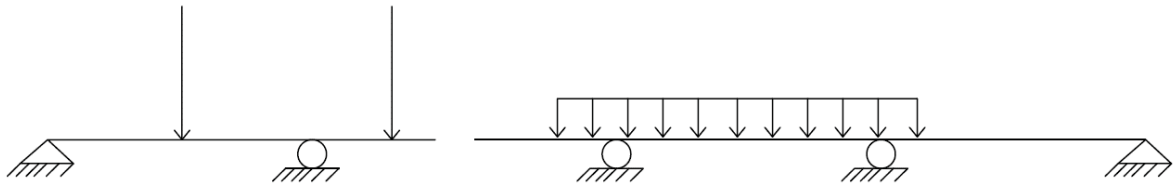

Fig.2.8 Four-span continuous beam (Damage case-2)

2.4 Qualitative Measure of Redundancy

The rational evaluation of structural redundancy is a difficult task because of the variety of triggering events, the number of parameters that can influence the behavior of structural systems, and the difficulty of performing a cost–benefit analysis that would account for the costs of improved topological configurations while considering the importance of the structure in terms of the economic, social, political, and environmental consequences of its failure (Anitori et al., 2013). Traditionally, redundancy of a bridge structure is judged merely based on the alternative load path provided by the system. Most would consider multi-girders bridge as redundant bridge system, and simply supported truss bridge would be considered as non-redundant bridge system. In the actual bridge systems, factors contributed to the quality of the bridge redundancy level can be classified into three main categories: load path redundancy, structural redundancy, and internal redundancy. Despite that, in the application, only load path redundancy is normally considered during the design phase. Consideration of structural redundancy is more likely only during the inspection and retrofitting process. The internal redundancy, on the other hand, is currently not recognized in the classification of Fracture Critical Members for either design and fabrication or in-service inspection (FHWA, 2012b).

2.4.1 Load path redundancy

Load path redundancy generally is referring to the capability of the system to redistribute the load from the damaged member to other adjacent members. This kind of redundancy can be clearly defined in the multi girders bridge. If one of the main girders failed, the load is expected to be carried by the adjacent girders. However, the existing of the load path redundancy will not guarantee the redundancy level of the bridge structure. In fact, it depends on the capability of the adjacent girders to continue to carry the load transfer from the damaged girder. If the adjacent girders are incapable of carrying the load from the damaged girder, progressive failure is expected and the whole bridge system is a collapse. Somehow, in multi

girders bridge system, the numbers of main girders are directly proportioned to the redundancy level of the bridge structure as a higher number of main girders results in a higher level of load-path redundancy. It can be concluded that a system showing more options of alternative load path generally considered as having a higher level of redundancy but the level of the redundancy cannot be determined merely by looking at the number of alternative load path.

2.4.2 Structural redundancy

Structural redundancy is referring to the capability of the bridge structure to continue to carry the load if the boundary condition of the structure was to change due to any unpredictable event. An example of structural redundancy is the failure of negative bending moment region of a continuous beam. The failure of the section at the negative bending moment region (support) is not necessarily lead to the failure of the entire structure provided that the positive moment region has enough reserve strength to carry the extra bending moment transfer from negative bending moment to positive bending moment at mid-span section. In contrast, if the mid-span section of a continuous beam failed, the collapse can also be guaranteed if the adjacent beam can carry the extra negative and positive bending moment causing by cantilever action of the damaged span. In general, a bridge with continuous span is normally considered as having structural redundancy.

2.4.3 Internal redundancy

Internal redundancy is referring to the capability of the structure itself to limit the extent of the damage after some parts of members are subjected to damage. For example, the connection method using to connect the web and flange for the main girder is related to internal redundancy. In the first case, if bolt connection would provide internal redundancy to the main girders as if the fracture is to initiate on the bottom flange, it will not continue to the web and the damage is limited to the flange only. In the second case, if weld connection is used instead of bold connection, there is a high possibility that the fracture initiated on the flange will continue to the web and the whole section will be subjected to full fracture which is more dangerous than the first case.

2.4.4 Qualitative measure of redundancy for composite twin I-girder bridges

In general, bridges system does not require to possess all three criteria of redundancy in order to qualify as redundant bridge systems. Some bridge systems that possess only one

criterion of redundancy can have a higher level of redundancy than bridge systems possess two or three criteria of redundancy. For example, if we compare the redundancy of continuous twin I-girder bridge system with the simply supported six I-girder bridge system, the simply supported six I-girder bridge system, which possesses only load-path redundancy, can be more redundant than the continuous twin I-girder bridge system which possesses both load-path and structural redundancy. From the viewpoint of engineering practice which considers only load path redundancy, all types of two girders systems including composite twin I-girder bridge system is classified as non-redundant bridge system. However, in the actual three-dimensional bridge system, not only the adjacent girder acts as the alternative load path, the concrete deck in composite twin I-girder bridge system is also a crucial member that transfers the load from the damaged girder to the adjacent girder and to the support or bearing. Furthermore, in the case of damage resulted from fracture, the fracture normally stops at the top flange of the I section which represents a property of internal redundancy. In addition, the composite twin I-girder bridge system with continuous span possesses the structural redundancy which further contributes to the overall redundancy level of the bridge system. Furthermore, previous studies also proved that composite twin I-girder bridge system does not collapse in the severe fracture condition and somehow manage to carry some extra live load. From the qualitative measure of redundancy, composite twin I-girder bridge system may have sufficient level of redundancy considering the actual three-dimensional behavior of the bridge system.

2.5 Quantitative Measure of Redundancy

To define the redundancy level of the bridge systems, a uniform quantitative measure for redundancy is required. During the early 1980s, the degree of indeterminacy was considered as the key aspect to evaluate bridge redundancy. As shown in **Eq.2.1**, a structure with a higher level of degree of indeterminacy is considered as more redundant. This equation, however, has been proved as not an adequate measure of structural redundancy (Frangopol, 1987). The later development of the quantitative measure of redundancy is focusing on the load carrying capacity aspect following the more commonly used nonlinear analyses in bridge design and analyses. Several alternative measures are proposed as deterministic approaches of structural redundancy as shown in **Eq.2.2**, **Eq.2.3**, and **Eq.2.4** (Furuta, 1985).

Degree of indeterminacy: $$R_1 = F - E \tag{2.1}$$

Reserve redundant factor: $$R_2 = \frac{L_{intact}}{L_{design}} \tag{2.2}$$

Residual redundant factor: $R_3 = \frac{L_{damage}}{L_{intact}}$ (2.3)

Strength redundant factor: $R_4 = \frac{L_{intact}}{L_{intact} - L_{damage}}$ (2.4)

where

F: number of unknown reactive forces,

E: number of independent equilibrium equations,

L_{intact}: load carrying capacity of the intact structure,

L_{damage}: load carrying capacity of the damaged structure,

L_{design}: design load of the intact system

In Europe, unlike in the United States, the term "robustness" is frequently used instead of "redundancy" in evaluating the structure in damaged condition (COST, 2011). Several approaches have also been proposed to quantify the safety of the structure in the damaged condition which refers as redundancy in this context. System inspection and repair are seen to increase the robustness of systems by lowering the probability that a damaged system will fail in the future (Baker et al., 2008). Several measures to account for the robustness of the system based on global stiffness, damage extent, and energy release upon damage as shown in **Eq.2.5**, **Eq.2.6**, and **Eq.2.7** (Starossek and Haberland, 2007, 2008, 2009, 2011). The measure based on the global stiffness, which is shown in **Eq.2.5**, is proved to be not an adequate measure based on the sensitivity tests performed by Haberland (Anitori, 2013). The measure based on damage extent, presented in **Eq.2.6**, is considered as theoretically correct and reasonable. However, such measure is hard to determine in the actual application due to the lack of specific guideline in the existing specifications. The measure based on energy released upon damage is shown in **Eq.2.**7. This measure requires dynamic analyses of the structural system which is difficult for most designers and in the determination of its parameter, the energies.

$$R_S = \min_j \frac{\det K_j}{\det K_0} \tag{2.5}$$

$$R_d = 1 - \frac{p}{p_{lim}} \tag{2.6}$$

$$R_e = 1 - \max_j \frac{E_{r,j}}{E_{s,k}} \tag{2.7}$$

where:

$\det K_0$: the determinant of the stiffness matrix of the intact system (Anitori et al., 2013)

$\det K_j$: the determinant of the stiffness matrix of the system with member j damaged (Anitori et al., 2013)

p: the maximum spread of damage caused by a given hazard (Anitori et al., 2013)

p_{lim}: the acceptable damage set by design or actual requirements (Anitori et al., 2013)

$E_{r,j}$: the energy released by the initial failure of an element j (Anitori et al., 2013)

$E_{s,k}$: energy required for the subsequent failure of element k (Anitori et al., 2013)

In the current design practice, AASHTO is one of a few specifications which include the measure of redundancy in the design phase. The AASHTO design specifications define redundancy as" the quality of a bridge that enables it to perform its design function in a damaged state" (AASHTO, 2012). Along with redundancy, a redundant member is a member whose failure does not cause the failure of the system or the entire bridge. The AASHTO Manual for Bridge Evaluation defines bridge redundancy as "the capability of a bridge structural system to carry the load after damage to or the failure of one or more of its members" (AASHTO, 2011). Despite its definitions related to structural behavior rather than single member's response, the current existing rating level is based on the judgment on single element behavior rather than overall system behavior. In current AASHTO specifications, the redundancy factor is including in the load modifier along with ductility factor and operational importance classification factor. This classification is rather simple and based on the qualitative measure of redundancy without requiring actual redundancy analysis base on the bridge response in damaged condition. The method is considered simplify because the designers don't have to calculate or consider in detail the redundancy level of the structure. A bridge contains non-redundant members will be subjected to 5% penalty to the load modifier factor while the bridge considered as very redundant will be subjected to 5% reduction (as a reward) to the load modifier factor. Besides, a bridge that classified as having a conventional level of redundancy will be ignored from the design consideration. AASHTO Specifications also recommends the use of multiple load paths and continuous structure. This is to ensure the existing of load path redundancy and structural redundancy. However, because of the simplicity of the method, its redundancy rating level is somehow considered as oversimplified which does not reflect the

response of the actual bridge structure. For example, in the current situation, all multiple girders bridges are considered as redundant only when the numbers of the main girder exceed three. To this point, all twin girder system is considered as non-redundant despite several past experiences shown that this type of bridge is normally survived even full crack is generating on one of the two main girders at the critical location. This classification will result in much stricter provisions than a non-fracture-critical bridge, such as hands-on inspections, nondestructive inspections on welded connections, and the mandated use of high-fracture-toughness materials (Kim and Williamson, 2014). These restrictions not only increase construction costs compared with non-fracture-critical bridges, they also increase the maintenance costs of the bridge (Kim and Williamson, 2014). A better evaluation of redundancy is required in the design phase to ensure the new design bridge is both safety and economy optimized.

2.6 Probabilistic Measure of Redundancy

2.6.1 Probability of failure and the reliability index β

In engineering practice, the probability of failure can be defined as the probability in which the action *S* is larger than the resistance *R*. The probability of failure P_f is express in **Eq.2.8** and shown in **Fig.2.9**. In the reliability of structural system, the first order second moment method (FORM) are often used in practical reliability assessment of the structural performance and safety level. This method, however, require the random variable to follow the normal or lognormal distribution in order to achieve a high level of accuracy in the reliability analyses. With the FORM, the reliability index β is defined as the negative value of a standardized normal variable corresponding to the probability of failure P_f (Holicky and Vrouwenvelder, 2005). In mathematical terms, the following relation can be defined for probability of failure and reliability index:

$$P_f = P\{(R - S) < 0\} \text{ or } P_f = P\left\{\left(\frac{R}{S}\right) < 1\right\} \tag{2.8}$$

$$\beta = -\Phi^{-1}(P_f) \tag{2.9}$$

Φ: is the cumulative distribution function

If both *R* and *S* follow the independent normal distribution, which means:

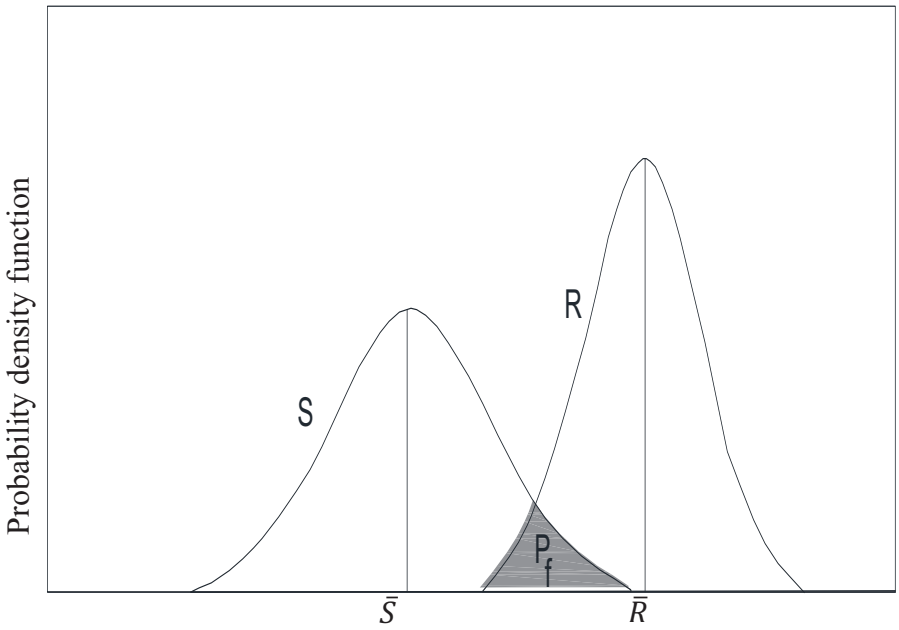

Fig.2.9 Definition of Probability of failure

$$\{R\} \sim N(\mu_R; \sigma_R^2)$$

$$\{S\} \sim N(\mu_S; \sigma_S^2)$$

Then

$$\{R - S\} \sim N(\mu_R - \mu_S; \sigma_R^2 + \sigma_S^2)$$

$$\Rightarrow \qquad \beta = -\Phi^{-1}(P_f) = -\Phi^{-1}(P\{(R - S) < 0\}) = \frac{\mu_R - \mu_S}{\sqrt{\sigma_R^2 + \sigma_S^2}} \qquad (2.10)$$

where:

μ_R: mean value of variable *R*

μ_R: mean value of variable *S*

σ_R : standard deviation of variable *R*

σ_S : standard deviation of variable *S*

If both *R* and *S* instead follow the independent lognormal distribution, which means:

$$\{lnR\} \sim N(\mu_{lnR}; \sigma_{lnR}^2)$$

$$\{lnS\} \sim N(\mu_{lnS}; \sigma_{lnS}^2)$$

Then

$$\{lnR - lnS\} \sim N(\mu_{lnR} - \mu_{lnS}; \sigma_{lnR}^2 + \sigma_{lnS}^2)$$

$$\Rightarrow \quad \beta = -\Phi^{-1}(P_f) = -\Phi^{-1}\left(P\left\{\frac{R}{S} < 1\right\}\right) = -\Phi^{-1}\left(P\left\{\ln(\frac{R}{S}) < 0\right\}\right) \tag{2.11}$$

$$\Rightarrow \quad \beta = -\Phi^{-1}(P\{\mathrm{lnR} - \mathrm{lnS}) < 0\}) \tag{2.12}$$

$$\Rightarrow \quad \beta = \frac{\mu_{lnR} - \mu_{lnS}}{\sqrt{\sigma_{lnR}^2 + \sigma_{lnS}^2}} \tag{2.13}$$

where :

μ_{lnR}: mean value of variable *lnR*

μ_{lnR}: mean value of variable *lnS*

σ_{lnR}: standard deviation of variable *lnR*

σ_{lnS}: standard deviation of variable *lnS*

Since *R* and *S* follow lognormal distribution, the mean $(\bar{R}; \bar{S})$ and standard deviation $(\sigma_R;\ \sigma_S)$ of the parameters *R* and *S* can be expressed as below:

$$\begin{cases} \bar{R} = e^{\mu_{lnR} + \left(\frac{{\sigma_{lnR}}^2}{2}\right)} \\ \bar{S} = e^{\mu_{lnS} + \left(\frac{{\sigma_{lnS}}^2}{2}\right)} \\ \sigma_R^2 = \left(e^{{\sigma_{lnR}}^2} - 1\right) e^{2\mu_{lnR} + {\sigma_{lnR}}^2} \\ \sigma_S^2 = \left(e^{{\sigma_{lnS}}^2} - 1\right) e^{2\mu_{lnS} + {\sigma_{lnS}}^2} \end{cases} \tag{2.14}$$

$$\begin{cases} ln\bar{R} = \mu_{lnR} + \left(\frac{{\sigma_{lnR}}^2}{2}\right) \\ ln\bar{S} = \mu_{lnS} + \left(\frac{{\sigma_{lnS}}^2}{2}\right) \\ \sigma_R^2 = \left(e^{{\sigma_{lnR}}^2} - 1\right)\bar{R}^2 \\ \sigma_S^2 = \left(e^{{\sigma_{lnS}}^2} - 1\right)\bar{S}^2 \end{cases} \tag{2.15}$$

$$\begin{cases} \mu_{lnR} = ln\bar{R} - \left(\frac{{\sigma_{lnR}}^2}{2}\right) \\ \mu_{lnS} = ln\bar{S} - \left(\frac{{\sigma_{lnS}}^2}{2}\right) \\ \frac{\sigma_R^2}{\bar{R}^2} = \left(e^{{\sigma_{lnR}}^2} - 1\right) => {\sigma_{lnR}}^2 = ln\left(\frac{\sigma_R^2}{\bar{R}^2} + 1\right) \\ \frac{\sigma_S^2}{\bar{S}^2} = \left(e^{{\sigma_{lnS}}^2} - 1\right) => {\sigma_{lnS}}^2 = ln\left(\frac{\sigma_S^2}{\bar{S}^2} + 1\right) \end{cases} \tag{2.16}$$

$$\begin{cases} \mu_{lnR} = ln\bar{R} - \left(\frac{{\sigma_{lnR}}^2}{2}\right) \\ \mu_{lnS} = ln\bar{S} - \left(\frac{{\sigma_{lnS}}^2}{2}\right) \\ {\sigma_{lnR}}^2 = ln\left(\frac{\sigma_R^2}{\bar{R}^2} + 1\right) \\ {\sigma_{lnS}}^2 = ln\left(\frac{\sigma_S^2}{\bar{S}^2} + 1\right) \end{cases} \tag{2.17}$$

$$\begin{cases} \mu_{lnR} = ln\bar{R} - \frac{1}{2}ln\left(\frac{\sigma_R^2}{\bar{R}^2} + 1\right) \\ \mu_{lnS} = ln\bar{S} - \frac{1}{2}ln\left(\frac{\sigma_S^2}{S^2} + 1\right) \\ {\sigma_{lnR}}^2 = ln\left(\frac{\sigma_R^2}{\bar{R}^2} + 1\right) \\ {\sigma_{lnS}}^2 = ln\left(\frac{\sigma_S^2}{\bar{S}^2} + 1\right) \end{cases} \tag{2.18}$$

The coefficient of variation V_R and V_S are defined as follow:

$$\begin{cases} V_R = \frac{\sigma_R}{\bar{R}} \\ V_S = \frac{\sigma_S}{S} \end{cases} \tag{2.19}$$

We get,

$$\begin{cases} \mu_{lnR} = ln\bar{R} - \frac{1}{2}ln(V_R^2 + 1) \\ \mu_{lnS} = ln\bar{S} - \frac{1}{2}ln(V_S^2 + 1) \\ {\sigma_{lnR}}^2 = ln(V_R^2 + 1) \\ {\sigma_{lnS}}^2 = ln(V_S^2 + 1) \end{cases} \tag{2.20}$$

Then the reliability index β can be expressed as:

$$\beta = \frac{\mu_{lnR} - \mu_{lnS}}{\sqrt{\sigma_{lnR}^2 + \sigma_{lnS}^2}} = \frac{\left[ln\bar{R} - \frac{1}{2}ln(V_R^2+1)\right] - \left[ln\bar{S} + \frac{1}{2}ln(V_S^2+1)\right]}{\sqrt{ln(V_R^2+1) + ln(V_S^2+1)}} \tag{2.21}$$

$$\beta = \frac{ln\left(\frac{\bar{R}}{\bar{S}}.\frac{\sqrt{1+V_S^2}}{\sqrt{1+V_R^2}}\right)}{\sqrt{ln\left[(1+V_S^2)(1+V_R^2)\right]}} \tag{2.22}$$

If V_R and V_S are less than 20%, **Eq.2.22** can be approximated as:

$$\beta = \frac{ln\left(\frac{\bar{R}}{\bar{S}}\right)}{\sqrt{V_S^2 + V_R^2}} \tag{2.23}$$

The **Eq.2.23** gives a very good approximation to the reliability index β even when the live load does not exactly follow a lognormal distribution (Saydam and Frangopol, 2013). It was also proved that the use of **Eq.2.23** produce a relatively small percentage of error when V_{LF} and V_{LL} are less than 30% and the reliability index β is smaller than 4.5 (Saydam and Frangopol, 2013).

2.6.2 Redundancy evaluation based on reliability index β

More studies are required to establish an accurate redundancy rating method for bridge structures. The effect of damage and redundancy on the reliability of structural system based on structural redundancy was investigated including both system reliability and damage assessment concepts (Frangopol, 1987). It was concluded that probabilistic concepts should be used to develop a redundancy evaluation method that can account for the random nature of the required information such as loads, strengths etc. It was more than 10 years later that a quantitative redundancy rating method based on the reliability concept is proposed in the United States (Ghosn and Moses, 1998). During the development of AASHTO LRFD, β_{member}=3.5 was taken as the target limit of the structural members (Nowak, 1995; Nowak, 1999). The use of reliability index to evaluate the bridge redundancy is proposed (Ghosn and Moses, 1998). By introducing the term reliability index, the redundant structure is designed with a smaller safety factor compared to the non-redundant structure to achieve the same level of safety between redundant and non-redundant structure. To link the reliability index with the bridge system capacity and redundancy, four loading factors were proposed for bridge system and represented in **Fig.2.10**. LF_1 is defined as the live load factor corresponding to first member failure. This load factor is generally referred as the design load which can be varied according to different specifications. LF_u is the live load factor at which the intact bridge system reached its ultimate state while LF_d is the live load factor at which the damaged bridge system reached its ultimate state. LF_f is the live load at which the displacement of the bridge reaches 1% of span length and the bridge is considered as unfit from using at this point (Ghosn and Moses, 1998).

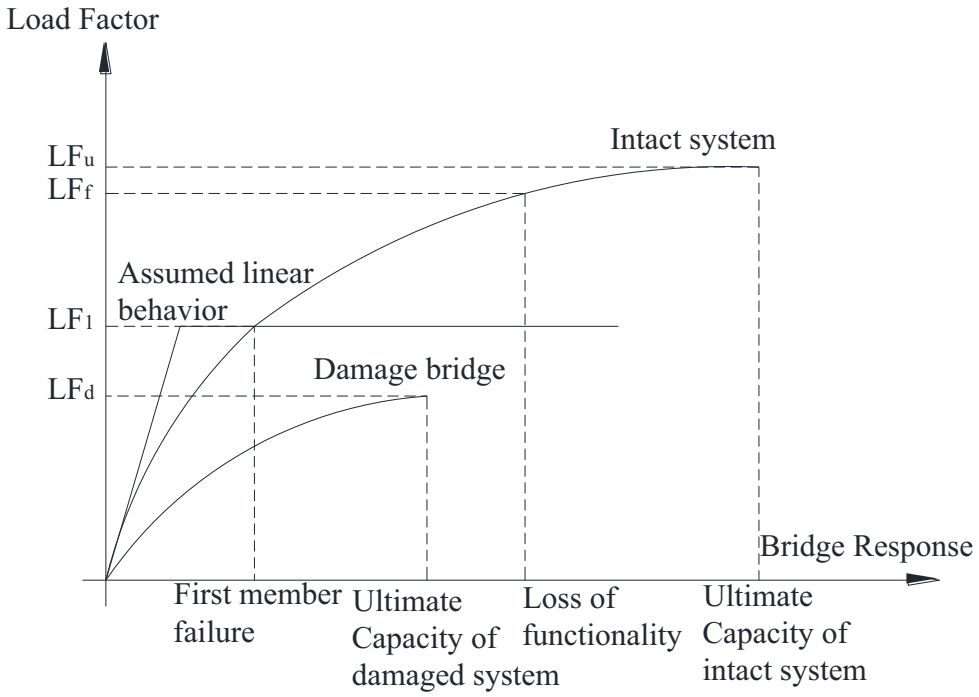

Fig.2.10 Typical behavior of bridge system (Ghosn et al, 2010)

Four reliability indexes were proposed according to the behavior of bridge system:

$$\beta_{member} = \frac{\ln\left(\frac{\bar{R}}{\bar{S}}\right)}{\sqrt{V_R^2+V_S^2}} = \frac{\ln\left(\frac{\overline{LF_1}}{\overline{LL_{75}}}\right)}{\sqrt{V_{LF}^2+V_{LL}^2}} \tag{2.24}$$

$$\beta_{ultimate} = \frac{\ln\left(\frac{\bar{R}}{\bar{S}}\right)}{\sqrt{V_R^2+V_S^2}} = \frac{\ln\left(\frac{\overline{LF_u}}{\overline{LL_{75}}}\right)}{\sqrt{V_{LF}^2+V_{LL}^2}} \tag{2.25}$$

$$\beta_{function} = \frac{\ln\left(\frac{\bar{R}}{\bar{S}}\right)}{\sqrt{V_R^2+V_S^2}} = \frac{\ln\left(\frac{\overline{LF_f}}{\overline{LL_{75}}}\right)}{\sqrt{V_{LF}^2+V_{LL}^2}} \tag{2.26}$$

$$\beta_{damaged} = \frac{\ln\left(\frac{\bar{R}}{\bar{S}}\right)}{\sqrt{V_R^2+V_S^2}} = \frac{\ln\left(\frac{\overline{LF_d}}{\overline{LL_2}}\right)}{\sqrt{V_{LF}^2+V_{LL}^2}} \tag{2.27}$$

The method proposed in NCHRP Report 406 was developed based on the live load according to AASHTO specifications (AASHTO, 2012) where:

β_{member}: reliability index corresponding to the first member failure (Ghosn and Moses, 1998)

$\beta_{ultiatme}$: reliability index corresponding to the ultimate state of the intact system (Ghosn and Moses, 1998)

$\beta_{function}$: reliability index corresponding to the service state of the intact system (Ghosn and Moses, 1998)

$\beta_{damaged}$: reliability index corresponding to the ultimate state of the damage system (Ghosn and Moses, 1998)

$\overline{LF_u}$: the mean value of the load factor corresponding to the ultimate limit state of intact system. (Ghosn and Moses, 1998)

$\overline{LF_f}$: the mean value of the load factor corresponding to the service limit state of intact system. (Ghosn and Moses, 1998)

$\overline{LF_d}$: the mean value of the load factor corresponding to the ultimate limit state of damaged system. (Ghosn and Moses, 1998)

LL_{75}: the maximum load expected in a 75-year design life expressed in terms of the number of AASHTO HS-20 trucks, (Ghosn and Moses, 1998)

LL_2 : the maximum load expected in a 2-year service life expressed in terms of the number of AASHTO HS-20 trucks. (Ghosn and Moses, 1998)

V_{LF}: Coefficient of variation of LF_1 (Ghosn and Moses, 1998)

V_{LL}: Coefficient of variation of the maximum expected live load LL_{75} (Ghosn and Moses, 1998)

The values of LL_{75}, LL_2, V_{LL} for different bridge configuration and span length are provided in NCHRP Report 406 (1998) and NCHRP Report 776 (2013). The measure of system redundancy can be obtained by comparing the overall capacity of originally intact and damaged bridge system (Ghosn and Moses, 1998). Three system reserve ratios and three reliability measures of redundancy which are defined in terms of relative reliability indices (Ghosn and Moses, 1998) were proposed as follows:

$$R_u = \frac{LF_u}{LF_1} \tag{2.28}$$

$$R_f = \frac{LF_f}{LF_1} \tag{2.29}$$

$$R_d = \frac{LF_d}{LF_1} \tag{2.30}$$

$$\Delta\beta_u = \beta_{ult} - \beta_{member} \tag{2.31}$$

$$\Delta\beta_f = \beta_{funct} - \beta_{member} \tag{2.32}$$

$$\Delta\beta_d = \beta_{damaged} - \beta_{member} \tag{2.33}$$

where:

R_u : system reserve ratio for the ultimate limit state (Ghosn and Moses, 1998)

R_f : system reserve ratio for the functionality limit state (Ghosn and Moses, 1998)

R_d : *system* reserve ratio for the damaged condition (Ghosn and Moses, 1998)

$\Delta\beta_u$: relative reliability index for the ultimate limit state (Ghosn and Moses, 1998)

$\Delta\beta_f$: relative reliability index for the functionality limit state (Ghosn and Moses, 1998)

$\Delta\beta_d$: relative reliability index for the damaged condition (Ghosn and Moses, 1998)

By using **Eq.2.24**, **Eq.2.25**, **Eq.2.26**, **Eq.2.27**, the **Eq.2.31**, **Eq.2.32** and **Eq.2.33** can be expressed as:

$$\Delta\beta_u = \frac{ln\left(\frac{\overline{LF_u}}{\overline{LL_{75}}}\right)}{\sqrt{V_{LF}^2+V_{LL}^2}} - \frac{ln\left(\frac{\overline{LF_1}}{\overline{LL_{75}}}\right)}{\sqrt{V_{LF}^2+V_{LL}^2}} = \frac{ln\left(\frac{\overline{LF_u}}{\overline{LF_1}}\right)}{\sqrt{V_{LF}^2+V_{LL}^2}} = \frac{ln(R_u)}{\sqrt{V_{LF}^2+V_{LL}^2}} \tag{2.34}$$

$$\Delta\beta_f = \frac{ln(R_f)}{\sqrt{V_{LF}^2+V_{LL}^2}} \tag{2.35}$$

$$\Delta\beta_u = \frac{ln\left(R_d \cdot \frac{\overline{LF_{75}}}{\overline{LL_2}}\right)}{\sqrt{V_{LF}^2+V_{LL}^2}} \tag{2.36}$$

The relative reliability indices in the proposed method give measures of the additional safety provided by the system compared to the safety against the first member failure (Anitori

et al., 2013). As the target value of this relative reliability indices, a four beams simple span bridge is considered as redundant bridge system and was set as the limit in the classification of bridge redundancy. In the determination of the average value of $\Delta\beta_u$, $\Delta\beta_f$, and $\Delta\beta_d$, live load model HS20 used in the AASHTO Specifications is used as the target load factor applied on the bridge models. A parametric study was performed on a series of four beam steel I-girder bridge and four I-beam pre-stressed concrete bridge. Nonlinear analyses were used in the determination of LF_1, LF_u , LF_f, and LF_d. In the determination of LF_d, one of the four main girders is considered as damaged and removed from the numerical model. The average value of $\Delta\beta_u$, $\Delta\beta_f$, and $\Delta\beta_d$ was found as 0.85, 0.25 and -2.7, respectively (Ghosn and Moses, 1998). The details of the analyses results are provided in NCHRP Report 406, Appendix B, C, and D. (Ghosn and Moses, 1998). Based on this result, the value of R_u, R_f, and R_d can be obtained by using **Eq.2.34**, **Eq.2.35**, and **Eq.2.36**. The exact value is R_u=1.22, R_f=1.06, and R_d=0.48. If the load follows Gumbel distribution as suggested by Nowak, then by using level II reliability program, the R_u, R_f, and R_d were obtained as 1.28, 1.08 and 0.47 (Ghosn and Moses, 1998). These results have shown that the lognormal approaches, as mentioned, produce a relatively small error even the load and resistance didn't exactly follow the lognormal distribution. The target reserve ratios were proposed and approximated as follow (Ghosn and Moses, 1998):

$$\begin{cases} R_{u,target} = 1.3 \\ R_{f,target} = 1.1 \\ R_{d,target} = 0.5 \end{cases}$$

Based on the results mentioned above, the redundancy factor was proposed in the following form (Ghosn and Moses, 1998):

$$\varphi_R = min\left(\frac{R_u}{1.30}, \frac{R_f}{1.10}, \frac{R_d}{0.50}\right) \tag{2.37}$$

$$R_u = \frac{LF_u}{LF_1} \tag{2.38}$$

$$R_f = \frac{LF_f}{LF_1} \tag{2.39}$$

$$R_d = \frac{LF_d}{LF_1} \tag{2.40}$$

It is important to point out that a bridge that proves to have enough redundancy level according to this method is not necessary and guarantee as a fail-safe structure in accidental circumstance. In fact, it ensures that the bridge can sustain overload condition above design

limit for a certain amount and any bridge that can survive in accident circumstance will be able to continue to carry some load until the damage was discovered and the repair can be taken place before the bridge collapses. This method is logically direct with defined quantitative limits; further, it does not depend on the choice of the live load model and is based on system reliability evaluation of the bridge, whose redundancy is generally agreed upon (Hunley and Harik, 2011). This method is later developed for evaluating the redundancy of the bridge substructure (Liu et al., 2001) and also for the long span bridge structure (Ghosn and Yang, 2014). The application of this method has also gained acceptance from bridge designers and researchers in several projects (Wisniewsky et al., 2006; Lin et al., 2013; Ghosn and Yang, 2014; Lin et al., 2014; Lam et al., 2014; Gheitasi and Harris, 2016). Such a requirement guarantees the safety of the bridge from collapse and prevents the bridge from entering out-of-service or damaged states. Despite the logic of the method and quantifiable redundancy factor, such method requires three-dimensional nonlinear analyses of the bridge structure, which normally considered as complicated, and not yet applicable to general bridge designer. Moreover, as the method itself is developed based on the girder bridge models which normally used for medium-span bridge, its application to long span bridge is still doubtful. Furthermore, it is unclear whether the application of such method is depending on the choice of live load model or not since such statement has not been proved in any existing literature. But in current design practice concerning the evaluation of bridge redundancy, such method is unarguably the most acceptable and practical method before a uniform or general method is introduced. Despite this limitation, the method proposed in NCHRP Report 406, which based on the multi-girder bridge system, is undoubtedly applicable to the multi-girders bridge system including composite twin I-girder bridge systems. While a universally accepted method for redundancy is not yet available, the method proposed above (Ghosn and Moses, 1998) will be used as a principal method to investigate the redundancy of bridge systems in this study.

2.7 Conclusions

From the existing literature, although uniform redundancy evaluation criteria are currently not existed, it has been widely recognized by structural engineering community that redundancy is an important criterion that can guarantee the survival of the bridge in critical damaged condition. In current design specifications in Japan, Europe, United States and many others, the redundancy criteria or the criteria to prevent system collapse from single member failure have been introduced during the design and maintenance processes. Though only general prescriptions and very limited guidelines are provided, such requirement is still

essential to guarantee the bridge safety, especially for the rapidly increasing of the old bridge. From the engineering based viewpoint, the redundancy criteria are recognized as important, yet hard to define which required some detailed analyses that are complicated and time-consuming. A series of quantitatively based measures have been proposed by several researchers which lead to the development of the redundancy criteria method based on reliability analyses. In current research and design practice of bridge redundancy, the method based on reliability analyses is becoming more and more acceptance from engineering community due to its promising deterministic level of redundancy. However, such method requires nonlinear analyses which are complicated and very time-consuming. In conclusion, from the existing literature to the design practice, a uniform redundancy evaluation should consist of two important aspects: 1. providing a uniform level of reliability with an objective measure which is independent to design specifications, and 2. Do not require nonlinear analyses and applicable to most of the bridge designers.

References

AASHTO (American Association of State Highway and Transportation Officials), (2012). "AASHTO "LRFD Bridge Design Specification", 6th edition, Washington, DC.

AASHTO (American Association of State Highway and Transportation Officials). (2011). "AASHTO Manual for Bridge Evaluation." 2nd edition, Washington, DC.

Anitori, G., Casas, J.R., and Ghosn, M. (2013) "Redundancy and robustness in the design and evaluation of bridges: European and north American perspectives", Journal of Bridge Engineering, ASCE, Vol. 18, No 12, pp. 1241-1251.

ASCE-AASHTO Task committee. (1985) "State of the art report on redundant bridge systems", Journal of Structural Engineering, ASCE, Vol. 111, No. 12, pp. 2517-2531.

Baker, J.W., Schubert, M., and Faber, M.H., (2008). "On the assessment of robustness", Structural Safety, Vol. 30, No. 3, pp. 253– 267.

CNN Report by Carter J.C, Brumfiled B.m and Barrett, k., May 24th, 2013, available online from http://edition.cnn.com/2013/05/24/us/washington-bridge-collapse.

Connor, R.J., Dexter R., and Mahmoud H. (2005). "Inspection and Management of Bridges with Fracture Critical Details." NCHRP Synthesis 354, National Cooperative Highway Research Program, Washington, DC.

COST (European Cooperation in Science and Technology). (2011) "Robustness of Structures", Action TU0601, Brussels.

Csagoly, P. F., and Jaeger, L. G. (1979). "Multi-Load-Path Structures for Highway Bridges", Transportation Research Record 711, pp. 34-39.

Deng, L., Wang, W., and Yu, Y. (2016). "State-of-the-Art Review on the Causes and Mechanisms of Bridge Collapse" Journal of Performance Construction Facility, ASCE, Vol. 30, No. 2, 04015005.

Ellingwood, B.R. and Dusenberry, D.O. (2005). "Building design for abnormal loads and progressive collapse", Computer-Aided Civil and Infrastructure Engineering, Vol 20, No.3, pp. 194–205.

FHWA (Federal Highway Administration) (1996). "A Look at the History of the Federal Highway Administration", FHWA-PD-96-029 HPD, Washington, D.C. https://www.fhwa.dot.gov/byday/fhbd1215.htm.

FHWA (Federal Highway Administration) (2012a). "Clarification of requirements for Fracture Critical Members", Memorandum, Washington, D.C.

FHWA (Federal Highway Administration) (2012b). Steel Bridge Design Handbook: Redundancy, Vol. 9, No. FHWA-IF-12-052, Washington, D.C.

Frangopol, D.M. (1992). "Bridge loading, reliability and redundancy: concepts and applications", International Federation for Information Processing, Geneva.

Frangopol, D.M. and James Curley, P. "Effects of damage and redundancy of structural reliability", Journal of Structural Engineering, ASCE, Vol. 113, pp. 1533-1549.

Fujino, Y. (2006). "Steel Bridges in Japan-Current Circumstances and Future Tasks." Steel Construction Today and Tomorrow, Japan Society of Steel Construction, No. 15.

Furuta, H., Shinozuka, M., and Yao, J.T.P. (1985). "Probabilistic and Fuzzy Representation of Redundancy in Structural Systems", International Fuzzy Systems Associated Congress, Palma de Mallorca, Spain.

Gheitasi, A. and Harris, D.K. (2016). "Redundancy and Operational Safety of Composite Stringer Bridges with Deteriorated Girders", Journal of Performance of Constructed Facilities, ASCE, Vol. 30, No. 2, 04015022.

Ghosn, M. and Moses, F. (1998). "Redundancy in Highway Bridge Superstructure." NCHRP Report 406, National Cooperative Highway Research Program, Washington, DC.

Ghosn, M., Moses, F., and Frangopol, D.M. (2010). "Redundancy and Robustness of Highway Bridge Superstructures and Substructures." Structures and Infrastructure Engineering, Vol. 6, No. 1-2, pp. 257-278.

Ghosn, M. and Yang, J. (2014). "Bridge System Safety and Redundancy." NCHRP Report 776, National Cooperative Highway Research Program, Washington, DC.

Holicky, M. and Vrouwenvelder, T. (2005). "Chapter 1- Basic Concepts of Structural Reliability", Implementation of Eurocodes, Handbook 2: Reliability Backgrounds, Prague.

Hunley, C.T., and Harik, I.E. (2012). "Structural Redundancy Evaluation of Steel Tub Girder Bridges." Journal of Bridge Engineering, ASCE, Vol. 17, Issue 3, pp. 481 - 489.

JSCE Steel Committee. (2014). "Report on redundancy of steel structures,", subcommittee on the redundancy of Steel structures (In Japanese).

JRA (Japan Road Association). (2012). "Specifications for Highway Bridges." Part I Common, English edition, Tokyo.

Kim, J., and Williamson, E.B. (2015). "Finite-Element Modeling of Twin Steel Box-Girder Bridges for Redundancy Evaluation." Journal of Bridge Engineering, ASCE, Vol. 20, No. 10, 04014106(1-9).

Lam, H., Lin, W., and Yoda, T. (2014). “Effect of Bracing Systems on Redundancy of Three-span Composite Twin I-girder Bridge.” JSCE Journal of Structural Engineering, Vol. 60A, pp. 59-69.

Lichtenstein, Abba. (1993). “The Silver Bridge Collapse Recounted.” Journal of Performance of Constructed Facilities, ASCE, Vol. 7, No. 4, pp. 249-261.

Lin, W., Yoda, T., Kumagai, Y., Saigyo, T. (2013). “Numerical Study on Post-Fracture Redundancy of the Two-girder Steel-Concrete Composite Highway Bridges.” International Journal of Steel Structures, Vol. 13, No. 4, pp. 671-681.

Lin, W., Yoda, T., and Lam, H. (2014). “Reliability and Redundancy of two-girder, steel-concrete composite bridges under uncertainty.” Second International Conference on Vulnerability and Risk Analysis and Management (ICVRAM) and the Sixth International Symposium on Uncertainty, Modeling, and Analysis (ISUMA), pp. 86-95.

Liu, W.D., Ghosn, M., Moses, F., and Neuenhoffer, A. (2001). “Redundancy in Highway Bridge Substructures.” NCHRP Report 458, National Cooperative Highway Research Program, Washington, DC.

WTNH Television Station Report: NEWS8, June 28th, 1983, available online from http://interactives.wtnh.com/photomojo/gallery/8011/156993/1983-mianus-river-bridge-collapse/bridge-collapse/

Nowak, A.S. (1995). “Calibration of LRFD bridge code”, Journal of Bridge Engineering, ASCE, Vol.121, No. 8, pp. 1245-1251.

Nowak, A.S. (1999). “Calibration of LRFD bridge design code”, NCHRP Report 368, National Cooperative Highway Research Program, Washington, DC.

Pearson, C., and Delatte, N. (2005). "Ronan Point Apartment Tower Collapse and its Effect on Building Codes." Journal of Performance Construction Facility, Vol. 19, No. 2, pp. 172-177.

Saydam, D. and Frangopol, D.M. (2013). “Applicability of simple expressions for bridge system reliability assessment”, Journal of computer and structure, Vol 114-115, pp. 59-71.

Starossek, U., Haberland, M. (2011). “Approaches to measures of structural robustness”, Structure and Infrastructure Engineering Vol. 7, Nos. 7–8, pp. 625–631.

Starossek, U. and Haberland, M., (2008). “Measures of structural robustness – Requirements and applications”, ASCE Structures Congress: Crossing Borders, Vancouver.

Starossek, U. (2009). “Progressive Collapse of Structures”, 1st edition, Thomas Telford Limited, London.

Starossek, U., (2007). “Typology of progressive collapse”, Engineering Structures, Vol. 29, No. 9, pp. 2302–2307.

Tamakoshi, T., Yoshida, Y., Sakai, Y., and Fukunaga, S. (2006). “Analysis of Damage Occurring in Steel Plate Girder Bridges on National Roads in Japan.” Public Work Research Institute of Japan.

Wardhana, K., and Hadipriono, F. (2003). “Analysis of Recent Bridge Failures in the United States.” J. Perform. Constr. Facil., ASCE, Vol.17, Issue 3, pp.144-150.

Wisniewsky, D.F., Casas, J.R., and Ghosn, M., (2006). “Load-capacity evaluation of existing railway bridges based on robustness quantification”, Structural Engineering International, Vol. 16, No. 2, pp. 161–166.

3. Experimental Study on Redundancy Evaluation of Simply Supported Composite Twin I-Girder Bridges in Fracture Condition

3.1 Introduction

The large number of old bridges and rapid increase in traffic has led to concerns over bridge safety in Japan as well as other parts of the world. In Japan, it has been reported that around 10,000 bridges on the national highway and major expressways will have been in service for over 50 years by 2016, and this number is expected to double in the next five years as shown in **Fig.3.1** (Fujino, 2006; Takeshi, 2006). Meanwhile, in the United States, 503 bridge collapse cases were confirmed between 1989 and 2000, among which 18.3% were caused by overload, deterioration, and fatigue of steel members (Wardhana et al., 2003; Deng et al., 2016). Also in Japan, bridge members damage and fracture cases were reported on the girder bridge structure (Tamakoshi et al., 2006). Owing to the large number of old steel bridges, fatigue has emerged as a major reason for member fractures, which critically affect the load-carrying capacity and safety of the bridges.

In general, the fracture of steel members can be caused by many factors, among which fatigue cracking is probably the most common cause in modern steel bridges, especially in welded steel bridges. In engineering practice, there are several examples of fatigue-induced member fractures in steel bridges. A 7-ft long vertical crack was confirmed in the web of the Interstate 95 Brandywine River Bridge; the crack originated from weld defects at the intersection between the fillet welds connecting the longitudinal stiffeners to the girder web and the butt welds made for transverse splices in the longitudinal stiffeners (Haghani et al. 2012). In 2006, a crack originating from the web and lateral beam connection was observed in the main girder of Yamazoe Bridge (steel-concrete composite bridge) in Japan (Kakiichi et al., 2011). At nearly the same time, a diagonal member of a steel truss bridge on a national highway in Japan was fractured owing to fatigue after initial corrosion of the steel member (Lin et al. 2013). Such examples clearly indicate that fatigue-induced cracking is a serious problem in steel structures. Therefore, the post-fracture behavior of such structures needs to be investigated to ensure their safety, serviceability, and maintainability.

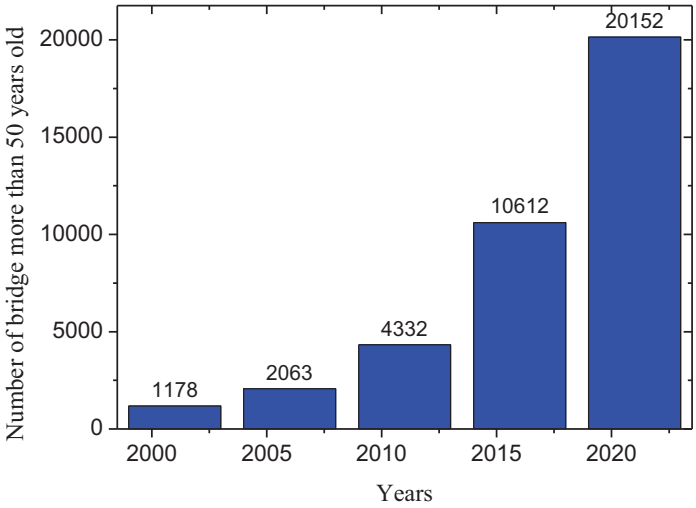

Fig.3.1 Number of bridge more than 50 years old in Japan (Fujino, 2006)

Fig.3.2 Fracture of the Interstate 95 Brandywine River Bridge (Haghani et al., 2012)

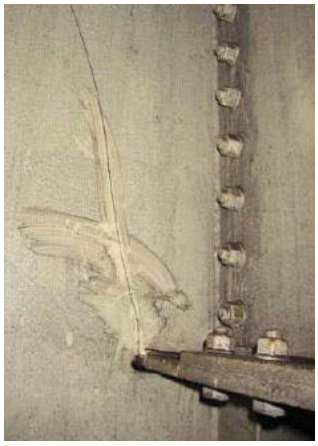

Fig.3.3 Fracture of Yamazoe Bridge (Kakiichi et al., 2011)

In Japan, the number of twin I-girder bridges has been significantly increasing in comparison with other bridge types in recent twenty years (Nagai, 2006). Despite being classified as fracture critical (AASHTO, 2012), several past experiences have shown that composite twin I-girder bridge systems do not collapse even after the severe fracture occurs on one of the main girder section (Daniels et al., 1988). This is due to the effect of concrete slab in three-dimensional space which is served as an alternative load path in redistributing the load from one girder to the other girder in the twin I-girder bridge system under fracture condition (Lam et al., 2014).

Thus far, most of the existing literatures are concerned with the performance of the bridge in the damaged or fracture condition. A study based on a field test on a three-span continuous two girder steel bridge (I-40) in fracture condition concluded that the cantilever action against the interior supports after the fracture occurred is the main reason that the bridge can redistribute the load in the damaged system (Idriss et al., 1995). Another experimental study on the composite twin I-girder bridge which focuses on effect of secondary member concluded that the use of bottom cross bracing can significantly increase the redundancy level of the composite twin I-girder bridge systems (Park et al., 2012). Laboratory experiments or field tests have been rarely conducted to compare the pre- and post-fracture mechanical behavior and safety of composite twin I-girder bridges in the fatigue crack condition. With this background, the present study involves an experimental program, including pre- and post-fracture conditions, carried out to investigate the performance and safety of a composite twin I-girder bridge system in fatigue induced crack condition. Meanwhile, the effect of the fracture on the performance and redundancy of the composite twin I-girder bridge systems is discussed.

3.2 Experimental Program

3.2.1 Test specimens

Two test specimens of composite twin I-girder bridges were fabricated including one intact specimen and one damaged specimen. The intact specimen, hereafter called Specimen-1, is used for investigating the behavior and response of the bridge without any damage. The damaged specimen, hereafter called Specimen-2, is used for investigating the behavior and response of the bridge after fracturing of full web and bottom flange, which had been imposed on one of the two main girders at the mid-span section. In both specimens, girder-1 pays attention to the main girder side subjected to loading and girder-2 pays attention to the other main girder side without any loading application. The overviews of Specimen-1 and Specimen-

2 are shown in **Fig.3.4** and **Fig.3.5**, respectively. The dimensions of the two specimens are identical. There is no damage imposed on the Specimen-1. For Specimen-2, as mentioned above, artificial fracture of full web and bottom flange had been imposed on mid-span section of girder-1 before loading were performed as can be seen at the bottom left corner of **Fig.3.5**.

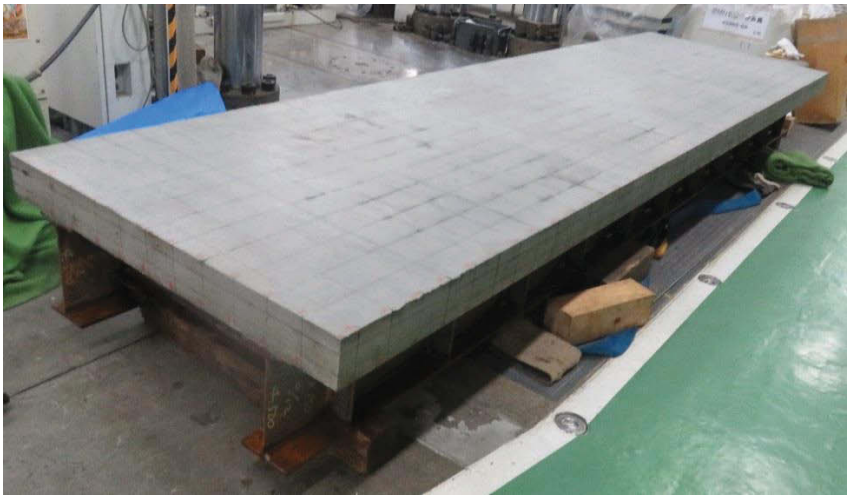

Fig.3.4 Overviews of Specimen-1

Fig.3.5 Overview of Specimen-2

Two row of shear stud connectors with the diameter of 19mm and the height of 80 mm were employed on top of the flanges of the main girders to achieve composite action between the concrete slab and steel girders as shown in **Fig.3.6**. The dimensions of the cross sections of the test specimens are shown in **Fig.3.7(a)**. Full connection design was employed according to the Japanese Specifications to obtain full composite condition between main steel girders and concrete slab (JSCE, 2007). The dimensions of stud connectors are shown in **Fig.3.7(b)**, and their arrangement can be seen in **Fig.3.7(d)**. The dimensions and positions of vertical stiffeners and transverse beams are shown in **Fig.3.7(b)** and **Fig.3.7(c)**. To comply with JRA specifications for reinforcement concrete of bridge structures, two layers of reinforcement are installed in the slab (JRA, 2002). As shown in **Fig.3.7(e)**, reinforcing bar type SD345 with 10 mm in diameter are used with the 100 mm spacing for both longitudinal and transversal directions.

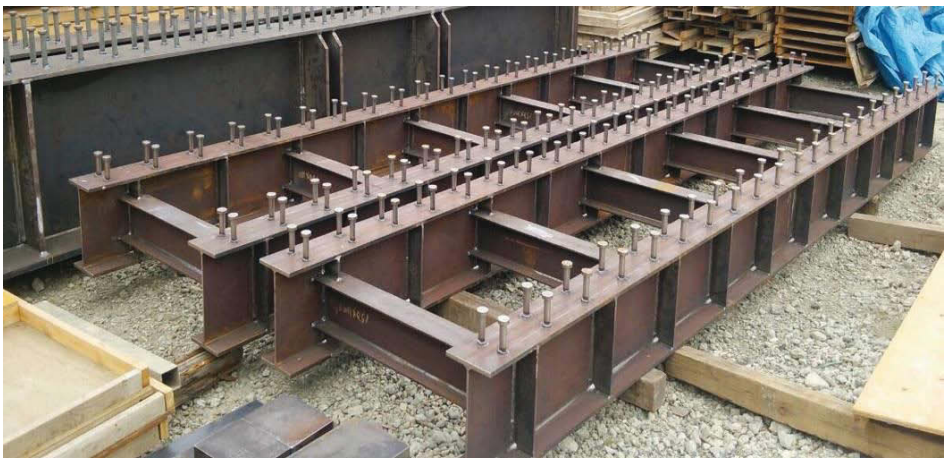

Fig.3.6 Main Girders, transverse beams, and stud arrangement of test specimens

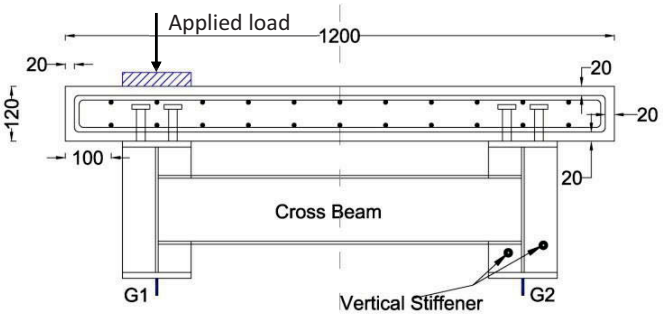

(a) Cross section

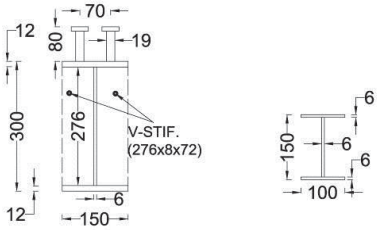

(b) Detail of main girder, crossbeam and stud

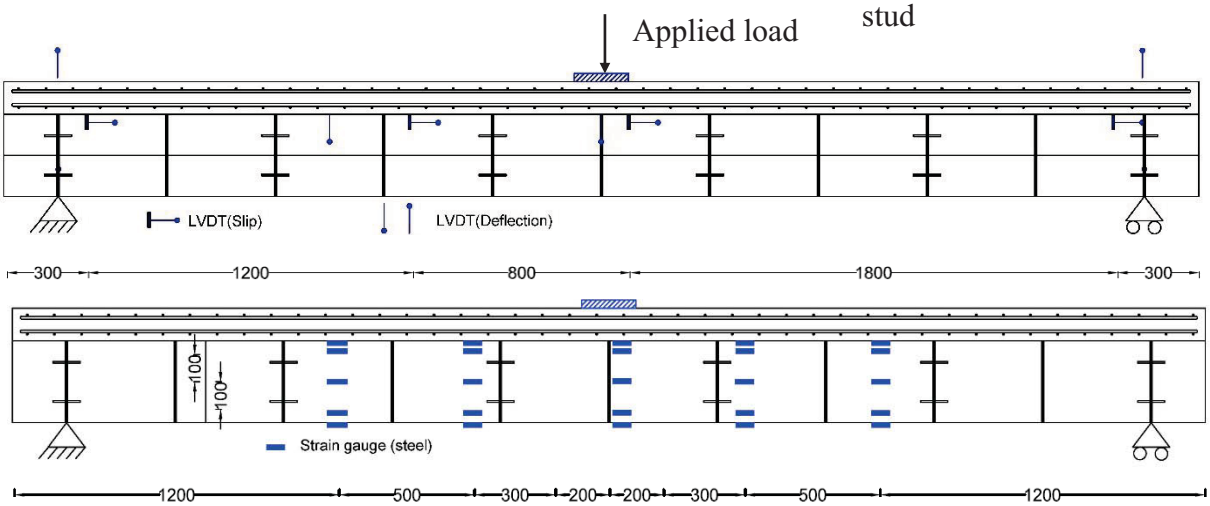

(c) Side view of test specimens

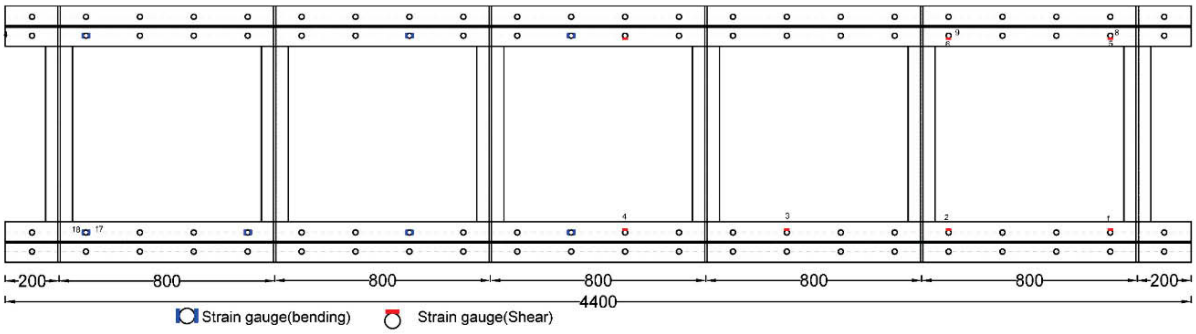

(d) Top view of steel girder

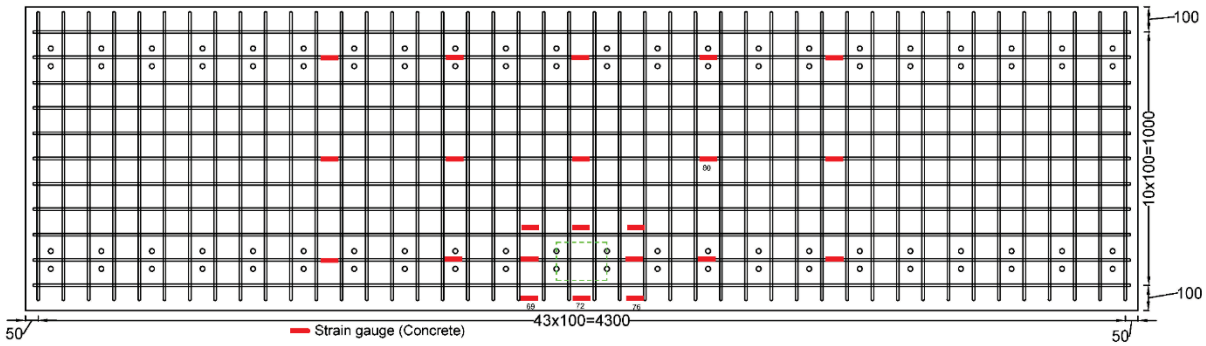

(e) Layout of reinforcement

Fig.3.7 Configuration of test specimens

3.2.2 Instrumentation

Strain gauges were used to measure the strain at various location of the specimens during loading test. **Fig.3.8** shows the strain gauges attached to the steel girders, reinforcing bars, and concrete slab, respectively. The location of the strain gauges attached on the main steel girders is shown in **Fig.3.7(c)** and **Fig.3.7(d)**. The location of the strain gauges attached on the concrete slab is shown in **Fig.3.7(e)**. Linear Variable Displacement Transducers (LVDTs) were used for measuring the deflections, out of plane displacement, and slip between steel girder and concrete slab as shown in **Fig.3.9(a)**, **Fig.3.9(b)**, and **Fig.3.9(c)**, respectively. The location of the LVDTs attached on the test specimens is shown in **Fig.3.7(c)**.

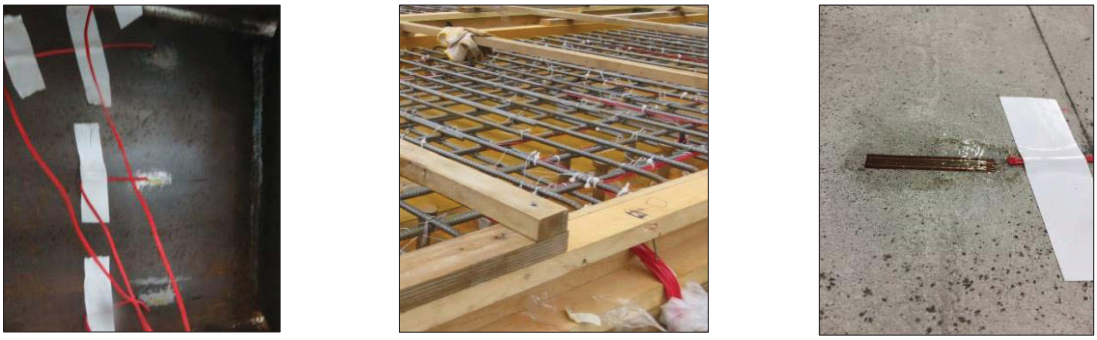

(a) steel (b) reinforcing bars (c) concrete slab

Fig.3.8 Strain gauges attached on steel, reinforcing bars, and concrete slab

(a) Vertical displacement (b) Out of plane displacement (c) Interface slip

Fig.3.9 Arrangement of LVDTs for measuring vertical displacement, out of plane displacement, and interface slip

3.2.3 Material properties

(a) Concrete

Cylinder concrete specimens were prepared when casting the concrete slab. The design compressive strength of the concrete specimen is 27 MPa. The mean compressive strength obtained from the three cylindric specimens from laboratory testing at 28th days is 33.5 MPa. The mix proportion of concrete and compression test results at 7th day and at 28th day is provided in **Table.3.1**.

Table.3.1 Property of the concrete specimens

Test specimen	Concrete Type	Design Strength (MPa)	Aggregate size (mm)	Slump (mm)	Water content (kg/m^3)	Air (%)	Unit salinity (kg/m^3)	7th day strength (MPa)	28th day strength (MPa)
1								23.3	34.1
2	Normal	27	≤ 20	90	166	4.7	0.057	22.8	33.5
3								24.3	33.0
Average								23.5	33.5

(b) Structural steel and reinforcing bar

According to the welding requirement, construction steel SM490 was used for the main girders, transverse beams, and the stiffeners. The reinforcing bar used in the slab is type SD345. The details of the materials properties are shown in **Table.3.2**.

Table.3.2 Materials properties of steel and reinforcing bar

Material	Yield Strength (MPa)	Ultimate Strength (MPa)
Steel Plate (6 mm)	450	577
Steel Plate (8 mm)	427	556
Steel Plate (12 mm)	389	548
Reinforcing bar (D10)	406	544

3.2.4 Test setup and loading conditions

The loading test was performed at the structural laboratory of Waseda University. The loading machine has the maximum capacity of 5000 kN. In the static load test, displacement control method was employed. The one-point load is imposed on girder-1 for both specimens to create the most critical loading condition (uneven loading condition) in a multi-girder bridge system (Hendawi and Frangopol, 1994). The loading point is set in the mid-span section of the damaged girder (girder-1) to produce the most critical scenario for the damaged specimen (Specimen-2) as shown in **Fig.3.10**. For the boundary conditions, a pinned support was used at one end, and a roller support was used at the other end.

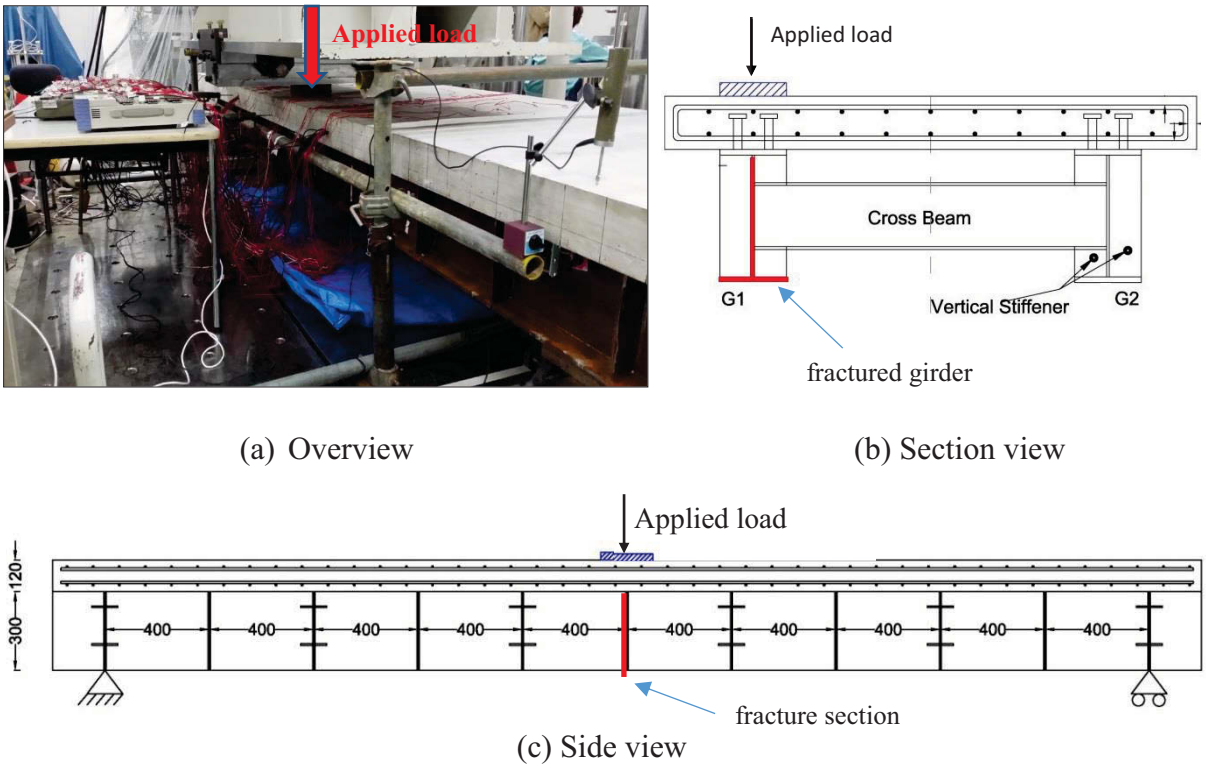

(a) Overview (b) Section view

(c) Side view

Fig.3.10 Loading condition

3.2.5 Damaged conditions

Fracture of steel members is commonly developed from the fatigue crack. A fatigue crack is the results of cracks originating from the microscopic flaws in steel plates, such as defects in welds or notches and dents. Such a crack will slowly grow under the effect of live load (cyclic load). The entire process of fatigue failure can be classified into three main phases: the crack initiation phase, the sub-critical crack propagation phase, and the fracturing phase (ASCE Committee on Fatigue and Fracture Reliability, 1982). In general, in the initiation phase, the

fatigue crack cannot be detected using the existing inspection and fracture control methods. For decades, efforts have been devoted toward ensuring that fatigue cracks can be found and repaired during the sub-critical crack propagation phase; however, fractures of steel members resulting from fatigue crack continue to occur. For I-girder steel-concrete composite sections, the fatigue crack commonly starts at the bottom flange or web near the weld defect area between the stiffener and the main girder. Such a crack then propagates on the web through the entire bottom flange, resulting in fracture of the bottom flange and entire web. To simulate and study this behavior of composite twin I-girder bridges, the fracture of the entire web and bottom flange is simulated by a torch cut at the mid-span section. As shown in **Fig.3.11**, the fracture of whole web and bottom flange on the specimen-2 was imposed next to the welding area of the stiffener and the main girder, where fatigue cracks or fractures are frequently observed in the actual bridges.

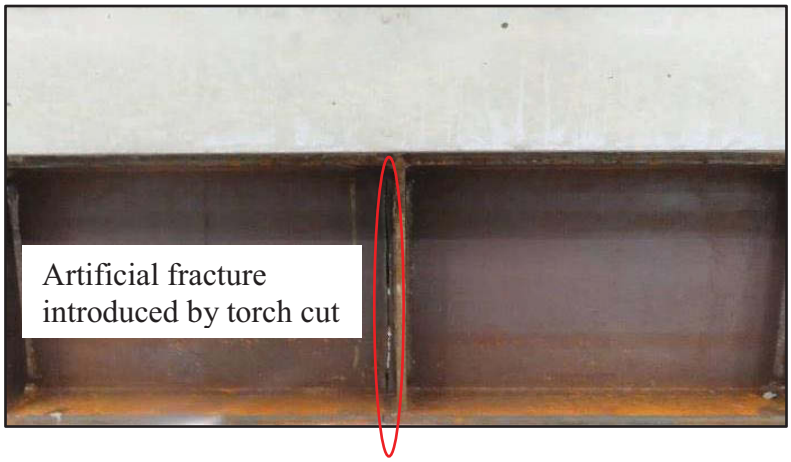

Fig.3.11 Artificial fracture imposed on the Specimen-2 (by torch cut)

3.3 Discussion of Experimental Results

3.3.1 Elastic system stiffness

Fig.3.12 shows the load-deflection curves of the Specimen-1 and Specimen-2 in the elastic stage. The line labeled K(Intact) represents the system stiffness of the intact specimen in the elastic state, and the line labeled K(Damage) represents the structural stiffness of the damaged specimen. The system stiffness of the Specimen-1 and Specimen-2 in the elastic state is presented in **Table.3.3**. The effect of the fracture on system stiffness is represented by calculating the difference between intact and damaged specimen. The ratio of the elastic system stiffness between damaged specimen and the intact specimen is found as 29 %. According to this result, the system stiffness in the elastic stage is reduced as large as 71 % after the fracture

occurs. The results from experimental programs clearly indicate a significant reduction of system stiffness between damaged bridge system and intact bridge system. It can be concluded that after fracture of full web and bottom flange occurs on the mid-span section of the simply supported composite twin I-girder bridge, a large decrease of system stiffness is expected and may lead to large deflection under a certain loading level. In this sense, the bridge may become out of service due to the large deformation resulting from the fracture of the whole web and bottom flange.

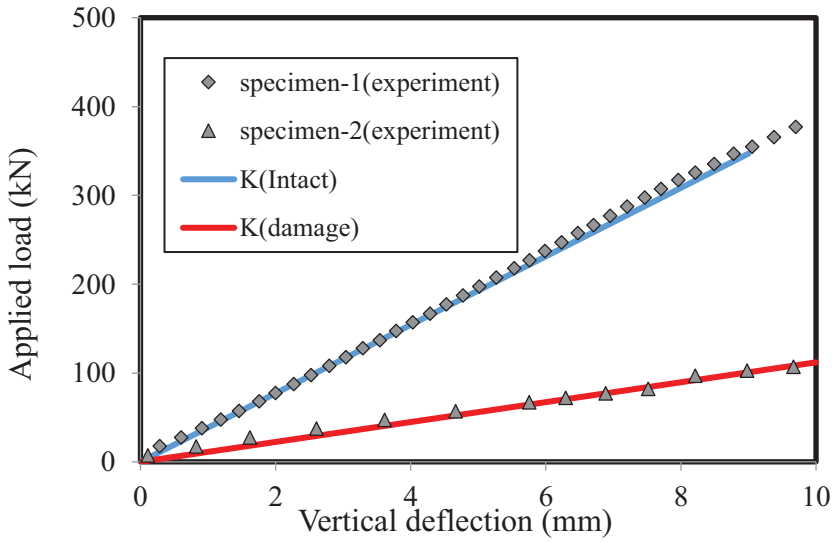

Fig.3.12 Load-deflection curves in the elastic state (mid-span section)

Table.3.3 Elastic system stiffness and load carrying capacity of the test specimens

	Elastic system stiffness (K)
Specimen-1	38.50 kN/mm
Specimen-2	11.20 kN/mm
Ratio (Damage/Intact)	29%
Reduction	71%

3.3.2 Load deflection responses at mid-span section

Fig.3.13 shows the load-deflection curves at the mid-span section of girder-1 for Specimen-1 and Specimen-2. For the Specimen-1, the first yield point is determined as the minimum applied load corresponding to the yield point of the steel or the yield point of the reinforcing bars. For the specimen-1, the data from strain gauge indicated that the bottom flange steel firstly reaches the yield point at 426kN before the reinforcing bar. At 580 kN, the crush of the concrete slab at the loading point is observed and the applied load slightly declined to 560 kN. This failure is concluded as a local failure because the applied load could steadily

increase with the increment of the displacement (displacement control was used during the loading test). The crack pattern from the bottom of the test specimen as shown in **Fig.3.14(a)** indicated that this local failure is resulted from the punching shear due to the stress concentration at the loading point. As the loading continue the concrete slab reaches its ultimate limit state, and the crush of the concrete slab can be observed from the side view of the test specimen at 668kN as shown in **Fig.3.15(a)**. The loading was stopped at this point with the ultimate load determined as 668 kN.

For the Specimen-2, the results from experimental programs clearly indicate a significant reduction of system stiffness as well as load carrying capacity due to the fracture of web and bottom flange at the mid-span section. The ultimate load of the Specimen-2 is determined as 275 kN when a large part of the concrete slab crush and can be observed from the side view during the loading test as shown in **Fig.3.15(b)**. Although no local failure can be detected during the loading phase, the local failure similar to Specimen-1 (punching shear) was confirmed by observing the crack pattern from the bottom of the test specimen as shown in **Fig.3.14(b)**. The load carrying capacity of the specimen after fracture is reduced as large as 59% as shown in **Table.3.4**. Both intact and damaged specimen show a similar failure pattern which is the combination of bending moment and torsional moment caused by unsymmetrical loading condition.

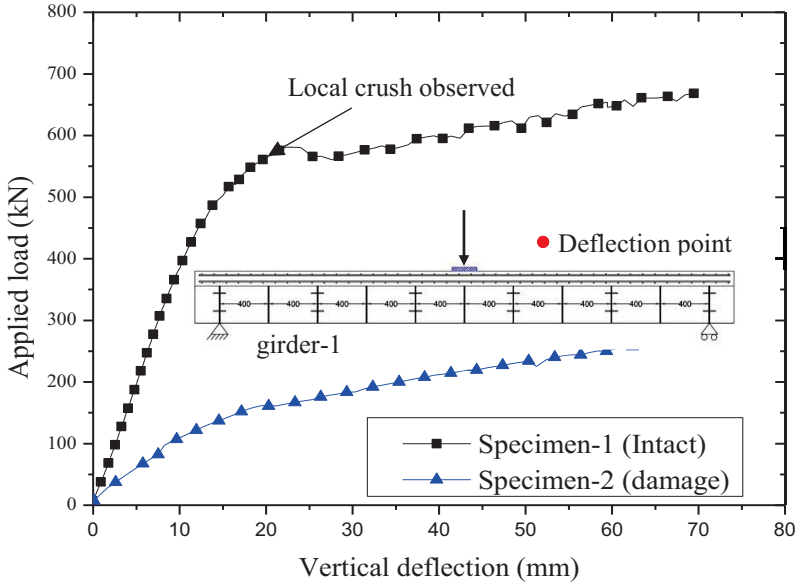

Fig.3.13 Load-deflection curves of Specimen-1 and Specimen-2 at the mid-span section

(a) Specimen-1 **(b)** Specimen-2

Fig.3.14 Crack pattern of concrete slab resulted from punching shear (bottom view)

(a) Crush of the concrete of Specimen-1

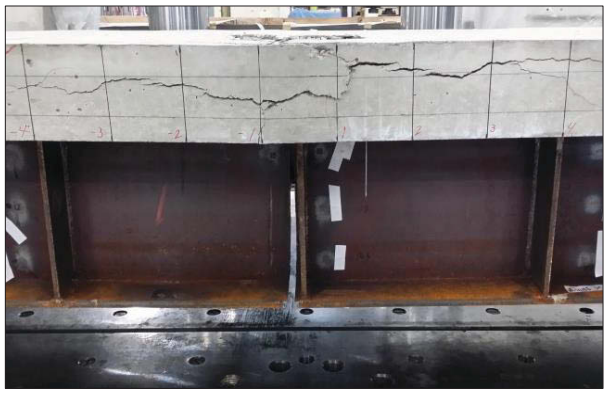

(b) Crush of the concrete of Specimen-2

Fig.3.15 Failure mode of the test specimens

Table.3.4 Load carrying capacity of the test specimens

	Load carrying capacity
Specimen-1	668 kN
Specimen-2	275 kN
Ratio (Damage/Intact)	41 %
Reduction	59 %

3.3.3 Load-strain curves of main girders

(a) Load-strain curves of steel girders at mid-span section

Strain gauges were attached to the bottom flange at the mid-span section to measure the maximum tensile strain of the steel strain of girder-1 and girder-2 during the loading test as shown in **Fig.3.16** for both specimens. For the Specimen-1, the yield point of the steel is determined as 426 kN when the strain of the bottom flange reaches 1945 μ as shown in **Fig.3.17(a)**. At the ultimate load governed by the crush of the concrete slab, the strain of the steel reaches almost 4.5%, and neither buckling nor obvious out of plane displacement is observed. The intact specimen is classified as a ductile section. For the Specimen-2, due to the fracture of the web and bottom flange, the girder-1 acts like those of cantilever system and the strain of the bottom flange near mid-span section is relatively small (almost zero) comparing to the intact specimen as can be seen in **Fig.3.17(b)**.

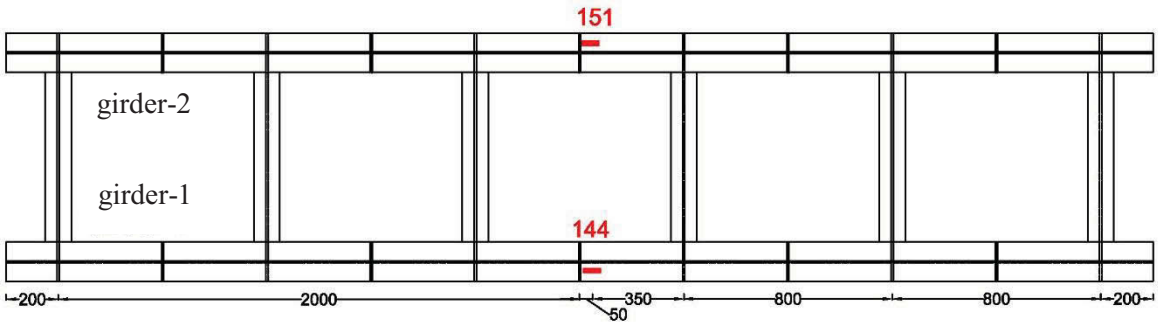

Fig.3.16 Location of strain gauge attached to the bottom flange of steel girders

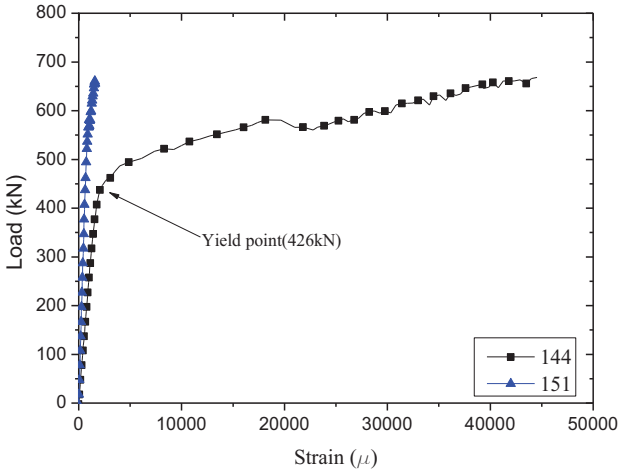

(a) Specimen-1

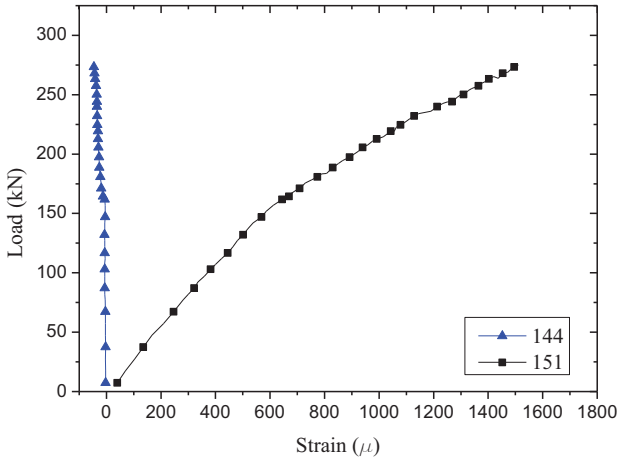

(b) Specimen-2

Fig.3.17 Load-strain curves at the bottom flange of the mid-span section

(b) Characteristic of load redistribution in the composite twin I-girder bridge system

The behavior of load redistribution of the composite twin I-girder bridge system during loading test was measured by the strain gauges attached to the flanges and web of the girder-2. As shown in **Fig.3.18** and **Fig.3.20**, three of the strain gauges located at the bottom flange and three strain gauges located near the bottom part of the web from girder-2 is selected as study target. The load-strain curves of the selected strain gauges from the bottom flange and Web of the girder-2 are shown in **Fig.3.19** and **Fig.3.21**. For the Specimen-1, as shown in **Fig.3.19 (a)** and **Fig.3.21 (a)**, before the yield load of Specimen-1, the strain of the test specimen increases linearly with the loading. Beyond this yield point, the strain of the girder-2 largely increases despite being still in the elastic state. This behavior proved that after the girder-1 reach plastic zone, more percentage of applied load is redistributing from girder-1 to girder-2 by the secondary member and the concrete slab. For the Specimen-2, as shown in **Fig.3.19 (b)** and

Fig.3.21 (b), the strain of the girder-2 begin to rapidly increase after a certain load level (around 160 kN). Torsional strength of the section is one of the main factors that contribute to this behavior. For both specimens, the results indicate that larger portion of the load is transferred from girder-1 to the girder-2 in the post-elastic stage or after a certain level of deflection.

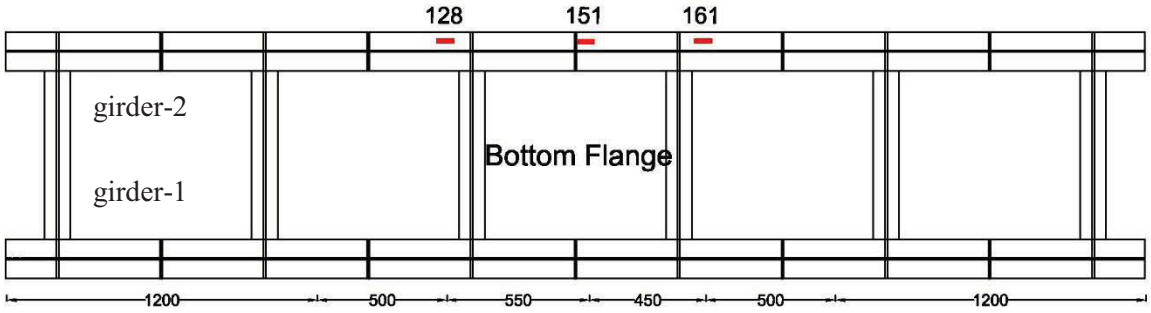

Fig.3.18 Strain gauge attached on the bottom flange of girder-2

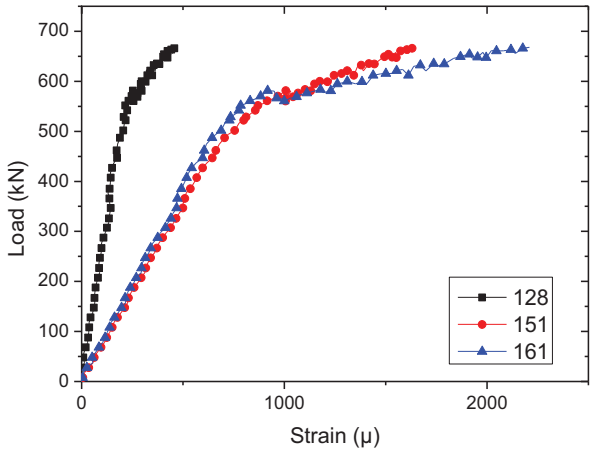

(a) Specimen-1

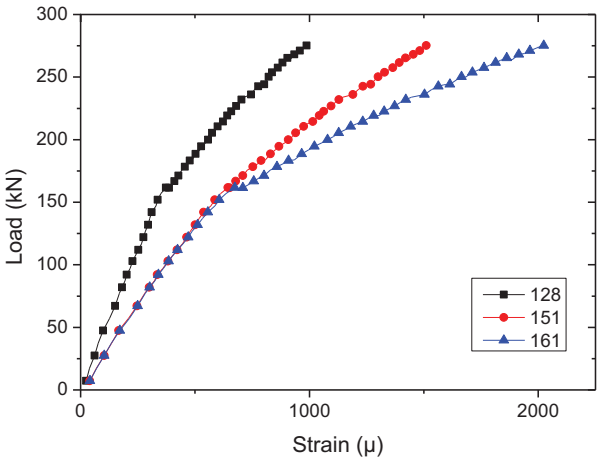

(b) Specimen-2

Fig.3.19 Load-strain curves of the bottom flange (girder-2)

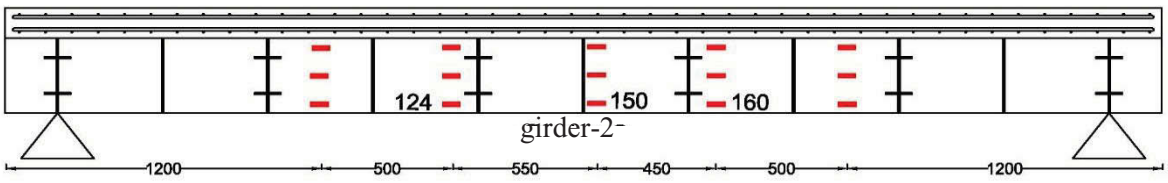

Fig.3.20 Location of strain gauge attached on the Web

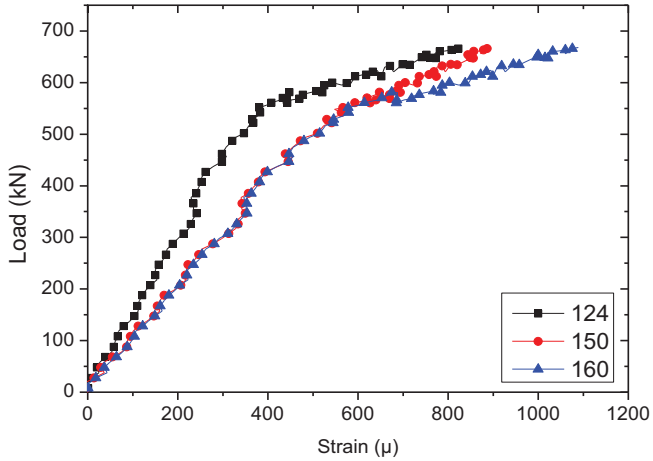

(a) Specimen-1

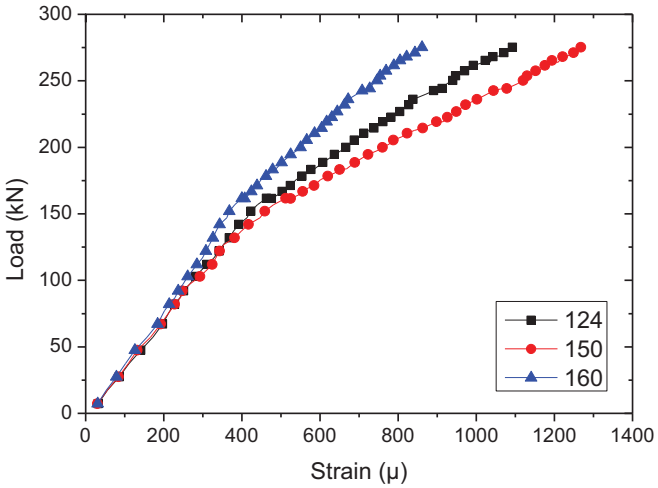

(b) Specimen-2

Fig.3.21 Load-strain curves of the web (girder-2)

3.3.4 Load-strain curves of reinforcing bars

Several of strain gauges were attached to the longitudinal and transversal reinforcing bars before casting of the concrete slab to measure the strain of the rebar during the loading test as shown in **Fig.3.22**. The gauges were attached at the same location for both specimens. For the longitudinal reinforcing bars, one gauge was attached to the top reinforcing bar and one gauge was attached to the bottom reinforcing bar at the same cross section. For the transversal reinforcing bar, the strain gauge was attached to the top reinforcing bar as shown in **Fig.3.22**.

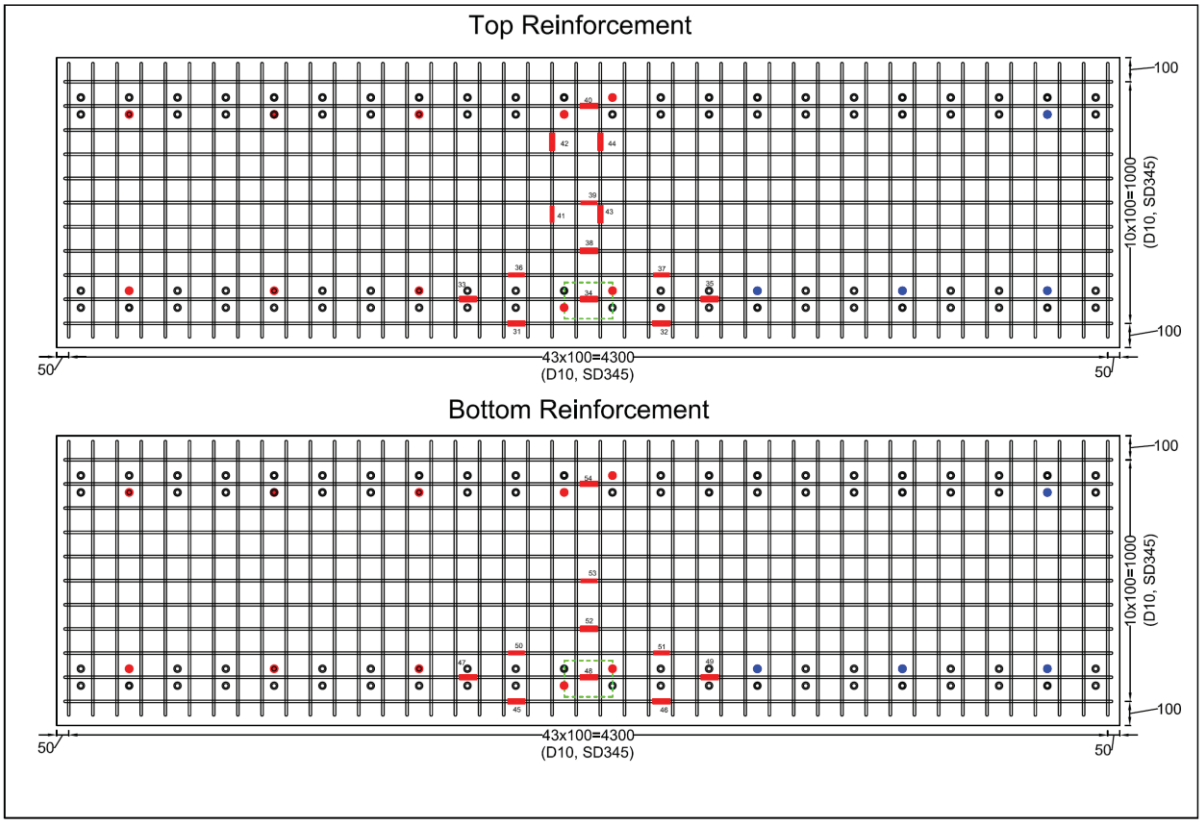

Fig.3.22 Strain gauge location attached to the reinforcing bars

(a) Load-strain curves of the longitudinal reinforcing bars for specimen-1

The load-strain curves of the longitudinal reinforcing bar for the Specimen-1 were shown in **Fig.3.23**. The positive strain data represents the tension strain while the negative strain data represent compression strain. A few strain gauges were broken before the loading test due to the concreting process including gauges CH040, CH052, and CH053. As mentioned, the local failure of the concrete slab is observed at 580kN for Specimen-1. Before the local failure occurs, the concrete slab is subjected to compression as indicated by the strain gauges data. The reinforcing bars are still in the elastic state before the first yield of the test specimen that is governed by the yielding of the bottom flange. After the first yield, the neutral axis of the mid-span section moved upward as indicated by the load-strain curve of the CH034 and CH048 at mid-span section. After the local failure at 580 kN, the behavior is becoming complicated due to the bond slip between the concrete slab and reinforcing bar affected by the local failure, especially near the loading section. The ultimate failure of the concrete at the ultimate load of 668kN can be confirmed by the compression strain of the reinforcing bar CH038 which is located at the loading section.

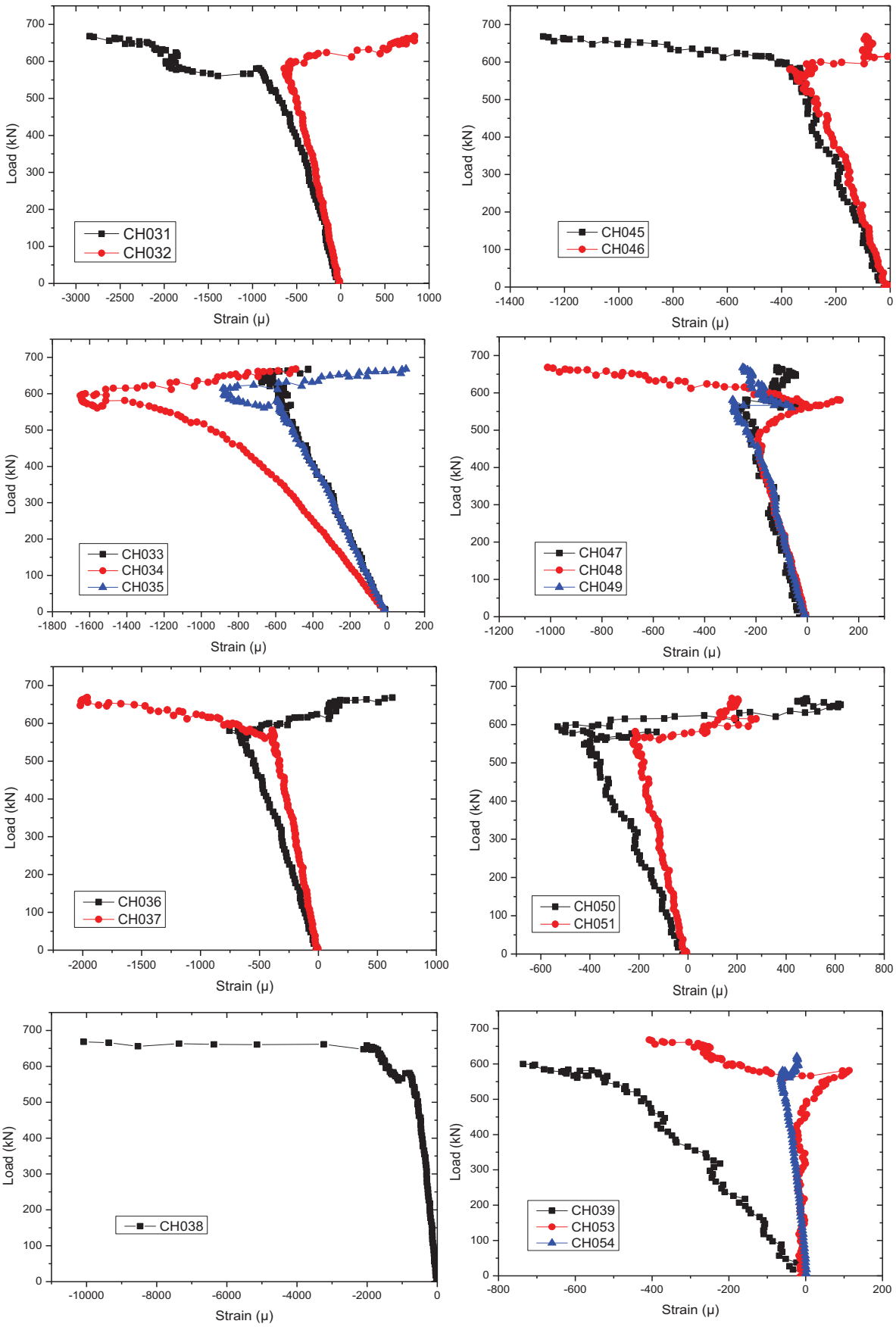

Fig.3.23 Load-strain curves of longitudinal reinforcing bars (Specimen-1)

(b) Load-strain curves of the longitudinal reinforcing bars for specimen-2

The load-strain curves of the longitudinal reinforcing bar for the Specimen-2 were shown in **Fig.3.24**. Gauge CH052 was broken before the loading test due to the concreting process. While the concrete slab is subjected to the compression for the specimen-1, the strain results in specimen-2 indicated that the top reinforcing bars are subjected to compression while the bottom reinforcing bars are subjected to tension resulted from the fracture of the web and bottom flange of the steel girder. Furthermore, the load corresponding to local failure of the concrete slab at the loading point can be detected based on the load-strain curves of the reinforcing bars. As shown in **Fig.3.24**, most of the curves indicated that the local failure occurs at 160kN. This local failure, which is governed the punching shear, results in the break of the bond of the reinforcing bar and concrete slab near the loading section.

(c) Load-strain curves of the transversal reinforcing bars

As shown in **Fig.3.24**, four strain gauges were attached to the top transversal reinforcing bar. Unfortunately, for the specimen-1, gauge CH043 was broken before the loading test. For the specimen-2, gauges CH041 and CH043 were also broken before the loading test. The load-strain curves of the top transversal reinforcing bars for Specimen-1 and Specimen-2 are shown in **Fig.3.25** and **Fig.3.26**, respectively. The results further justified that the load redistribution in composite twin I-girder bridge system become more effective with the increment of the applied load and deflection. However, the behavior of the transversal reinforcing bars after the local failure of both specimens are irregular due to the break of the bond between reinforcing bars and concrete slab.

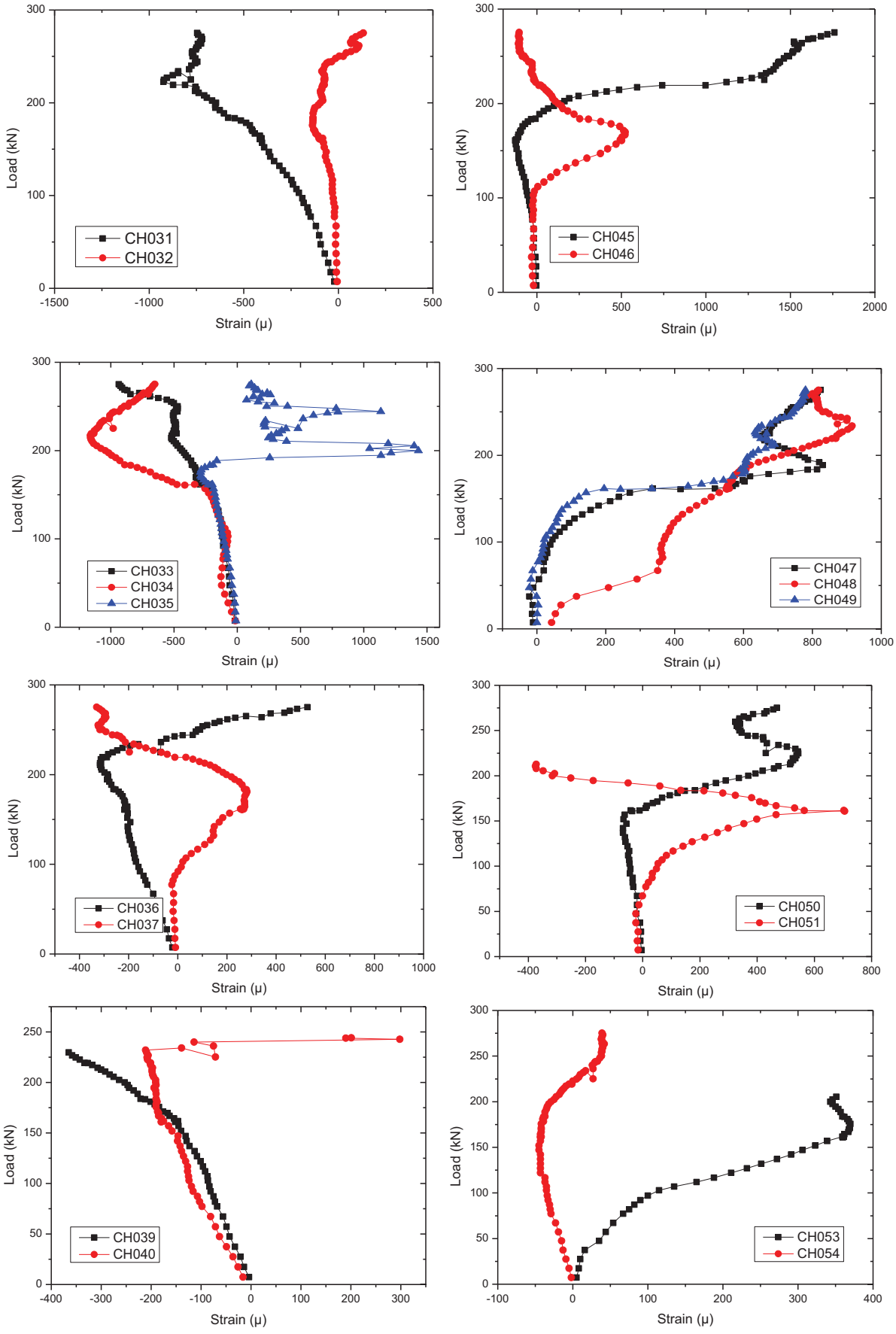

Fig.3.24 Load-strain curves of longitudinal reinforcing bars (Specimen-2)

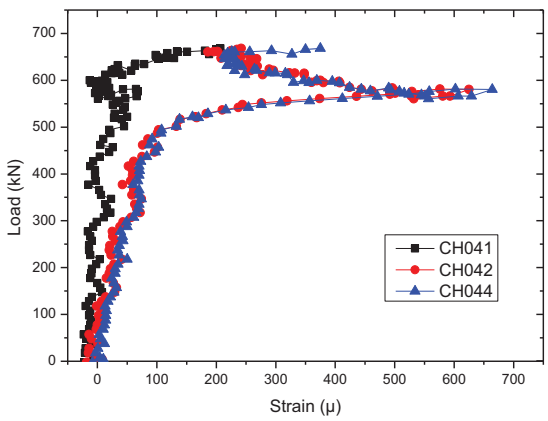

Fig.3.25 Load-strain curves of transversal reinforcing bars (Specimen-1)

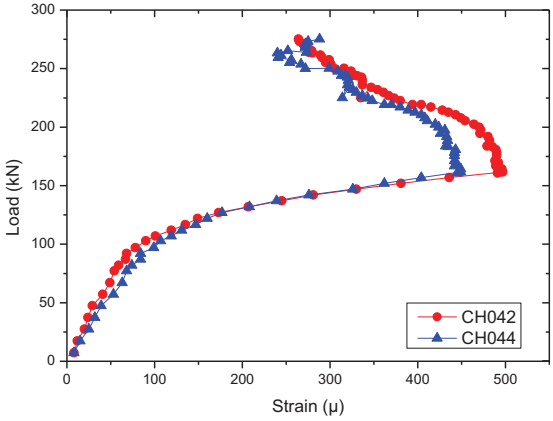

Fig.3.26 Load-strain curves of transversal reinforcing bars (Specimen-2)

3.3.5 Load-strain curves of the concrete slab

Several strain gauges were attached to the top surface of concrete slab to measure the strain of concrete as shown in **Fig.3.27**. The gauges were attached at the same location for both Specimen-1 and Specimen-2 to investigate the behavior of the concrete slab in pre- and post-fracture conditions. **Fig.3.28** shows the load-strain curves of the concrete slab at different locations for Specimen-1. The data further justified the local failure of the concrete slab at 580 kN. **Fig.3.29** shows the load-strain curves of the concrete slab at different locations for Specimen-2. The data further justified the local failure of the concrete slab at 161 kN.

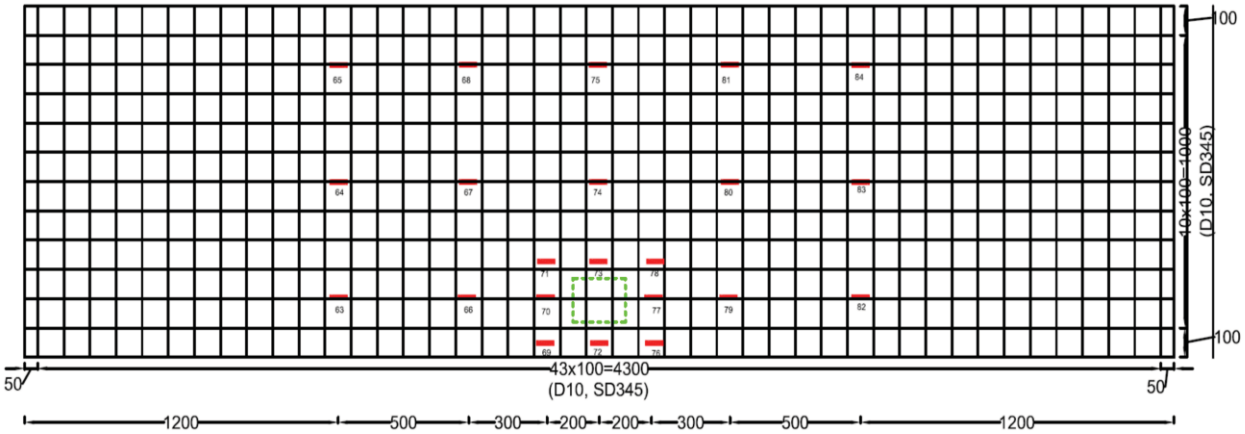

Fig.3.27 Strain gauge locations attached to the top surface of concrete slab

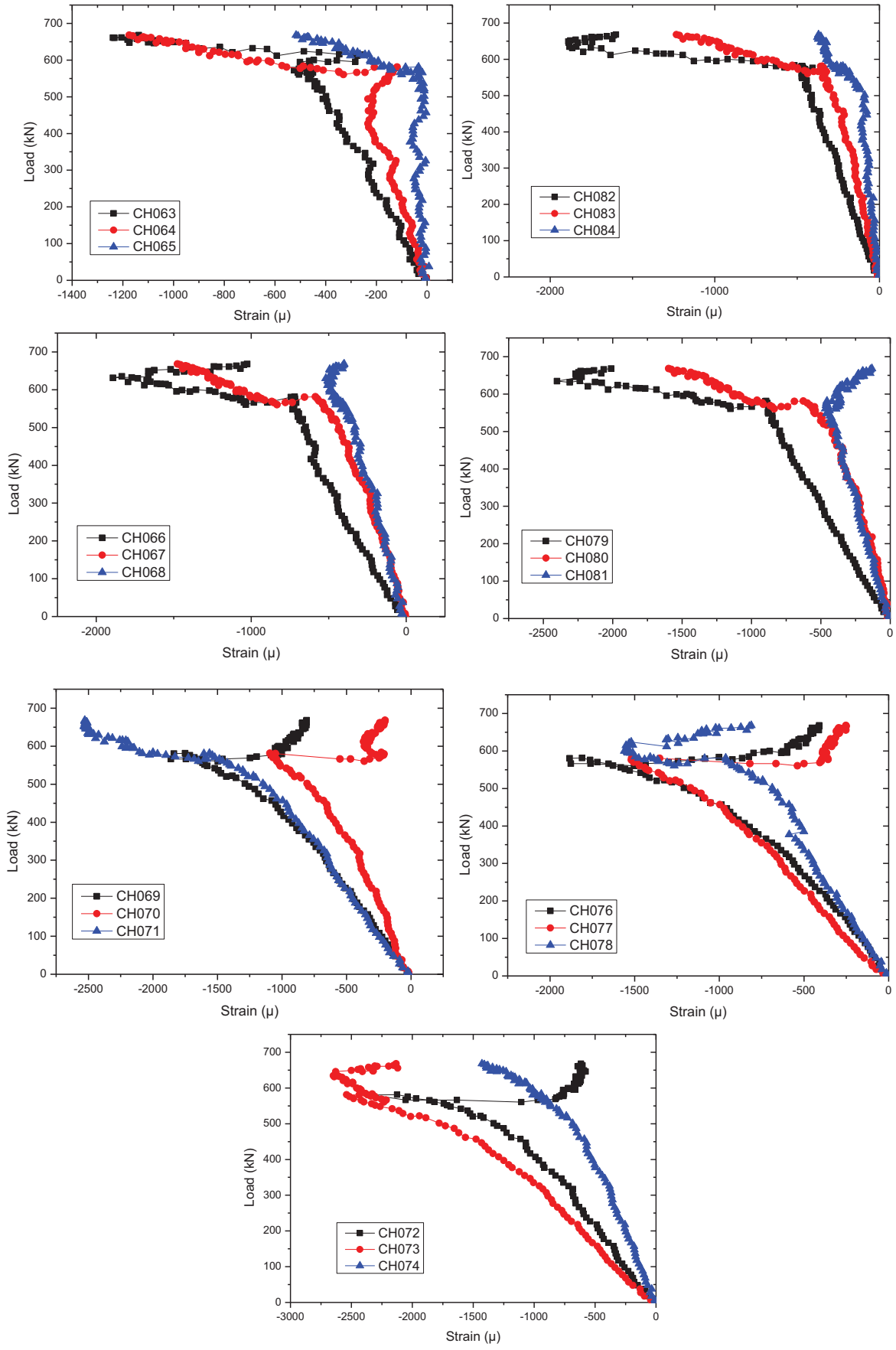

Fig.3.28 Load-strain curves of concrete slab (Specimen-1)

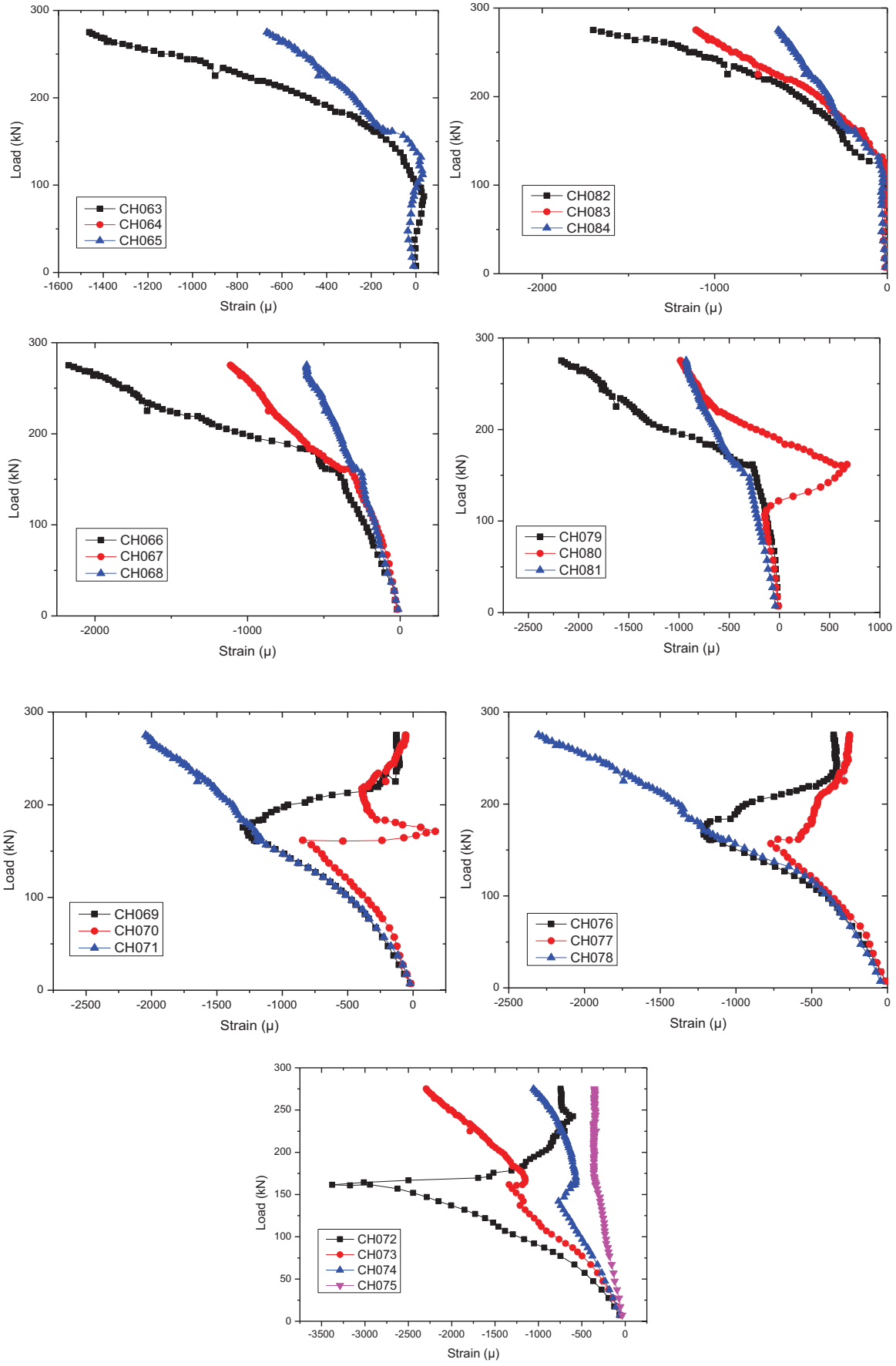

Fig.3.29 Load-strain curves of concrete slab (Specimen-2)

3.3.6 Performance of shear stud in pre- and post-fracture condition

For the steel-concrete composite twin I-girder bridge system, the shear studs play an important role in guaranteeing the composite behavior between the deck and the main steel girders. The damage of the shear studs will highly affect the performance of the composite section in terms of system stiffness as well as ultimate load carrying capacity and safety level of the bridge structure. **Fig.3.30** shows the location of the strain gauges attached to the shear stud connectors during the fabrication of the test specimens. The strain gauges applied on both specimens are identical in terms of attached location and types. For girder-1, a total of 8 studs at different locations was selected to measure the strain, including four bending strain locations and four shear strain locations for both specimens. The bending strain on the stud was measured by two one-direction strain gauges attached to the stud, as shown in **Fig.3.31(a)**, and the shear strain on the stud was measured by a shear gauge attached to the stud, as shown in **Fig.3.31 (b)**. **Fig.3.32(a)** and **Fig.3.33(b)** show the shear strain distribution of the right half of girder-1 of Specimen-1 and Specimen-2, respectively. **Fig.3.32(a)** and **Fig.3.33(b)** show the bending strain distribution of the left half of girder-1 of Specimen-1 and Specimen-2, respectively. The experimental results indicated that for the intact specimen, both the shear strain and the bending strain distributions are not uniform, as can be seen in **Fig.3.32(a)** and **Fig.3.33(a)**. From the results of the intact specimen, the maximum strain occurs in the area around 1/5 of the span length. For the damaged specimen, the shear strain gauge near the support location is broken during the casting of the concrete slab. The shear strain of three studs was measured, and the results are shown in **Fig.3.32(b)**. At the same loading level, the shear strain of the stud in the damaged specimen increased significantly (more than 10 times) compared to the intact specimen. The same behavior was observed in the case of the bending strain, as shown in **Fig.3.33(b)**. This result indicates that the fracture of the web and bottom flange will result in a sharp increase in the shear stress on the shear stud near the fracture location and thus reduce the lifespan of the shear stud against fatigue significantly.

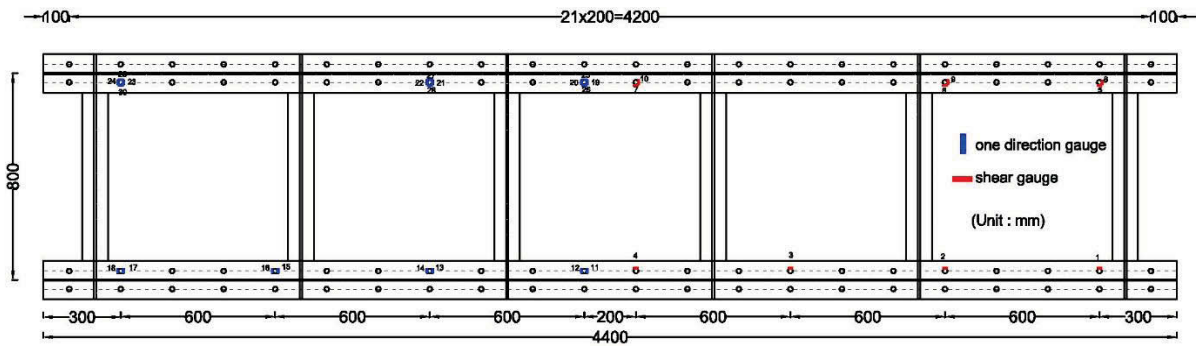

Fig.3.30 Location of strain gauges attached on the shear stud

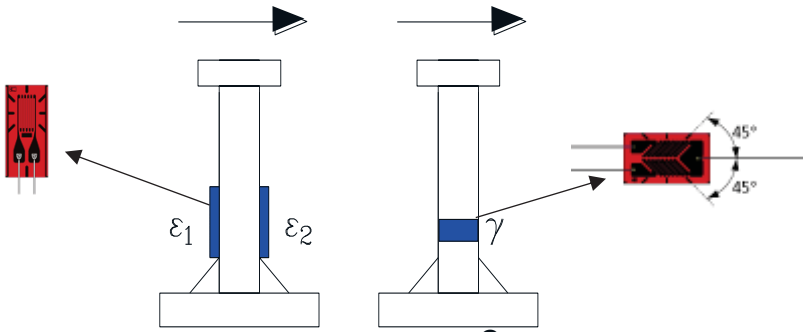

(a) One direction gauges (Bending) (b) Shear gauge (Shear)

Fig.3.31 Strain gauge patterns on the shear stud

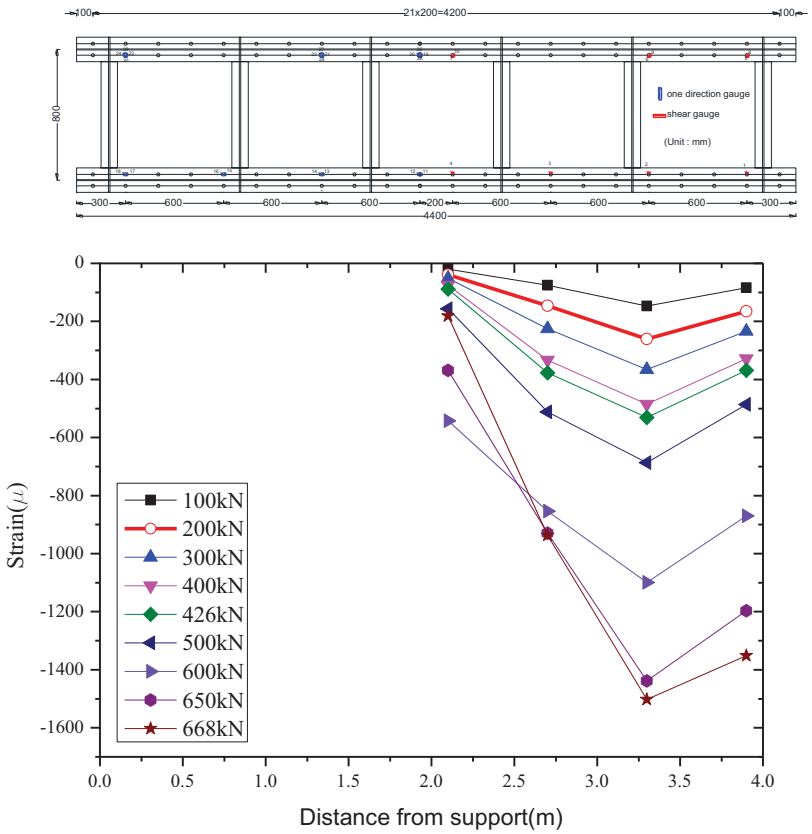

(a) Shear strain of Specimen-1

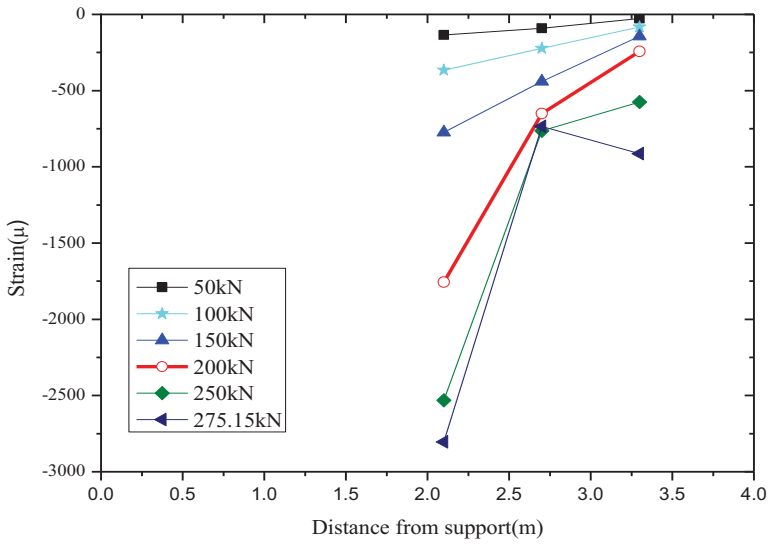

(b) Shear strain of Specimen-2

Fig.3.32 Shear strain distribution of the shear stud

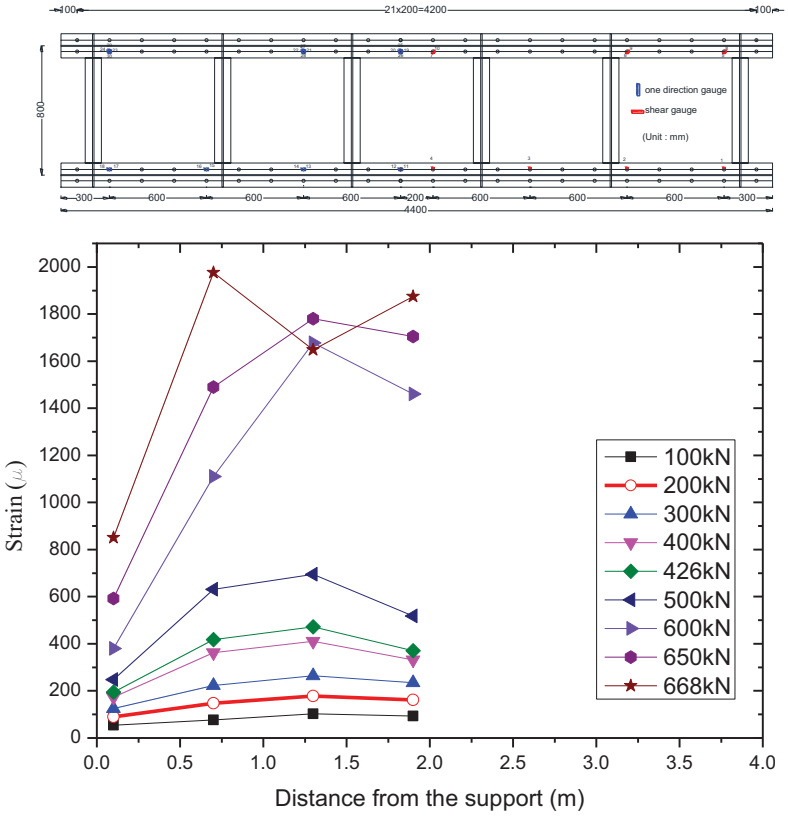

(a) Bending strain of Specimen-1

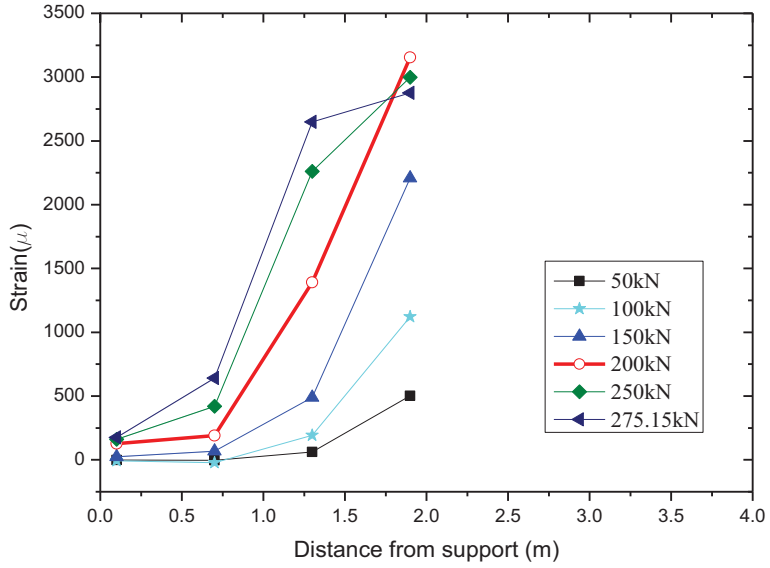

(b) Bending strain of Specimen-2

Fig.3.33 Bending strain distribution of the shear stud

3.4 Redundancy Analyses

Up to now, no specific redundancy evaluation method existed in any standard specifications (FHWA, 2012). To quantify the redundancy level of a bridge structure, the redundancy rating method proposed in the NCHRP is employed in this study (Ghosn and Moses, 1998; Ghosn et al., 2008; Liu et al., 2001; Ghosn and Yang, 2014). This method is logically direct with defined quantitative limits, does not depend on the choice of the live load model, and is based on system reliability evaluation of the bridge, whose redundancy is generally agreed upon (Hunley and Harik, 2011). The application of this method has also gained acceptance from the bridge designers and researchers in several projects (Wisniewsky et al., 2006; Lin et al., 2013; Ghosn and Yang, 2014; Lam et al., 2014; Gheitasi and Harris, 2016). Such a requirement guarantees the safety of the bridge from collapse and prevents the bridge from entering out-of-service or damaged states, but it does not guarantee that the bridge will function normally in the damaged condition. **Fig.3.34** shows the load-displacement curves of typical bridge behavior under increasing of vertical load. The curve labeled with "Intact System" represents the bridge system without any structural or elemental damage. The curve labeled with "Damage System" represents the bridge system with initial member damage. For the intact system, the load that results in first member failure or reaches design limit is defined as LF_1. LF_u is the ultimate load carrying capacity of the intact structure. Before bridge collapse, large displacements may occur at certain load level, which makes the bridge unfit for using and is defined as LF_f which corresponds to the deflection level of span-length/100 (Ghosn and Moses, 1998). For the damaged bridge, only the ultimate failure load is concerned and defined as LF_d. Finally, the redundancy factor was proposed in the following form:

$$\varphi_R = min\left(\frac{R_u}{1.30}, \frac{R_f}{1.10}, \frac{R_d}{0.50}\right) \tag{3.1}$$

$$R_u = \frac{LF_u}{LF_1} \tag{3.2}$$

$$R_f = \frac{LF_f}{LF_1} \tag{3.3}$$

$$R_d = \frac{LF_d}{LF_1} \tag{3.4}$$

where:

- φ_R : Redundancy factor of bridge system (Ghosn and Moses, 1998)
- R_u : System reserve ratio for the ultimate limit state (Ghosn and Moses, 1998)
- R_f : System reserve ratio for the functionality limit state (Ghosn and Moses, 1998)
- R_d : System reserve ratio for the damaged condition (Ghosn and Moses, 1998)

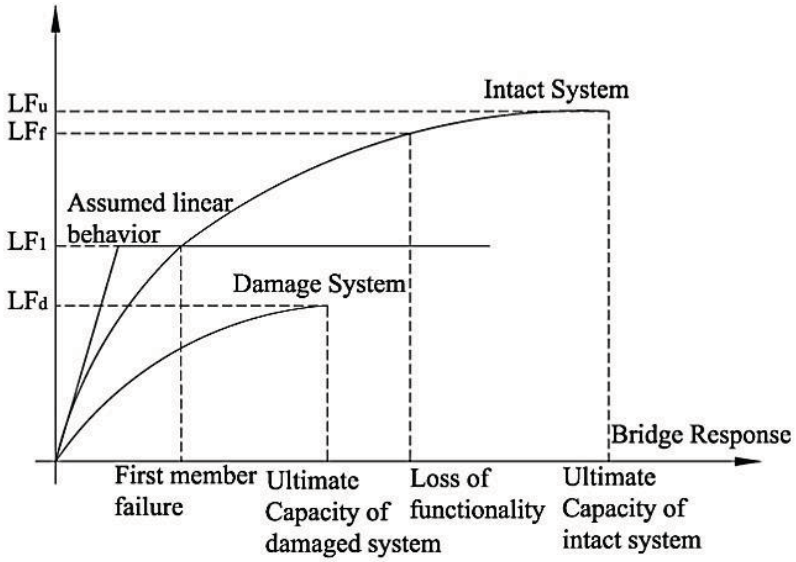

Fig.3.34 Typical behavior of bridge system (Ghosn and Moses, 1998)

By using the redundancy factor proposed in **Eq.3.1**, the redundancy level of the composite twin I-girder bridge used in this study can be evaluated based on the value of ϕ_R. A higher value of ϕ_R means a higher redundancy level of the bridge system. If $\varphi_R \geq 1$, the bridge system can be concluded as redundant bridge system. And if $\varphi_R < 1$, the bridge system is not redundant. For the specimen used in this study, LF_1 is the yield load of the test specimen and is taken as 426 kN. LF_u is the ultimate load which covers by the total failure of the concrete slab, in this case, is taken as 668 kN. LF_f is the load level which causes the deflection reached 1% of the span length (in this case 40mm) and is determined as 599 kN. LF_d, the ultimate load of damaged structure (specimen-2), which covers by the failure of the concrete slab, is found as 275 kN. According to the result summarized in **Table.3.5**, the specimens tested in this study have the minimum redundancy ratio of 1.21. Following the method proposed in the NCHRP Report 406, simply supported composite twin I-girder bridge used in this study are proved to be redundant with a reserve capacity of 21 % for the test specimens used in this study.

Table.3.5 Redundancy evaluation of the test specimens

Model	LF_1 (kN)	LF_u (kN)	LF_f (kN)	LF_d (kN)	$\frac{R_u}{1.30}$	$\frac{R_f}{1.10}$	$\frac{R_d}{0.50}$	φ_R
Experiment	426.00	668.00	599.00	275.00	1.21	1.28	1.29	1.21

3.5 Reliability Analyses of the Test Specimens

Assumes that the applied load and resistance S are two independent variables following lognormal distribution, then the probability of failure and reliability index can be determined based on the following equations:

$$P_f = \Phi(-\beta) \tag{3.5}$$

$$\beta = \frac{ln\left(\frac{\bar{R}}{\bar{S}}\cdot\frac{\sqrt{1+V_S^2}}{\sqrt{1+V_R^2}}\right)}{\sqrt{ln[(1+V_S^2)(1+V_R^2)]}} \tag{3.6}$$

where

R: resistance

S: load effect

V_i: coefficient of variation of parameter i,

$\bar{\imath}$: mean value of the parameter i.

Three limit states were defined to evaluate the safety of the bridge system based on the reliability index including the ultimate state of the intact system corresponding to the ultimate load of the intact system, the ultimate state of the damaged system corresponding to the ultimate load of the damaged system, and the design limit state corresponding to the yield load of the intact system.

$$\beta_{member} = \frac{ln\left(\frac{P_y}{P_{design}}\cdot\frac{\sqrt{1+V_S^2}}{\sqrt{1+V_R^2}}\right)}{\sqrt{ln[(1+V_S^2)(1+V_R^2)]}} \tag{3.7}$$

$$\beta_{ultimate} = \frac{ln\left(\frac{P_u}{S}.\frac{\sqrt{1+V_S^2}}{\sqrt{1+V_R^2}}\right)}{\sqrt{ln[(1+V_S^2)(1+V_R^2)]}} \tag{3.8}$$

$$\beta_{damaged} = \frac{ln\left(\frac{P_d}{P_{dd}}.\frac{\sqrt{1+V_S^2}}{\sqrt{1+V_R^2}}\right)}{\sqrt{ln[(1+V_S^2)(1+V_R^2)]}} \tag{3.9}$$

where:

β_{member} : reliability index of the design limit state corresponding to the yield load of the intact system

$\beta_{ultimate}$: reliability index of the ultimate state of the intact system corresponding to the ultimate load of the intact system

$\beta_{damaged}$: reliability index of the damaged system corresponding to the ultimate load of the damaged system

P_y : yield load of the intact system and is determined as 426kN in the experiment

P_u : ultimate load of the intact system and is determined as 668kN in the experiment

P_d : ultimate load of the intact system and is determined as 668kN in the experiment

P_{design} : design load for the intact bridge system during its service life

P_{dd} : expected design load for the bridge in damaged condition before the damaged can be detected during inspection

In this study, the design load for the intact bridge system is taken as the applied load level corresponding to the allowable stress level of the steel provided by JRA (JRA, 2002), which means:

$$P_{design} = P(\sigma_{allowable}) \tag{3.10}$$

According to the Japanese specifications (JRA, 2002), $\sigma_{allowable}$ for the steel SM490 used in this study is 185 MPa corresponding to the $\varepsilon_{allowable} = \frac{185MPa}{200GPa} = 925\mu$. According to the measured strain data, the design load is taken as follow:

$$P_{design} = P(\sigma_{allowable}) = P(\varepsilon_{allowable} = 925\mu) = 237kN \tag{3.11}$$

For the coefficient of variation, the following value is taken from the results reported by Ghosn and Moses used for the development of the redundancy (Ghosn and Moses, 1998):

$$V_S = 19\% \tag{3.12}$$

$$V_R = 13\% \tag{3.13}$$

$$P_{dd} = 0.93 \times P_{design} = 220kN \tag{3.14}$$

With the above assumptions, the reliability index and probability of each limit state for the test specimens can be calculated and shown in **Table.3.6**. The results indicate that the composite twin I-girder bridge in this study have a reliability index of 1.02 with the probability of failure of 15.44843%. As severely damaged condition imposed on the test specimen (fracture of whole web and bottom flange), 15% of failure rate is reasonable to classified the bridge as redundant bridge system which yields the same conclusion when the method proposed by Ghosn and Moses to quantify the redundancy of the bridge system was used.

Table.3.6 Reliability analysis of the test specimens

	Yield state	Ultimate state	Damaged state
$\bar{R}$ (kN)	426	668	275
$\bar{S}$ (kN)	237	237	220
V_R	0.13	0.13	0.13
V_S	0.19	0.19	0.19
Reliability index (β)	2.61	4.58	1.02
Probability of failure (P_f)	0.45685%	0.00024%	15.44843%

3.6 Conclusions

An experimental study was carried out to investigate the redundancy characteristic and the mechanical behavior of the composite twin I-girder bridge under the extreme loading and critical fracture conditions. Experimental studies were carried out for an intact system and a damage system of a simply supported composite twin I-girder bridge. The results obtained from the LVDTs, loading device, and strain gauges attached to the test specimens were presented in the study to investigate the post-fracture performance of the test specimens. The findings from the experimental program in this study can be summarized as follow:

- In the event of the fatigue crack occurrence and its propagation to the entire bottom flange and the web in one main girder of a composite twin I-girder bridge, a significant reduction in system stiffness and load-carrying capacity was confirmed. Furthermore, a combination of bending and torsional deformation was confirmed by observing the crack pattern from the experimental results.

- A comparison of the strain distribution between the intact and the damaged conditions shows that fracture of the whole web and bottom flange at the mid-span section can result in a considerable increase in the shear strain on the studs near the middle section, thus reducing the strength and lifespan of the shear studs against fatigue failure.

- The failure mode of the simply supported composite twin I-girder bridge model used in this study was governed by the crushing of the concrete slab. Both intact and damaged specimens show a similar failure pattern which was governed by the combining of bending moment and torsional moment.

- The damaged specimen in this study can sustain the damage without significant deformation under self-weight and manage to carry some impose live load. By using first order reliability analysis, the probability of failure of the test specimen in damaged condition is determined as 15% for the damaged specimen. Considered the severely damaged condition used in this study, this result can be concluded as consistent with the redundancy evaluation method proposed in NCHRP Report 406, which concludes the composite twin I-girder bridge model used in this study as redundant bridge system with a reserve capacity of 21 %.

References:

AASHTO (American Association of State Highway and Transportation Officials). (2012). AASHTO LRFD Bridge Design Specification." 6th edition, Washington, DC.

ASCE Committee on Fatigue and Fracture Reliability. (1982). "Fatigue reliability: introduction," Journal of the Structural Division, ASCE, Vol. 108, No. 1, pp. 3–23.

Connor, R.J., Dexter R., and Mahmoud H. (2005). "Inspection and Management of Bridges with Fracture Critical Details." NCHRP Synthesis 354, National Cooperative Highway Research Program, Washington, DC.

Daniels, J. H., Kim, W., and Wilson J.L. (1988). "Recommended Guidelines for Redundancy Design and Rating of Two-Girder Steel Bridges." NCHRP Report 319, National Cooperative Highway Research Program, Washington, DC.

Deng, L., Wang, W., and Yu, Y. (2016). "State-of-the-Art Review on the Causes and Mechanisms of Bridge Collapse" Journal of Performance Construction Facility, ASCE, Vol. 30, No. 2, 04015005.

FHWA (Federal Highway Administration) (2012). Steel Bridge Design Handbook: Redundancy, Vol. 9, No. FHWA-IF-12-052, Washington, D.C.

Fujino, Y. (2006). "Steel Bridges in Japan-Current Circumstances and Future Tasks." Steel Construction Today and Tomorrow, Japanese Society of Steel Construction, No. 15.

Gheitasi, A. and Harris, D.K. (2016). "Redundancy and Operational Safety of Composite Stringer Bridges with Deteriorated Girders", Journal of Performance of Constructed Facilities, ASCE, Vol. 30, No. 2, 04015022.

Ghosn, M. and Moses, F. (1998). "Redundancy in Highway Bridge Superstructure." NCHRP Report 406, National Cooperative Highway Research Program, Washington, DC.

Ghosn, M., Moses, F., and Frangopol, D.M. (2010). "Redundancy and Robustness of Highway Bridge Superstructures and Substructures." Structures and Infrastructure Engineering, Vol. 6, No 1-2, pp. 257-278.

Ghosn, M. and Yang, J. (2014). "Bridge System Safety and Redundancy." NCHRP Report 776, National Cooperative Highway Research Program, Washington, DC.

Haghani, R., Al-Emrani, M., and Heshmati, M. (2012). "Fatigue-Prone Details in Steel Bridges." Buildings, MDPI, Vol. 2, No. 4, pp. 456-476.

Hendawi, S. and Frangopol, D.M. (1994). "System Reliability and Redundancy in Structural Design and Evaluation." Journal of Structural Safety, Vol. 16, N. 1-2, pp. 47-71.

Idriss, R. L., White, K. R., Woodward, C. B., and Jauregui, D.V. (1995). “After-fracture redundancy of two-girder bridge: Testing I-40 bridges over Rio Grande”, Proc. 4th International Bridge Engineering Conference, pp. 316-326.

JRA (Japan Road Association). (2012). "Specifications for Highway Bridges." Part I Common, English edition, Tokyo.

JRA (Japan Road Association). (2002a). "Specifications for Highway Bridges." Part II Steel Bridges, English edition, Tokyo.

JRA (Japan Road Association). (2002b). "Specifications for Highway Bridges." Part III Concrete Bridges, English edition, Tokyo.

JSCE (Japanese Society of Civil Engineers). (2002). "Standard Specifications for Concrete Structures", Tokyo.

JSCE (Japanese Society of Civil Engineers). (2007). "Standard Specifications for Steel and Composite Structures", Tokyo.

Kakiichi, T., Ishikawa, T., Ojio, T., Yamada, K. (2011). “Stress Measurement and Fatigue Durability Evaluation of Plate Girder Web Detail at Cross Beam”, JSCE Journal of Structural Engineering, Vol. 57A, pp. 852-859. (in Japanese)

Lam, H., Lin, W., and Yoda, T. (2014). “Effect of Bracing Systems on Redundancy of Three-span Composite Twin I-girder Bridge.” JSCE Journal of Structural Engineering, Vol. 60A, pp. 59-69.

Lin, W., Yoda, T., Kumagai, Y., Saigyo, T. (2013). “Numerical Study on Post-Fracture Redundancy of the Two-girder Steel-Concrete Composite Highway Bridges.” International Journal of Steel Structures, Vol. 13, No. 4, pp. 671-681.

Lin, W., and Yoda, T. (2013). “Experimental and Numerical Study on Mechanical Behavior of Composite Girders under Hogging Moment.” International Journal of Advanced Steel Construction, Vol. 9, No. 4, pp. 309-333.

Liu, W.D., Ghosn, M., Moses, F., and Neuenhoffer, A. (2001). “Redundancy in Highway Bridge Substructures.” NCHRP Report 458, National Cooperative Highway Research Program, Washington, DC.

Nagai, M. (2006). “Steel Bridges in Japan- Rationalized Design Methods in Japan.” Japanese Society of Steel Construction, No. 15.

Park Y., Joe, W., Park, J., Hwang, M., and Choi, B.H. (2012) “An experimental study on after-fracture redundancy of continuous span two-girder bridges”, Int. J. Steel Struct., Vol. 12, No. 1, pp. 1-13.

Takeshi, M. (2006). “Improvement of Steel Bridge Durability”, Steel Construction Today and Tomorrow, Japanese Society of Steel Construction, No. 15.

Tamakoshi, T., Yoshida, Y., Sakai, Y., and Fukunaga, S. (2006). “Analysis of Damage Occurring in Steel Plate Girder Bridges on National Roads in Japan.” Public Work Research Institute of Japan.

Wardhana, K., and Hadipriono, F. (2003). “Analysis of Recent Bridge Failures in the United States.” J. Perform. Constr. Facil., ASCE, Vol.17, Issue 3, pp.144-150.

Wisniewsky, D.F., Casas, J.R., and Ghosn, M., (2006). “Load-capacity evaluation of existing railway bridges based on robustness quantification”, Journal of Structural Engineering International, Vol. 16, No. 2, pp.161–166.

4. Numerical Study on Redundancy Evaluation of Simply Supported Composite Twin I-Girder Bridges

4.1 Introduction

Steel-concrete composite twin I-girder bridges are commonly used as highway bridges in Europe, Asia, and other part of the world owing to their low cost, high span-to-depth ratio, and simple construction procedure compared to other types of bridges. However, such bridges are classified as non-redundant and fracture-critical (AASHTO, 2012). Such classification is the result of oversimplified assumptions normally used in the design, but not on the realistic behavior of the as-built three-dimensional structure (Daniels et al., 1988). The terms oversimplified here is referred to the two-dimensional assumption used in the design which consider twin girders alone as the design load path available for transmitting the vertical load like dead load, live load, and impact load to the substructure. The secondary members, including diaphragms and bottom lateral bracings, are neglected in sharing or resisting the vertical load. Furthermore, the torsional strength of the deck in balancing the live load is also not considered. From past experiences, composite twin I-girder bridge systems do not collapse even after the severe fracture occurs in one of the main girder sections (Daniels et al., 1988). This is also justified by the experiment performed and reported in the **Chapter 3**. The cantilever action against the interior supports after fracture occurred is the main reason the bridge can redistribute the load in the damage system (Idriss et al., 1995). A recent study also points out that many bridges have had a full-depth fracture of the main girder and did not collapse, usually owing to the alternative-load-carrying mechanism of catenary action of the deck under large rotations at the fracture (Connor et al., 2005). With this background, the present study is carried out to investigate the post-fracture behavior and redundancy analyses of a composite twin I-girder bridge system in the fracture condition based on the numerical analyses. Finite Element Method (FEM) with nonlinear analyses are carried out to investigate the performance of the composite twin I-girder bridge under different fracture locations. Load-deflection curves and load-strain curves from the experimental results were used for verifying the validating the numerical models. Then, parametric studies were conducted to investigate the effects of structural indeterminacy and the effect of the concrete slab on the safety of the composite twin I-girder bridge in the fracture condition.

4.2 Configuration of the Bridge Model

A small scale simply supported composite twin I-girder bridge model is shown in **Fig.4.1.** The total length of the model is 4.4 m with the span length of 4m in the loading test. The cross section of the bridge model is shown in **Fig.4.1(a)**. The side view and top view is shown in **Fig.4.2** and **Fig.4.3**, respectively. Two row of shear stud connectors with the diameter of 19mm and the height of 80mm were employed on top of the flanges of the main girders to ensure the composite action between the concrete slab and the steel girders. The details of the shear stud connectors are shown in **Fig.4.1(b)** and its arrangement can be seen in **Fig.4.3**. To comply with JRA specification for reinforcement concrete of bridge structures, two layers of reinforcement are installed in the slab. As shown in **Fig.4.5**, reinforcing bar type SD345 with 10mm in diameter are used with the 100mm spacing in both longitudinal and transversal direction. The dimensions and positions of vertical stiffeners and details of transverse beams are shown in **Fig.4.1(b)** and **Fig.4.2**, respectively.

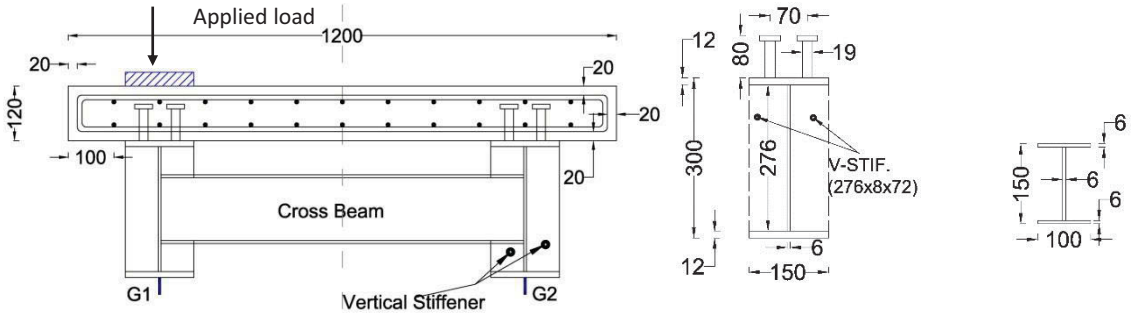

(a) Cross section **(b)** Details of girders and studs

Fig.4.1 Cross section of the bridge model

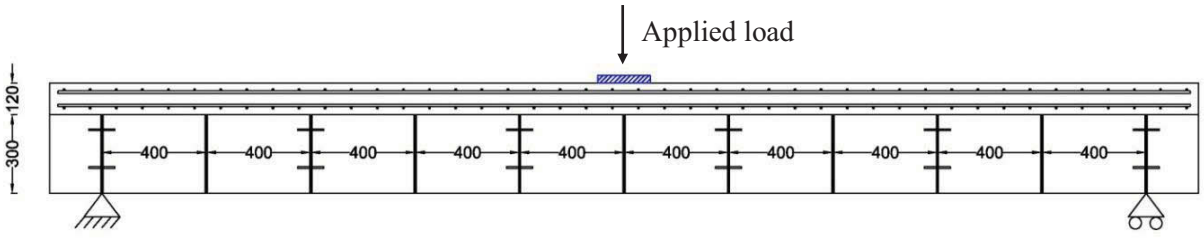

Fig.4.2 Side view of the test specimens

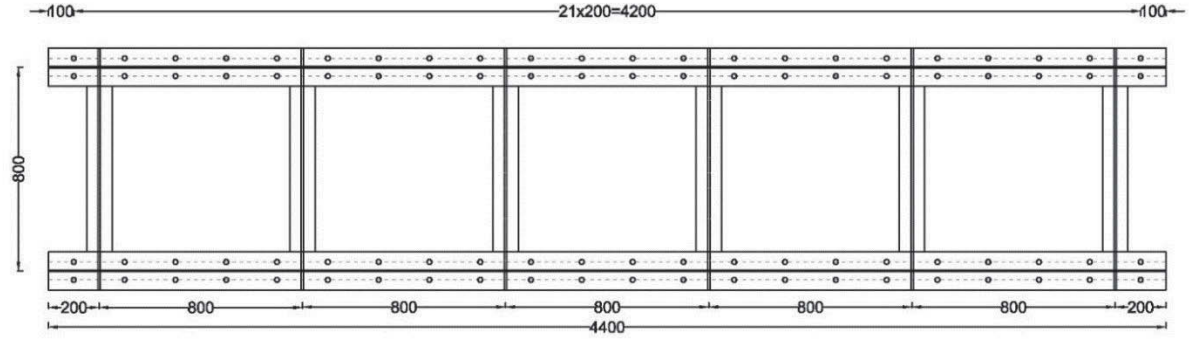

Fig.4.3 Top view of the steel girders

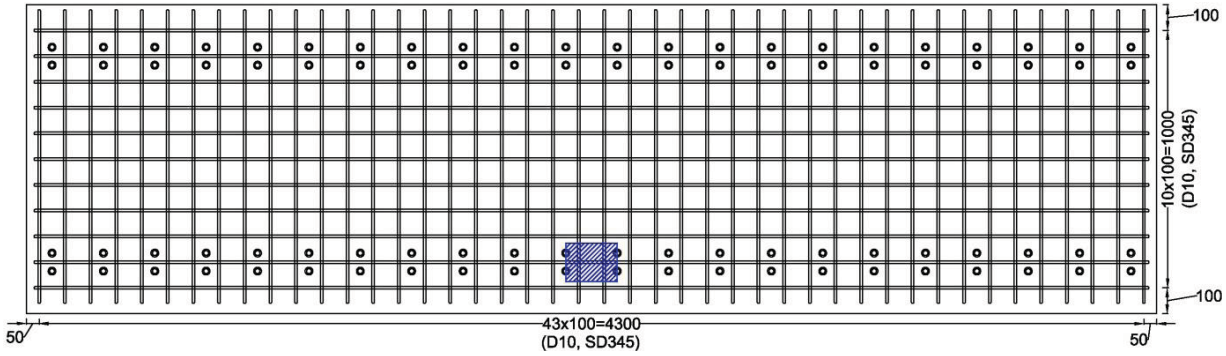

Fig.4.4 Layout of the reinforcement

4.3 Numerical Models

In the numerical model, finite element method with the aid of TNO Diana 9.4.4 software was employed for modeling and analyzing the bridge model (Diana user manual, 2012). Both material non-linearity and geometrical non-linearity were included in the nonlinear analyses. The concrete slab is modeled by using the 8-node solid element with 24 degrees of freedom. The reinforcing bars are modeled by using embedded bar elements. The steel girders, transverse beams, and vertical stiffeners are modeled by 4-node curve shell elements. Spring elements were used for modeling the shear studs and interface elements were used for simulating the interface friction between the concrete slab and main girders top flanges. Phase analyses and load increment method were employed to analyze the bridge model. The dead load (self-weight) is analyzed in the first phase following by the applied live load in the second phase. In this study, similar to previous study (Hunley and Harik, 2011), the dynamic effect of crack propagation is not included. This approach is further justified by the dynamic response of a twin girder bridge fracture test conducted at the University of Texas at Austin, in which the

bridge deflection did not increase significantly after the fracture of one box girder(Neuman, 2009; Veggeberg, 2011; Samaras, 2012). The overview of the numerical models is shown in **Fig.4.5**.

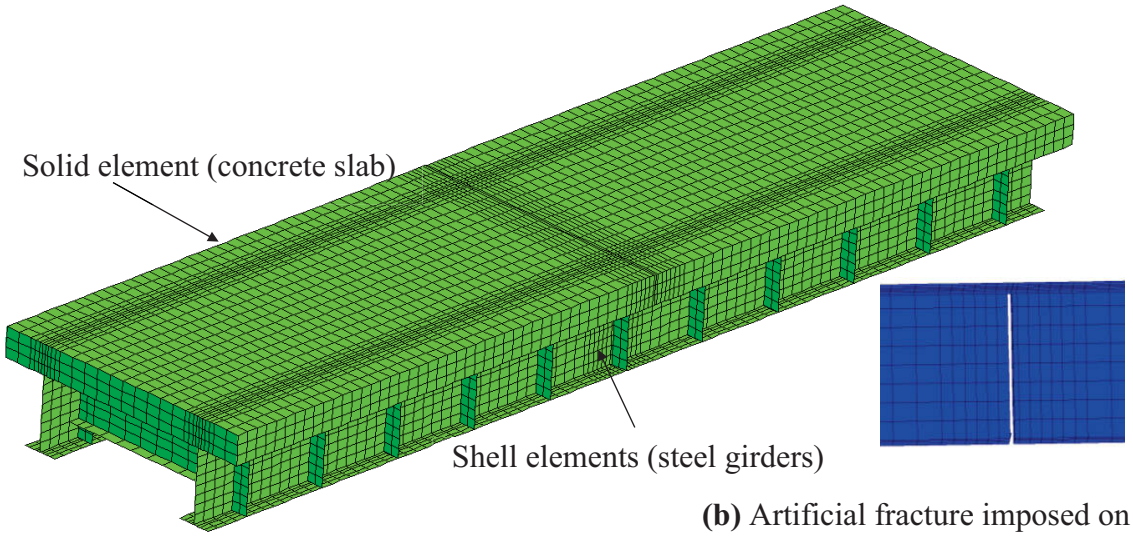

(b) Artificial fracture imposed on girder

(a) Overview of numerical model

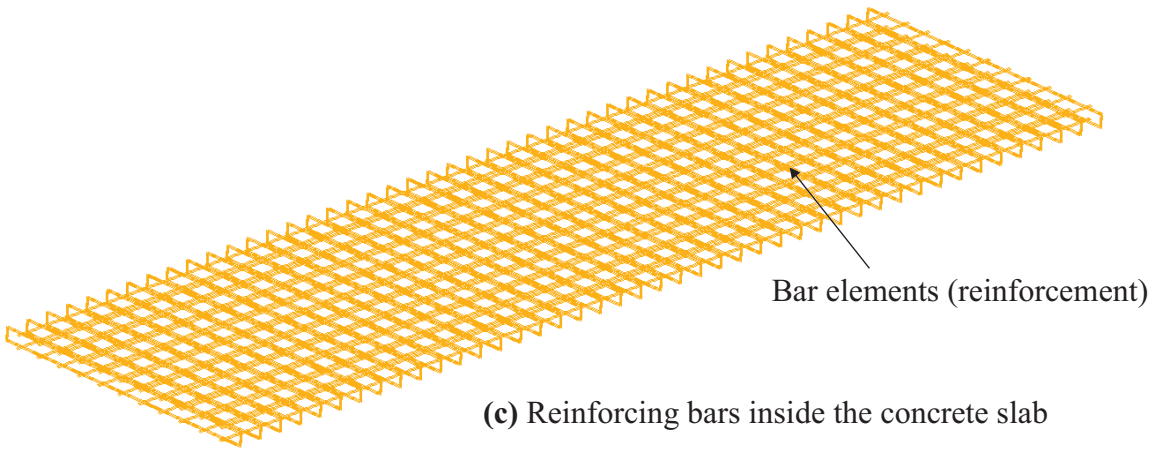

(c) Reinforcing bars inside the concrete slab

Fig.4.5 Numerical models

4.3.1 Material properties

(a) Concrete

In the numerical models, the total strain crack model was used to simulate the three-dimensional constitutive model of the concrete (Vecchio and Collins, 1986; Selby and Vecchio, 1993), and the smeared cracking model was employed for the cracking of the concrete slab. The stress-strain curve shown in **Fig.4.6** was used to simulate the compression and tension behavior of concrete. The tensile strength of the concrete was calculated according to **Eq.4.1** based on the JSCE specification for concrete structures (JSCE, 2002), in which f_t and f'_{ck} denote the tensile and compression strengths of concrete, respectively. The tension-stiffness curve as shown in **Fig.4.6** was used in the numerical analyses to reflect the softening of concrete according to **Eq.4.2** (Nakasu et al., 1996). The stress-strain relationship in compression was determined according to **Eq.4.3**. The ultimate compression strain ε'_{cu} is taken as 0.0035. This value is suggested in the Japanese specifications (JRA, 2002; JSCE, 2002) and Eurocode 2 (CEN, 1992).

$$f_t = 0.28{f'_{ck}}^{2/3} \tag{4.1}$$

$$\sigma_t = f_t\left(\frac{\varepsilon_t}{\varepsilon}\right)^{0.4} \tag{4.2}$$

$$\sigma_c = \begin{cases} k_1 f'_{cd}.\frac{\varepsilon'_c}{0.002}.\left(2-\frac{\varepsilon'_c}{0.002}\right); & \varepsilon'_c \le 0.002 \\ k_1 f'_{cd}; & \varepsilon'_c \ge 0.002 \end{cases}; \quad k_1 = 1 - 0.003 f'_{ck} \tag{4.3}$$

$$\varepsilon'_{cu} = \frac{155 - f'_{ck}}{3000}\,; 0.0025 \le \varepsilon'_{cu} \le 0.003 \tag{4.4}$$

where:

- σ_c : Compression stress of concrete
- ε'_c : Compression strain of concrete
- f'_{cd} : design compression stress of concrete

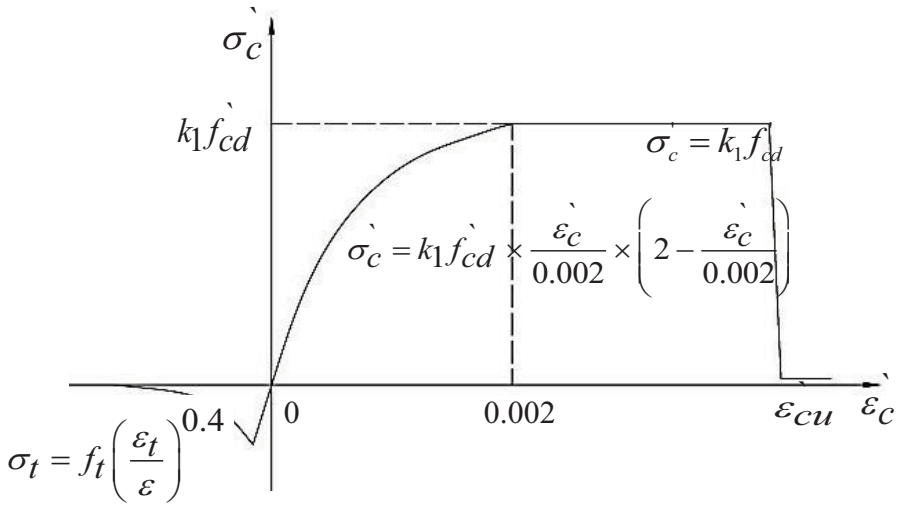

Fig.4.6 Stress-strain relationship of the concrete

(b) Structural steel and reinforcing bars

Table.4.1 provides details of material properties of reinforcing bars and steel plates including yield strength and ultimate strength. The Young Modulus is take as 200 GPa. As suggested in Japanese specifications (JSCE, 2007), the stress-strain relationship for structural steel as shown in **Fig.4.7(a)** was adopted in the numerical analyses. The stress-strain relationship of the rebar is adopted from JSCE specification for concrete structure and is shown in **Fig.4.7(b)** (JSCE, 2002).

Table.4.1 Materials properties of steel and reinforcing bars

Material	Young's modulus (MPa)	Poisson ratio	Yield Strength (MPa)	Ultimate Strength (MPa)
Steel Plate (6mm)	200000	0.3	450	577
Steel Plate (8mm)			427	556
Steel Plate (12mm)			389	548
Reinforcing bar (D10)			406	544

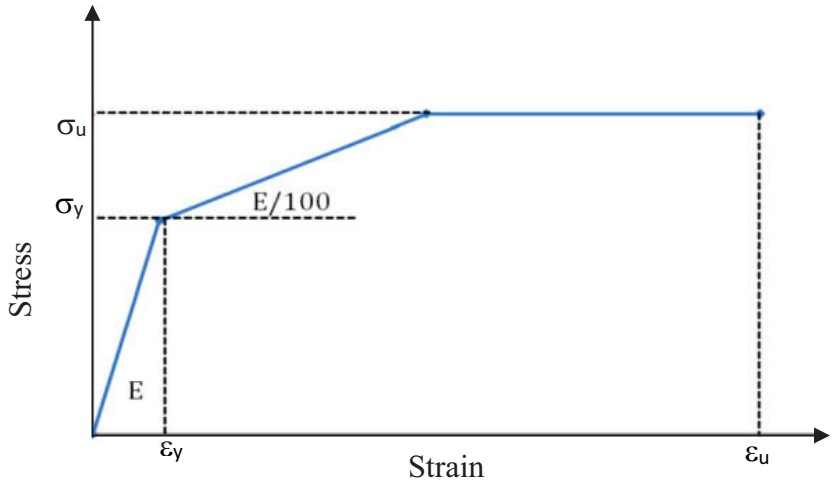

(a) Stress-strain relationship of the reinforcing bar (JSCE, 2002)

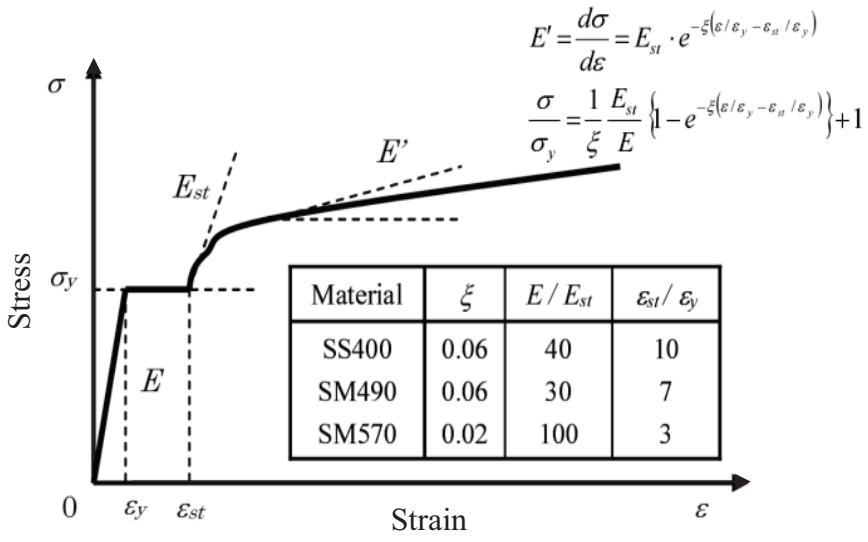

(b) Stress-strain relationship of the structural steels (JSCE, 2007)

Fig.4.7 Stress-strain relationship of reinforcing bar and structural steels

(c) Stud shear connectors

To model the shear stud inside the concrete slab, 3D nonlinear spring elements were employed (Lin et al., 2013). For each stud, one spring was used for modeling the behavior in the normal direction, and two other springs were used for modeling the behavior in tangential directions. The properties of the spring elements are given by **Eq.4.5** and **Eq.4.6**, as illustrated in **Fig.4.8** (Ollgaard et al., 1971). The ultimate shear strength of studs was calculated according to **Eq.4.6** as suggested in Japanese specifications (JSCE, 2002).

$$Q = Q_u(1 - e^{-07s})^{0.4} \tag{4.5}$$

$$Q_u = min\begin{pmatrix} (31A_{ss}\sqrt{\left(\frac{h_{ss}}{d_{ss}}\right)f'_{cd}} + 10000)/\gamma_b \\ A_{ss}f_{sud}/\gamma_b \end{pmatrix} \tag{4.6}$$

where:

- s: slip of the shear stud (mm)
- A_{ss}: area of the shank of the stud (mm^2)
- d_{ss}: diameter of the shank of the stud (mm)
- h_{ss}: height of the stud (mm)
- f'_{cd}: compressive strength of concrete (MPa)
- f_{sud}: design tensile strength of the stud (MPa)
- γ_c: material factor of concrete (=1.3)
- γ_s: material factor of the stud (=1.0)
- γ_b: member factor (=1.3)

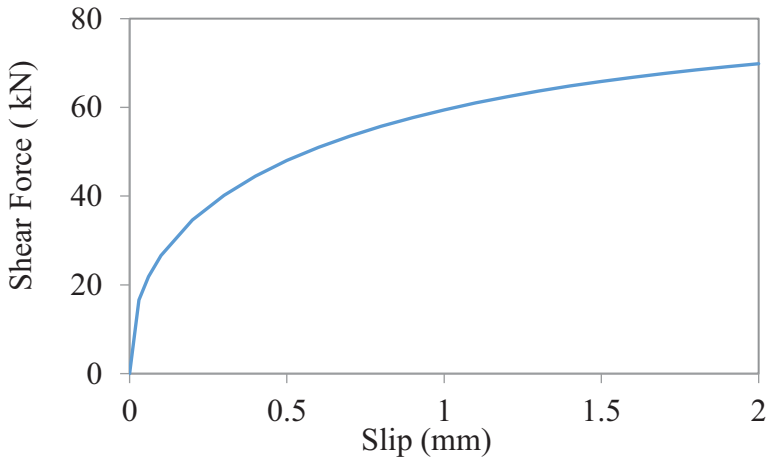

Fig.4.8 Shear force-slip relationship of shear stud

(d) Interface between steel and concrete

In this study, the interface model proposed by Okada et al., is used for simulating the interface between the top flange and concrete slab as shown in **Eq.4.7** and **Eq.4.8** (Okada et al., 2006). The constitution relationship is shown in **Fig.4.9**. The maximum bond stress f_{bo} which represented the strength of adhesion between steel flange and concrete slab is taken as 0.5 MPa derived from the push out test in the previous research (Yamada et al., 2001). The slip at the maximum bond stress is taken as 0.06 mm, which is the standard value of the slip at the peak chemical bond (DÖRR et al., 1980).

$0 \leq \Delta u_t \leq \Delta u_t{}^0$:

$$f_{tan} = \frac{f_{bo}}{1.9}\left(5\left(\frac{\Delta u_t}{\Delta u_t^0}\right) - 4.5\left(\frac{\Delta u_t}{\Delta u_t^0}\right)^2 + 1.4\left(\frac{\Delta u_t}{\Delta u_t^0}\right)^3\right) \tag{4.7}$$

$\Delta u_t \geq \Delta u_t{}^0$:

$$f_{tan} = f_{b0} \tag{4.8}$$

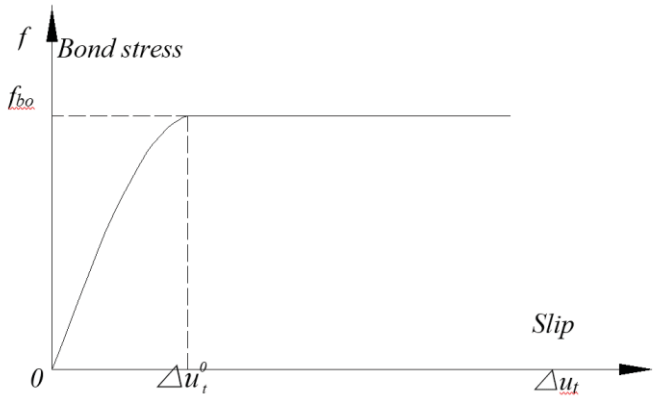

Fig.4.9 Bond stress slip relationship of interface between the steel and the concrete

4.3.2 Numerical model validation

To validate the numerical model, experimental results in **Chapter 3** is used to compare with the analysis results. The load-strain curves of the bottom flange at the middle section, the load-deflection curves at mid-span section, and load-strain curves of the concrete slab are used for verifying the mechanical behavior of the test specimens.

(a) Loading and boundary condition

As shown in **Fig.4.10**, one-point load is imposed on girder-1 for both specimens to create the most critical loading condition (uneven loading condition) in a multi-girder bridge system (Hendawi and Frangopol, 1994). The loading point is set in the mid-span section of the damaged girder (girder-1) to produce the most critical scenario for the damaged specimen (Specimen-2). For the boundary conditions, a pinned support is used at one end and a roller support is used at the other end.

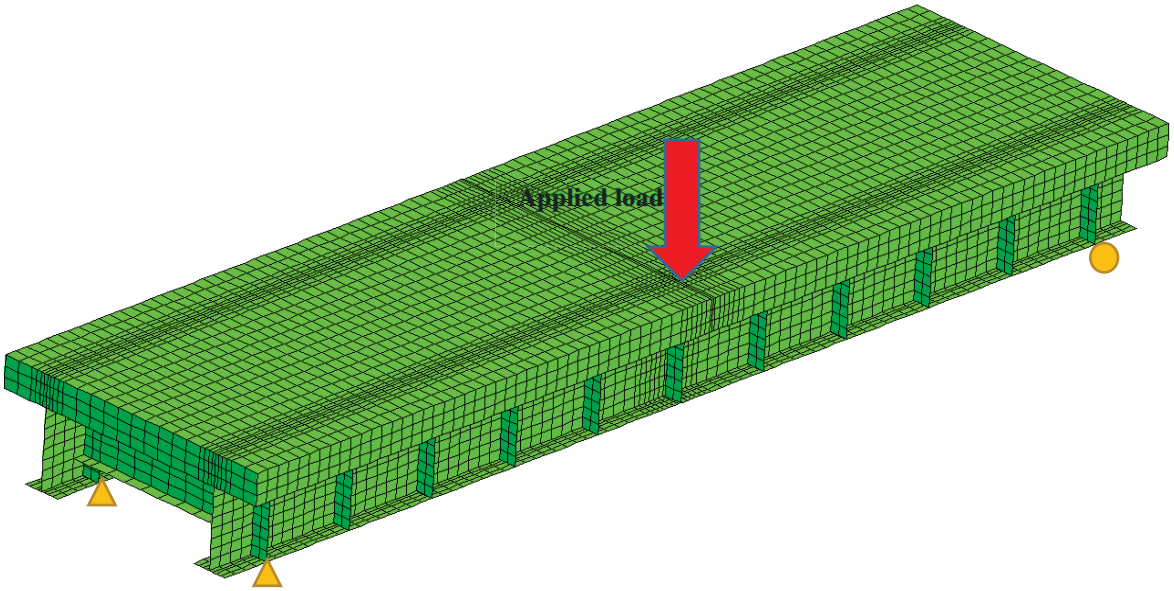

Fig.4.10 Boundary and loading condition in numerical models

(b) Load-strain curves of steel girders

On the experimental specimens, strain gauges were attached to the bottom flange at the mid-span section to measure the tensile strain of the bottom flange of girder-1 and girder-2 during the loading test, as shown in **Fig.4.11**. The load-strain curves from the experimental results and numerical analyses are shown in **Fig.4.12** and **Fig.4.13**, respectively. For the Specimen-1, before reaching the yield point, the load-strain curves of the bottom flange of both girder-1 and girder-2 from numerical results agree well with the strain data from experimental results as can be seen in **Fig.4.12**. The yield load is determined as 426 kN which associated with yield strain of 1945 μ. In the post-elastic region, the load-strain curves for the girder-1 and girder-2 are consistent well while slight difference can be seen for girder-1. One of the reasons that contribute to the difference is the use of a rigid plate in the numerical model to prevent stress concentration at the loading point. This difference is also caused by the imperfection of the boundary conditions, loading conditions, and the actual stress-strain curves of the materials used in the experimental program and used in the numerical models. For the specimen-2, due to the fracture of the web and bottom flange, the strain at the bottom flange and also along the web near the fracture section of girder-1 is almost zero. For girder-2, similar to the specimen-1, at the bottom flange of the mid-span section, the load-strain curve between experimental results and numerical results is well agreed as shown in **Fig.4.13**. In both cases, the ultimate load in the experiment (which is governed by the crush of concrete slab) is reached before the yield point of the girder-2.

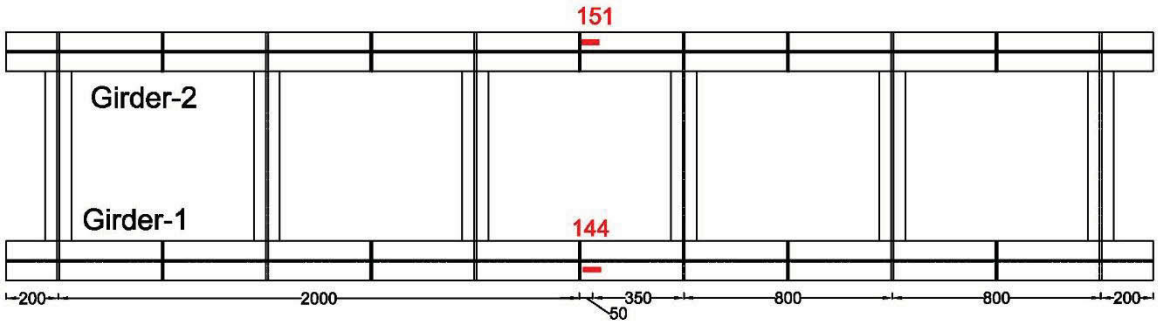

Fig.4.11 Strain gauges attached to the bottom flange of steel girders

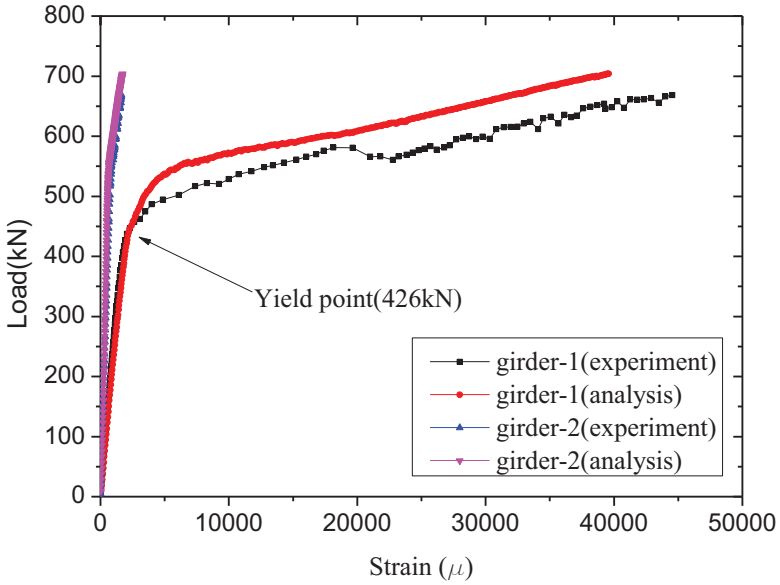

Fig.4.12 Load-strain curves at the bottom flange middle cross section of girder-1

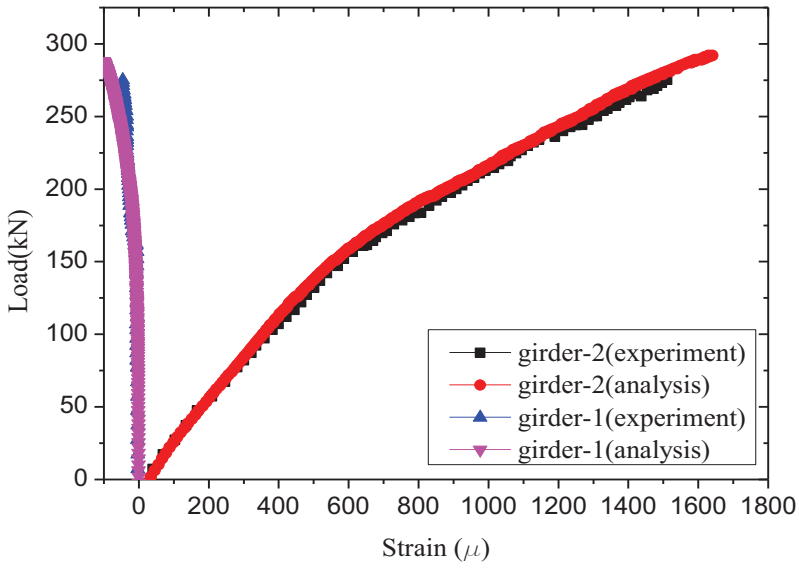

Fig.4.13 Load-strain curves at the bottom flange middle cross section of girder-2

(c) Load-deflection curves of bridge models

Fig.4.14 shows the load-deflection curves of the Specimen-1 and Specimen-2 from experimental results and numerical analyses. Consistent results between experimental models and numerical models can be observed. Slight difference in post-elastic response for both models is mainly due to the assumption of material properties for numerical model and imperfection of the experimental model as discussed above. The numerical models used in this study are proved to be accurate to predict the performance of both intact specimen and damaged specimen under vertical loading condition. The system stiffness of the experimental specimen and numerical model is well agreed for the elastic stage. As the loading continues, cracks were observed on the test specimen as can be seen in **Fig.4.15**. The crack pattern observed in the experiment is consistent with the deformation shape from the numerical result (as shown in **Fig.4.15(a)** and **Fig.4.16**) which is generated from the combination of bending moment and torsional moment. The ultimate load in the numerical analyses is slightly higher (704 kN) than the experimental results (668 kN). For the Specimen-2, due to the fracture of the web and bottom flange at mid-span, the system stiffness, as well as ultimate load, are much smaller than those of specimen-1. The crack pattern of the Specimen-2 (as shown in **Fig.4.15(b)** and **Fig.4.17**) is similar to those of Specimen-1 which is generated from the combining of bending moment and torsional moment. Similar to the Specimen-1, the ultimate load for the numerical model is determined as 292 kN which is slightly higher than that of the experimental specimen (275 kN). The deformation at the ultimate load from the numerical model is shown in **Fig.4.17**.

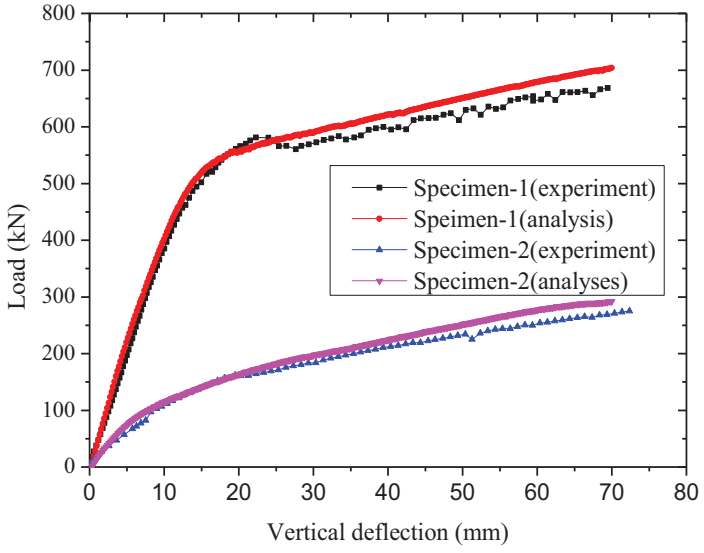

Fig.4.14 Load-deflection curves at middle section

(a) Specimen-1 (b) Specimen-2

Fig.4.15 Crack patterns on the concrete slab

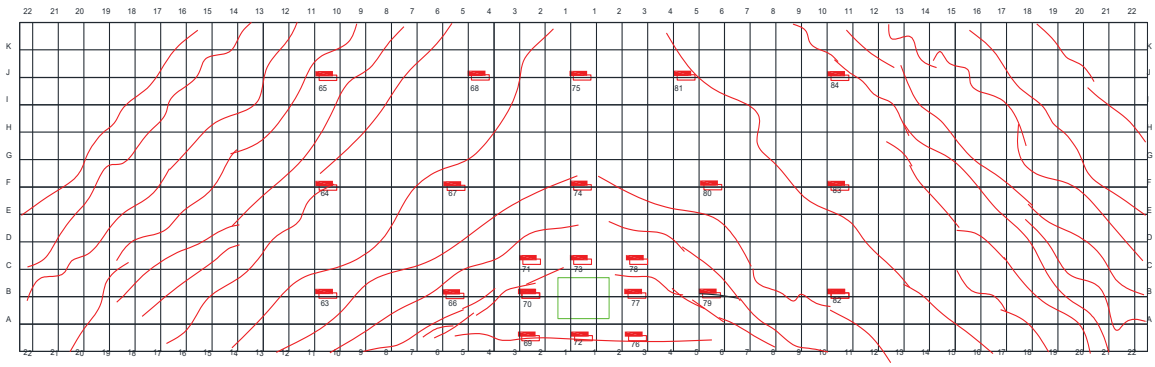

(a) Visible crack pattern on the top of the concrete slab (specimen-1)

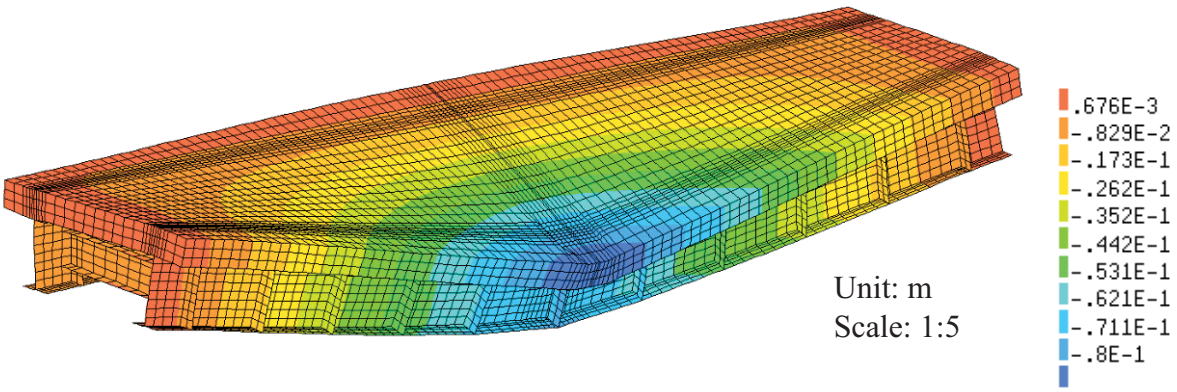

(b) Deformation of the intact specimen (Specimen-1)

Fig.4.16 Visible crack patterns and deformation of the intact specimen

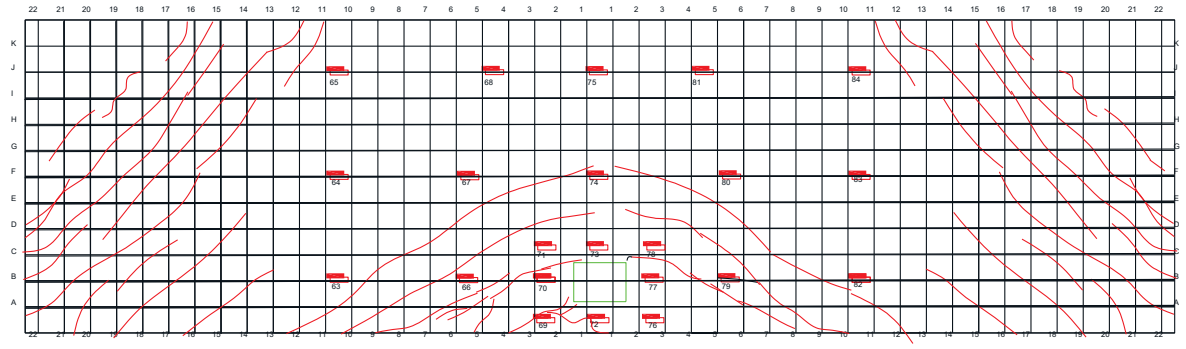

(a) Visible crack patterns on the top of the concrete slab (specimen-2)

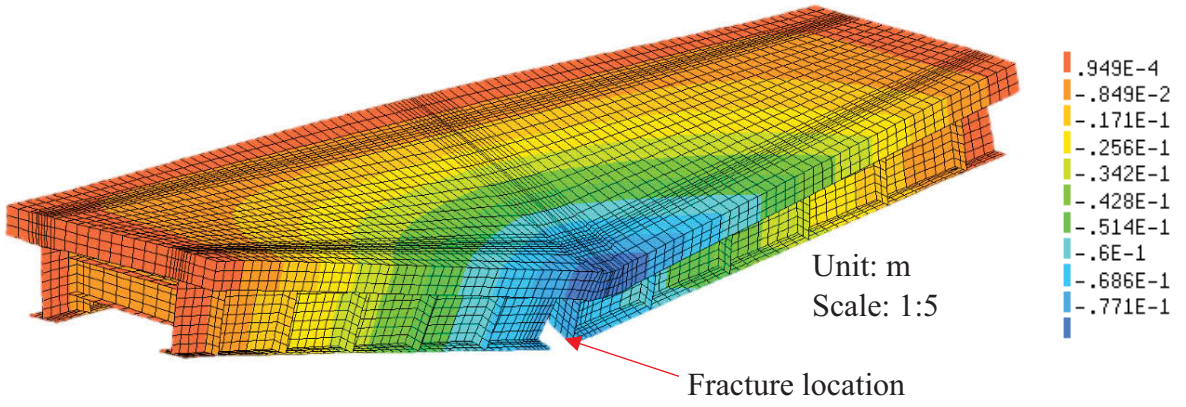

(b) Deformation of the damaged specimen (Specimen-2)

Fig.4.17 Visible crack pattern and deformation of the damaged specimen

(d) Load-strain curves of concrete slab

The strain results of the strain gauges CH66, CH70, and CH74 are compared with the results from numerical analyses. **Fig.4.19** presents the load-strain curves of the Specimen-1. The results show that the load-strain curves from the experimental results and numerical analyses are consistent well in the elastic stage, but not in the plastic stage and beyond the local failure of the concrete slab at 580kN. Similar results were observed for the Specimen-2. As shown in Fig.4.20, the load-strain curves of the concrete slab of the Specimen-2 from the numerical analyses is consistent well with the experimental result of the local failure of the concrete slab at 160 kN. The difference between the experimental results and numerical analyses concerning the concrete strain in post-elastic behavior can be concluded as due to the local failure of the concrete slab.

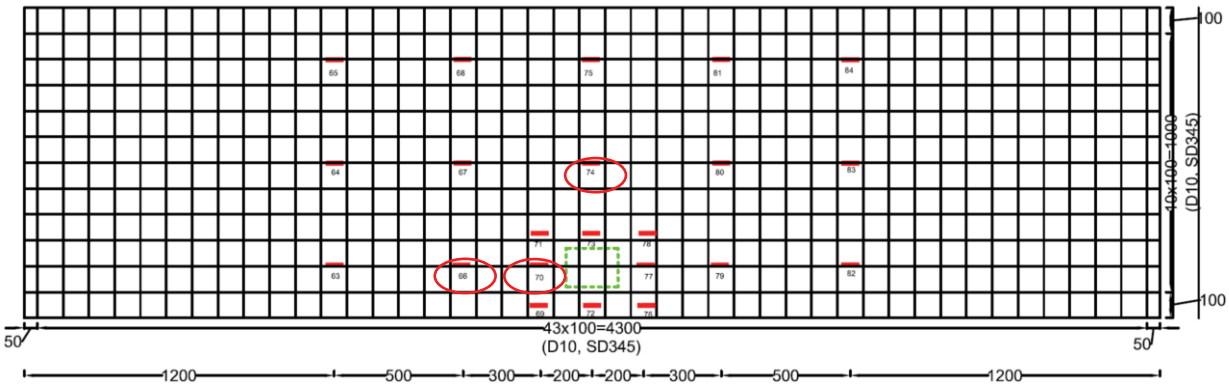

Fig.4.18 Strain gauge location attached on the top surface of concrete slab

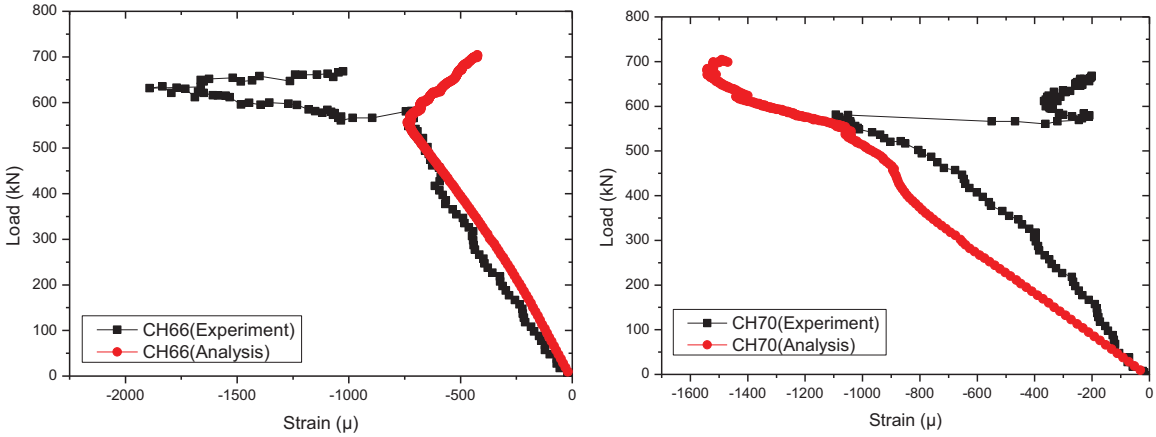

(a) CH66 (b) CH70

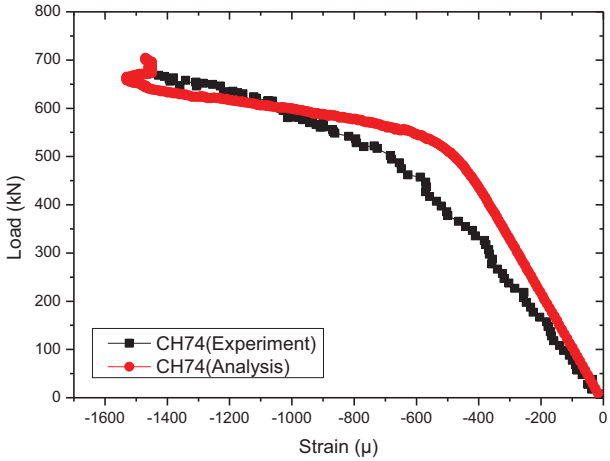

(b) CH74

Fig.4.19 Load-strain curve of the concrete slab for Specimen-1

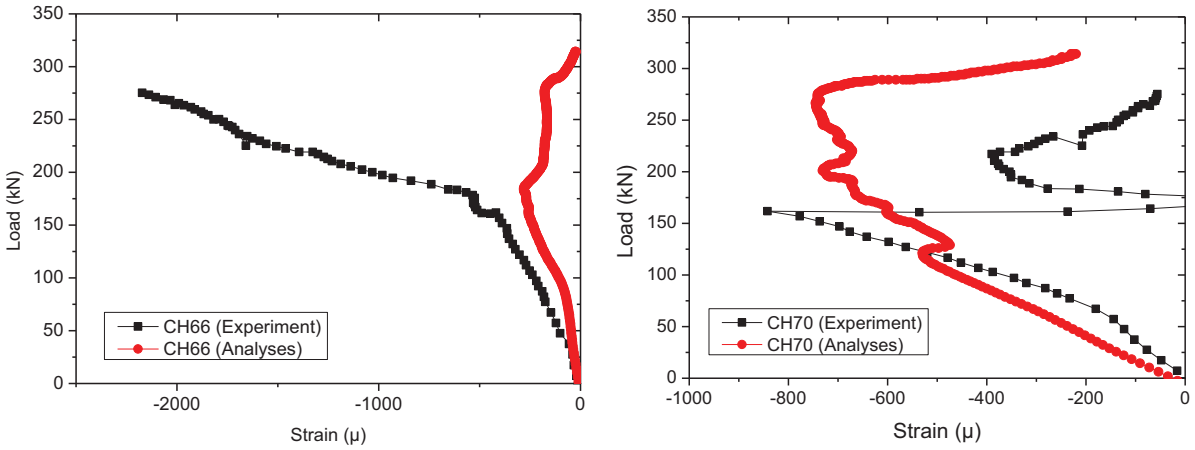

(a) CH66 (b) CH70

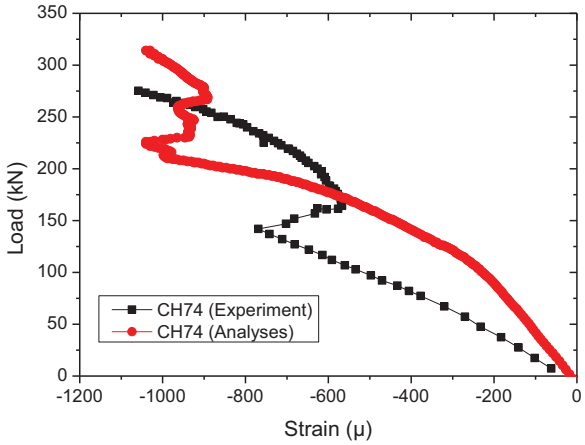

(c) CH74

Fig.4.20 Load-strain curves of the concrete slab for Specimen-2

(e) Redundancy factor

The redundancy rating method proposed in NCHRP is employed to quantify the redundancy level of the bridge models used in this study (Ghosn and Moses, 1998; Liu et al., 2001; Ghosn et al., 2008; Ghosn and Yang, 2014). The redundancy factor proposed in the following form is used:

$$\varphi_R = min\left(\frac{R_u}{1.30}, \frac{R_f}{1.10}, \frac{R_d}{0.50}\right) \tag{4.9}$$

$$R_u = \frac{LF_u}{LF_1} \tag{4.10}$$

$$R_f = \frac{LF_f}{LF_1} \tag{4.11}$$

$$R_d = \frac{LF_d}{LF_1} \tag{4.12}$$

where:

- φ_R : Redundancy factor of bridge system
- R_u : System reserve ratio for the ultimate limit state (Ghosn and Moses, 1998)
- R_f : System reserve ratio for the functionality limit state (Ghosn and Moses, 1998)
- R_d : System reserve ratio for the damaged condition (Ghosn and Moses, 1998)
- LF_u : Load carrying capacity of the intact structure
- LF_1 : Load level corresponding to first member failure
- LF_f : Load level corresponding to the vertical deflection of 1 % of span-length
- LF_d : Load carrying capacity of the damaged structure

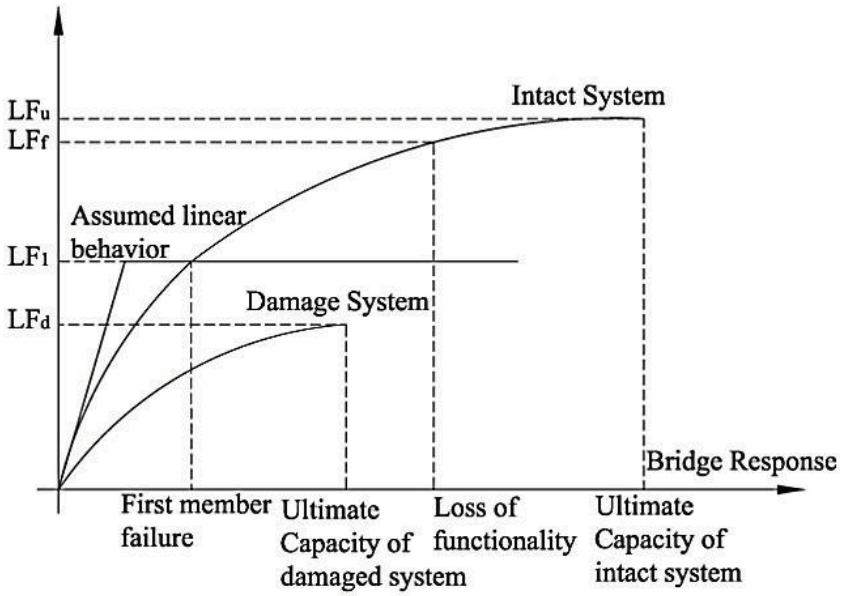

Fig.4.21 Typical behavior of bridge system (Ghosn and Moses, 1998)

Table.4.2 Redundancy evaluation of the test specimens

Model	LF_1 (kN)	LF_u (kN)	LF_f (kN)	LF_d (kN)	$\frac{R_u}{1.30}$	$\frac{R_f}{1.10}$	$\frac{R_d}{0.50}$	φ_R
Experiment	426.00	668.00	599.00	275.00	1.21	1.28	1.29	1.21
Analyses	427.00	704.00	621.00	292.00	1.27	1.32	1.36	1.27
Inaccurate percentage	0.20%	5.39%	3.67%	6.18%	4.96%	3.13%	5.43%	4.96%

As shown in **Table.4.2**, for the specimen used in this study, LF_1 is the yield load of the test specimen and is found as 426 kN for the experimental model and 427 kN for the numerical analyses. LF_u is the ultimate load which covers by the total failure of the concrete slab, and is taken as 668 kN for the experimental model and 704 kN for the numerical analyses. LF_f is the load level corresponds to the 40 mm deflection (1% of span length) and is determined as 599kN according to the experimental results and 621 kN according to the numerical analyses. LF_d, the ultimate load of damaged structure which covers by the failure of the concrete slab, is taken as 275 kN for the experimental model and 292 kN for the numerical analyses. According to the numerical result summarized in **Table.4.3**, the specimens tested in this study have the minimum redundancy ratio of 1.21 for the experimental result and 1.27 for the numerical result. Following the method used in this study, simply supported composite twin I-girder bridge used in this study are proved to be redundant with a reserve capacity of 21 % for the experimental model and 27 % for the numerical analyses. Concerning the redundancy factor φ_R, the difference of 4.96 % is found between experimental results and numerical analyses. For the other loading factors, the error is found between 0.2 % and 6.18 %. This difference is considered as small and acceptable considering the complex behavior of the bridge system in post-elastic and damaged conditions. From the comparison of the load-strain curves, load-displacement curves, failure modes, and redundancy level, the numerical models and analyzing method used in this study are proved to accurately simulate the bridge behavior in both intact and damaged conditions.

4.4 Fracture Critical Members (FCMs)

A survey report on bridge damage pointed out that the fracture of the steel or composite girder bridge happened randomly along the main girder (Tamakoshi et al., 2011). The fracture of whole web and bottom flange can be anywhere near the support region to the mid-span region. For this reason, fracture at the mid-span section, near the support, and at the 1/4 span section were compared to determine the most critical location which considered the possible FCMs. Five different scenarios (including one associated with experiment program), are included in determining the most severe fracture condition. The scenario having the lowest load carrying capacity is considered as the most critical damaged cases comparing to other cases.

4.4.1 Fracture near the support location

In this case, fracture of whole web and bottom flange is considered near the end support as shown in **Fig.4.22**. The damage is located at 0.2 m from the center of the support. Two loading cases were considered: one on the top of the damaged section (Case-2a) to create the maximum bending moment at the fractured section, and another one at the mid-span section (Case-2b). The deformation corresponding to each damaged case is shown in **Fig.4.24(a)** and **Fig.4.24(b)**. Load-displacement curves were shown in **Fig.4.23**. For Case-2a, when the load is applied on the fracture location, the bridge model failed at 532 kN. For Case-2b, when the load is applied at the mid-span section to produce maximum bending moment, the bridge model failed at 464 kN. Comparing to the fracture at mid-span section (Case-1), both cases in this damaged scenario has higher load carrying capacity which can be concluded as less critical for the studied bridge model.

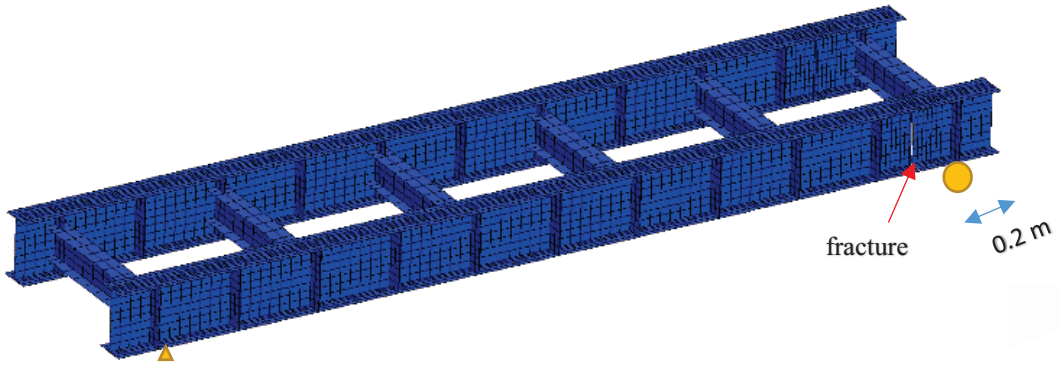

Fig.4.22 Fracture near the support location

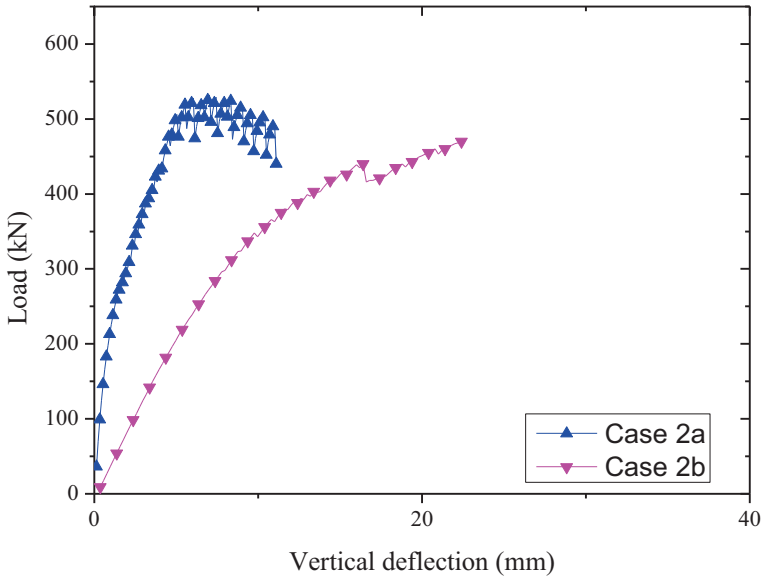

Fig.4.23 Load-displacement curve of Case-2a and Case-2b

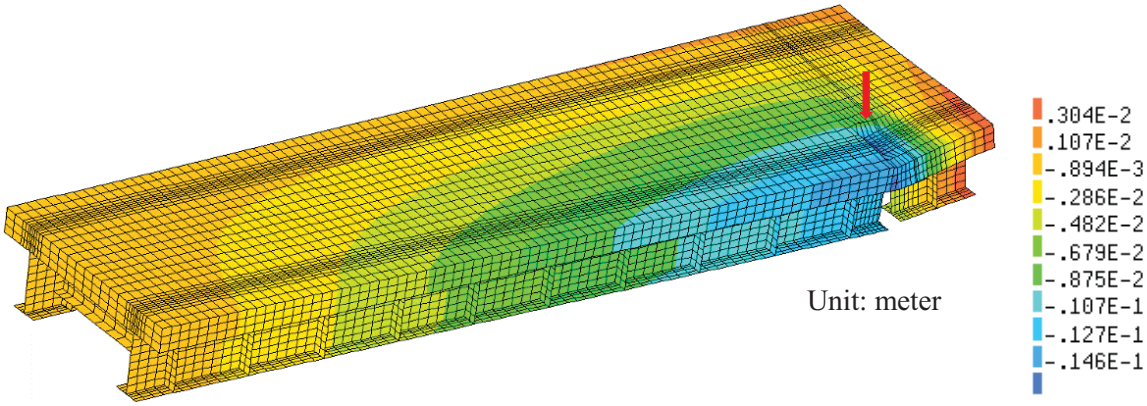

(a) Loading applied at the damaged section (Case-2a)

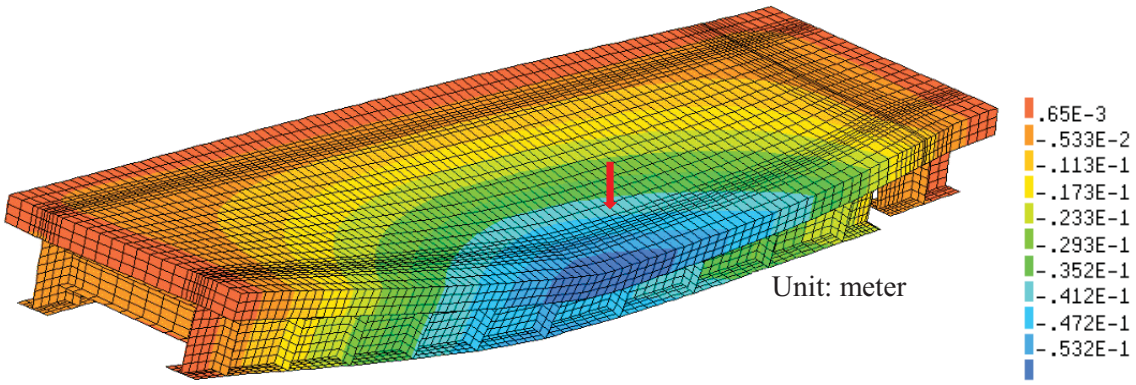

(b) Loading applied at the mid-span section (Case-2b)

Fig.4.24 Deformation of the bridge specimen (fracture near support)

4.4.2 Fracture at one-fourth of span

Fracture of whole web and bottom flange was assumed at one-fourth span section as shown in **Fig.4.25**. The damage is located at 1 m from the center of the support. Two loading cases were considered: one on the top of the damaged section (Case-3a), and another one at the mid-span section (Case-3b). The deformation corresponding to each damaged case is shown in **Fig.4.26(a)** and **Fig.4.26(b)**. Load-displacement curves were shown in **Fig.4.27**. For Case-3a, when the load is applied on the fracture location, the bridge model failed at 417kN. For Case-3b, the bridge model failed at 537kN. Comparing to the fracture at mid-span section (Case-1), both cases in this damage scenario have higher load carrying capacity which can be also considered as less critical damaged conditions for the studied bridge model.

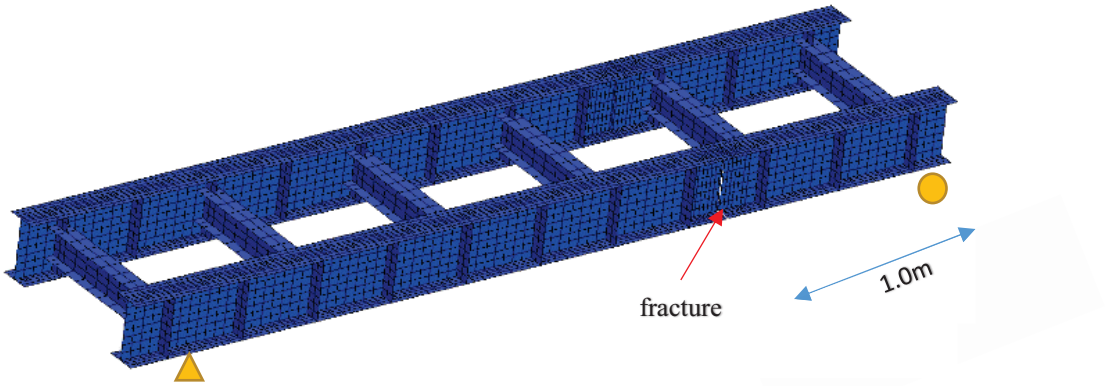

Fig.4.25 Fracture near the support location

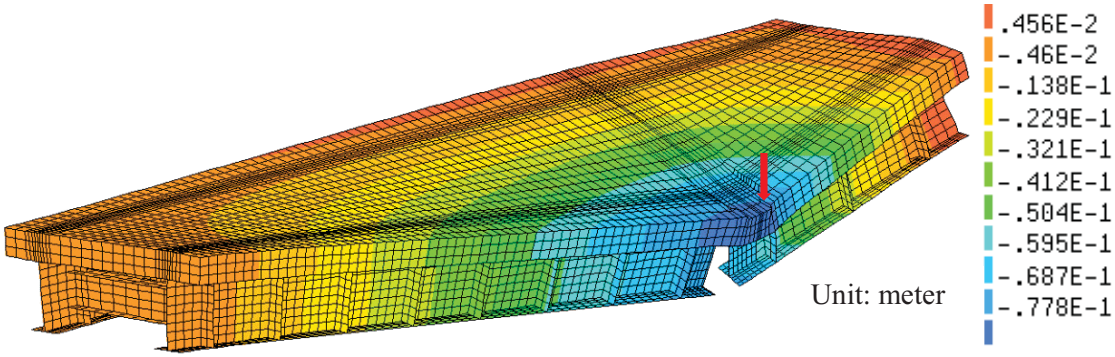

(a) loading applied at the damaged section (Case-3a)

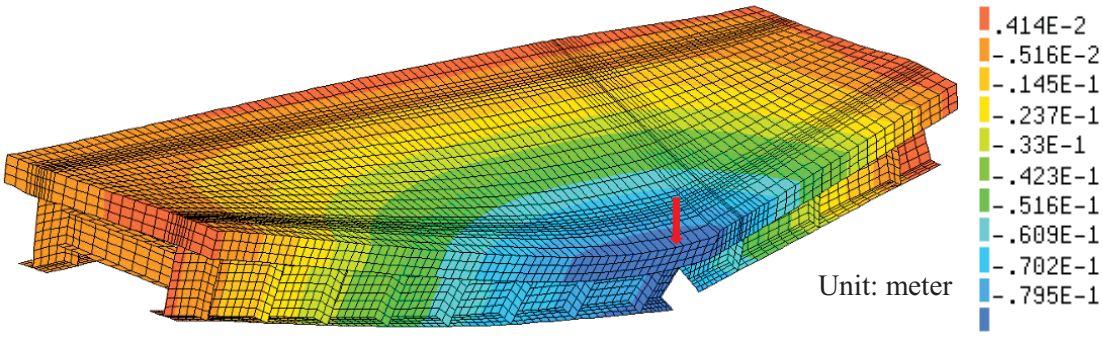

(b) loading applied at the mid-span section (Case-3b)

Fig.4.26 Deformation of the bridge specimen (fracture at one-fourth span)

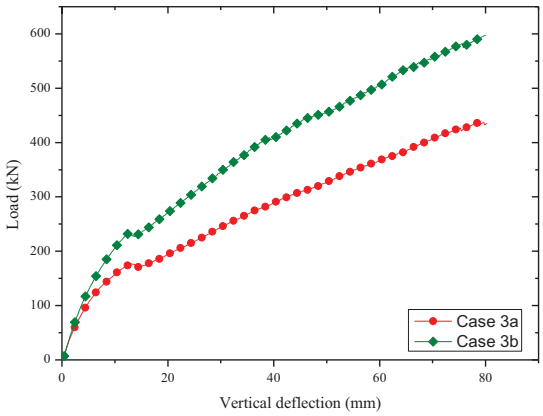

Fig.4.27 Load-displacement curves of Case-3a and Case-3b damaged cases

4.4.3 Discussion of results

Five different scenarios (including one associated with experiment program), as defined before, are included in determining the most severe fracture condition. The details of each damage case are summarized in **Table.4.3**. **Fig.4.28** summarize the load-deflection curves of all cases. According to the analyses results, two types of failures modes can be confirmed depending on the location of the fracture: bending failure and shear failure of the concrete slab. For Case-1 and Case-3a, the ultimate failure of the models is governed by bending failure which resulted in crushing of concrete slab at the fracture location. For Case-2b and Case-3b, the ultimate failure is also governed by bending failure resulted in crushing of concrete at the mid-span section, but not at the fracture section. For Case-2a, as loading condition and fracture condition is near the support section, the failure is governed by the shear force act on the concrete slab. This shear failure, which causes the sudden drop of the load carrying capacity, highly reduce the ductility of the bridge system. This kind of failure is considered as brittle and highly dangerous which can result in the sudden collapse of the bridge system. From the viewpoint of load carrying capacity and redundancy of damaged cases, it is clearly indicated that the damage imposed at the mid-span (Case-1) has the lowest load carrying capacity and redundancy level compared to other cases (as shown in Table.4.3) and can be considered as the most fracture critical location in this study. However, if a thinner (slender) slab is used, the most critical fracture location may shift from mid-span section to near support section depending on the shear strength of the concrete slab. Furthermore, the shear failure of concrete slab resulted from fracture near support location (Case-2a) is found brittle which can result in the catastrophic collapse of the bridge system. It is suggested that both fractures near the support and mid-span section should be considered in evaluating the performance and safety of the bridge in fracture condition for composite twin I-girder bridge system.

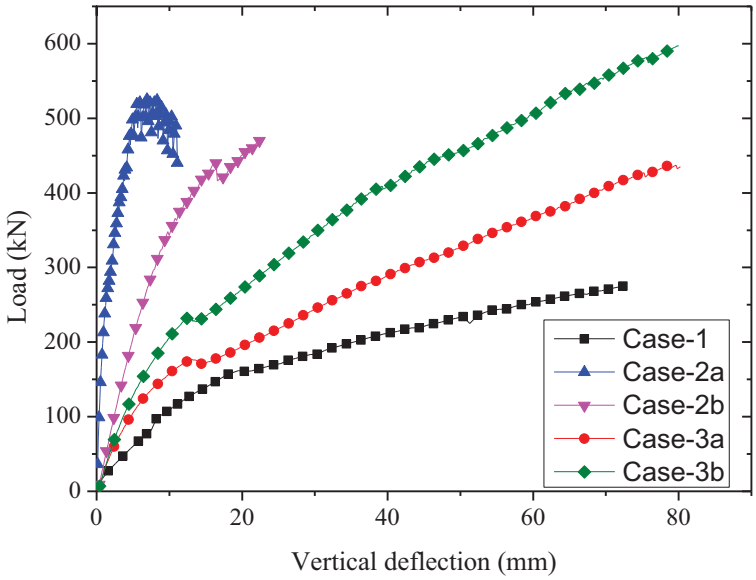

Fig.4.28 Load-deflection curves for different damaged conditions

Table.4.3 Details of each damaged case

Damaged cases	Damaged location	Loading point	LF_d (kN)	LF_1 (kN)	$R_d/0.5$
Case-1	mid-span	mid-span	292	427	1.36
Case-2a	near support	damaged section	532		2.49
Case-2b	near support	mid-span	464		2.17
Case-3a	1/4 span	damaged section	417		1.9
Case-3b	1/4 span	mid-span	537		2.51

4.5 Effect of Degrees of Indeterminacy

The previous study has concluded that degree of indeterminacy is not an adequate measure of the system redundancy level based on a truss model (Frangopol, 1987). However, for composite twin I-girder bridges, as systems supported by parallel girders, it is believed that degrees of indeterminacy will significantly affect the redundancy level. To evaluate the effect of degrees of indeterminacy on redundancy level of composite twin I-girder bridge, the numerical models used in this study are extended to two spans continuous and three spans continuous composite twin I-girder bridge models. Both models remain 4m in span length and all the parameters including cross section, and material properties remain the same.

4.5.1 Two-span continuous models

Fig.4.29 shows the numerical model of the two-span continuous model. One intact model and one damaged model are analyzed. The damaged model, like the simply supported span, has a fracture of the whole web and the bottom flange at the mid-span section of one main girder. The load-displacement curve is shown in **Fig.4.30**. For the intact specimen, the elastic stiffness, yield load, and the ultimate load are determined as 51.21 kN/mm, 491 kN, and 750 kN, respectively. For the damaged specimen, the elastic stiffness and ultimate load are determined as 23.13 kN/mm and 436 kN, respectively. The fracture of the whole web and bottom flange at mid-spans section results in 55% reduction of system stiffness and 42% reduction of ultimate load carrying capacity as shown in **Table.4.4**. In this study, the failure mode of both intact and damaged specimen is governed by the crush of the concrete slab at the loading point. The deformation of the both intact and damaged model at ultimate load is shown in **Fig.4.31** and **Fig.4.32**.

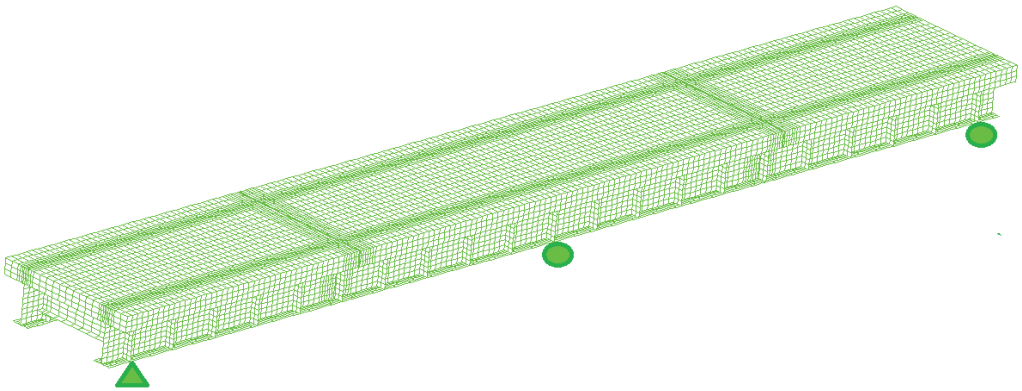

Fig.4.29 Overview of the 2-span bridge model

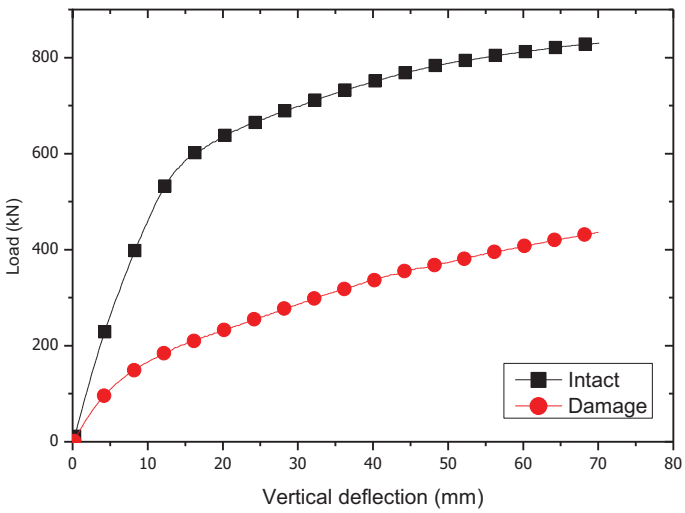

Fig.4.30 load-deflection curves of the 2-span bridge models

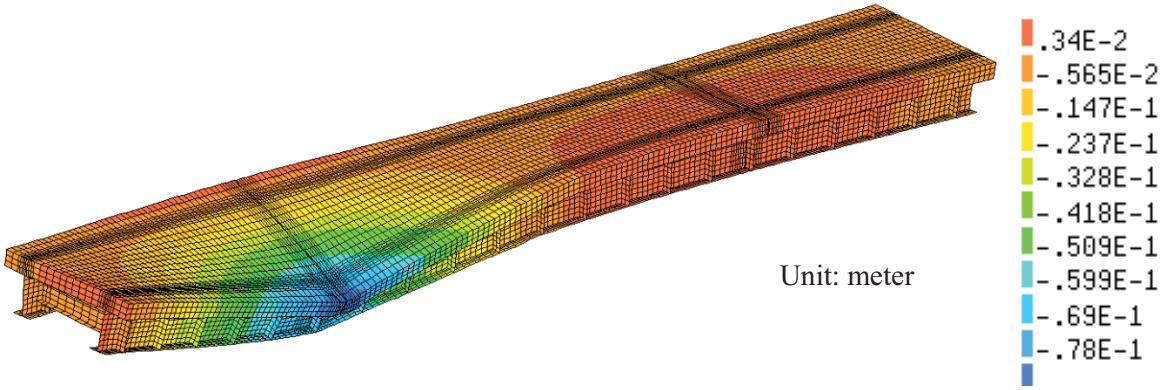

Fig.4.31 Deformation of intact specimen (2-span bridge model)

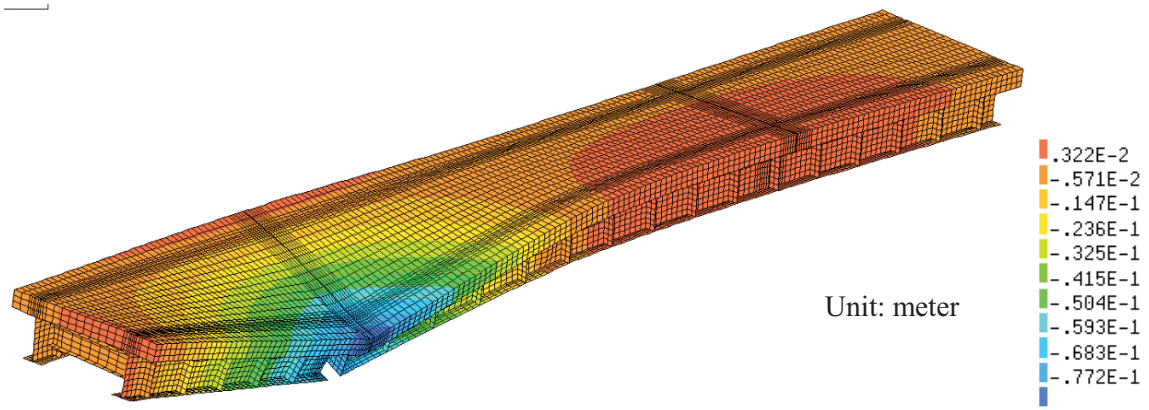

Fig.4.32 Deformation of damaged specimen (2-span bridge model)

Table.4.4 Summary of analyses results for 2-span continuous bridge models

	Elastic stiffness (kN/mm)	Yield load (kN)	Ultimate load (kN)	Failure mode
Intact	51.21	491	750	Concrete crush
Damage	23.13	-	436	Concrete crush
Ratio (D/I)	45%	-	58 %	
Reduction (D/I)	55%	-	42%	

4.5.2 Three-span continuous models

Fig.4.33 shows the numerical model of the three-span continuous model. One intact model and one damaged model are analyzed. The damaged model has a fracture of the whole web and the bottom flange at the mid-span section of one main girder. The damage is located at the side span which considered as more critical than the middle span. The load-displacement curve is shown in **Fig.4.34**. For the intact specimen, the elastic stiffness, yield load, and the ultimate load are determined as 51.24 kN/mm, 499 kN, and 879 kN, respectively. For the damaged specimen, the elastic stiffness and ultimate load are determined as 25.24 kN/mm and 445 kN, respectively. The fracture of the whole web and bottom flange at mid-spans section results in 49% reduction of system stiffness and 42% reduction of ultimate load carrying capacity as shown in **Table.4.5**. In this study, the failure modes of both intact and damaged specimens are governed by the crush of the concrete slab at the loading point. The deformations of the both intact and damaged model at ultimate load are shown in **Fig.4.35** and **Fig.4.36**.

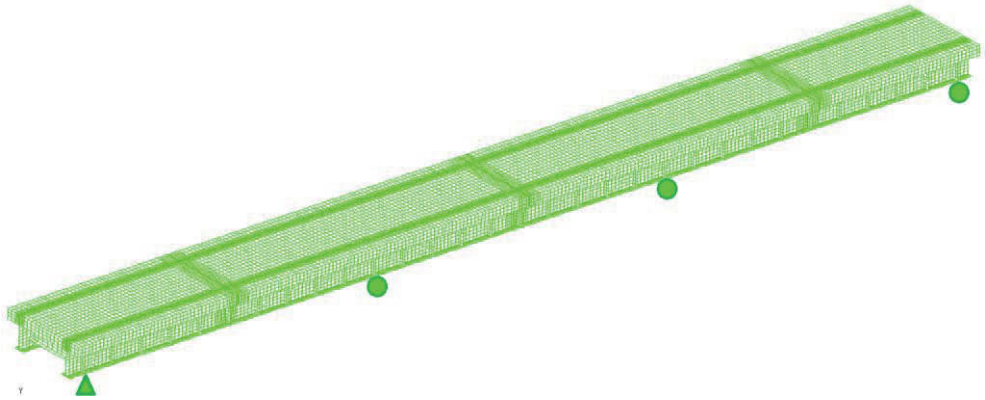

Fig.4.33 Overview of three-span model

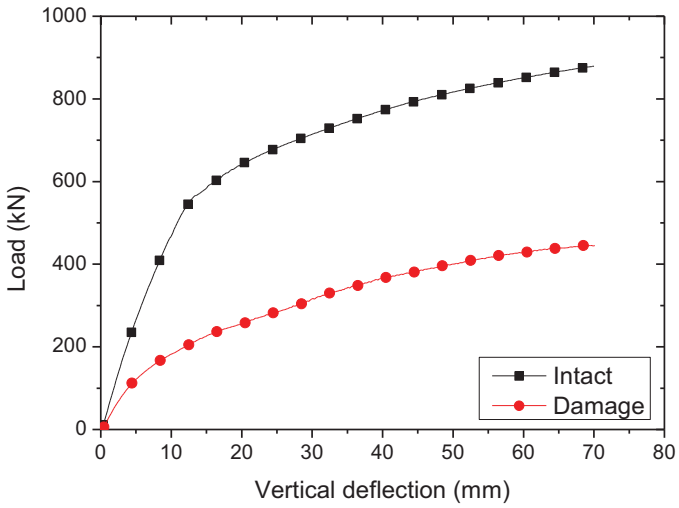

Fig.4.34 Load-deflection curves of 3-span bridge models

Table.4.5 Summary of analyses results for 3-span models

	Elastic stiffness (kN/mm)	Yield load (kN)	Ultimate load (kN)	Failure mode
Intact	51.24	499	879	Concrete crush
Damage	25.24	-	445	Concrete crush
Ratio (D/I)	49%	-	51%	
Reduction (D/I)	51%	-	49%	

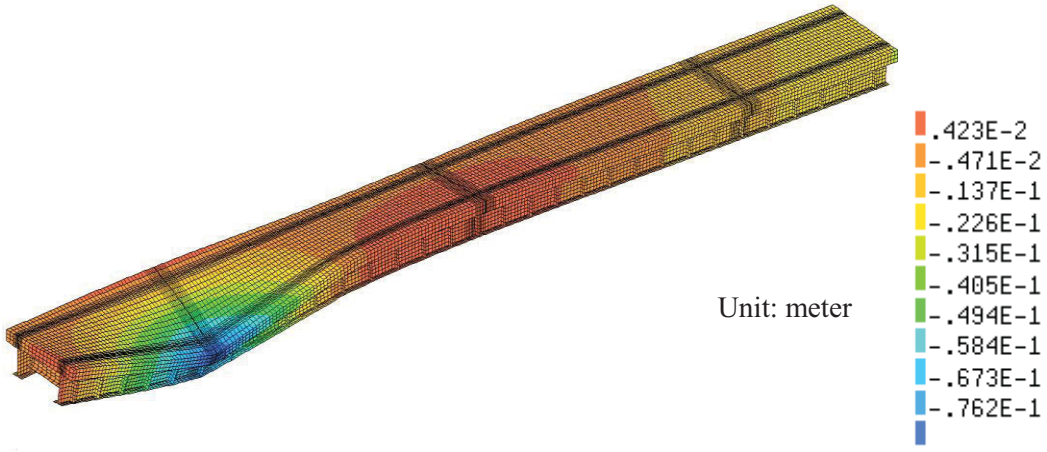

Fig.4.35 Deformation of intact specimen (3-span model)

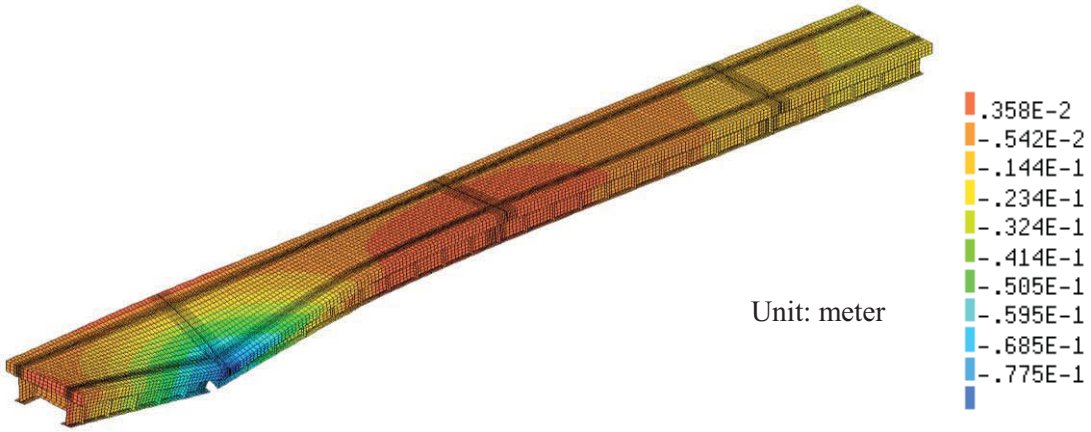

Fig.4.36 Deformation of damaged specimen (3-span model)

4.5.3 Discussion on the analyses results

From the numerical results, it is clearly indicated that the redundancy level of damage limit state highly increases when the model is extended from 1-span to 2-span. The less significant difference is found between the 2-span and 3-span comparing to those of 1-span and 2-span. From the load-deflection curves, as shown in **Fig.4.37**, the behaviors of the 2-span model and 3-span model are almost the same in the elastic state (deflection less than 18mm). The curve starts to deviate from each other after the yield point; the larger difference can be observed when the displacement becomes large enough. This can show that in the process of deformation, a portion of the load is redistributed from one span to another span. It can be concluded that the redundancy level of the bridge increases as the number of continuous span increases. The redundancy evaluation is summarized in **Table.4.6**. Results show that significant increase of redundancy level can be achieved especially in damaged condition by using the continuous span instead of the simply supported span for composite twin I-girder bridges. The alternative load paths in composite twin I-girder bridge system, to this point, are confirmed to transfer parallelly from damaged girder to intact girder in the transversal direction, and horizontally from damaged span to the intact span in the continuous systems. In both cases, the concrete slab is served as a very important member in load transfer.

Table.4.6 Effect of degree of indeterminacy on the redundancy factor

Model	LF_1 (kN)	LF_u (kN)	LF_f (kN)	LF_d (kN)	$\frac{R_u}{1.30}$	$\frac{R_f}{1.10}$	$\frac{R_d}{0.50}$	$\emptyset_R$
Simple span	427.00	704.00	621.00	292.00	1.27	1.32	1.37	1.27
Two-span continuous	491.00	830.00	750.00	436.00	1.30	1.39	1.78	1.30
Three-span continuous	499.00	879.00	772.00	445.00	1.36	1.41	1.78	1.36

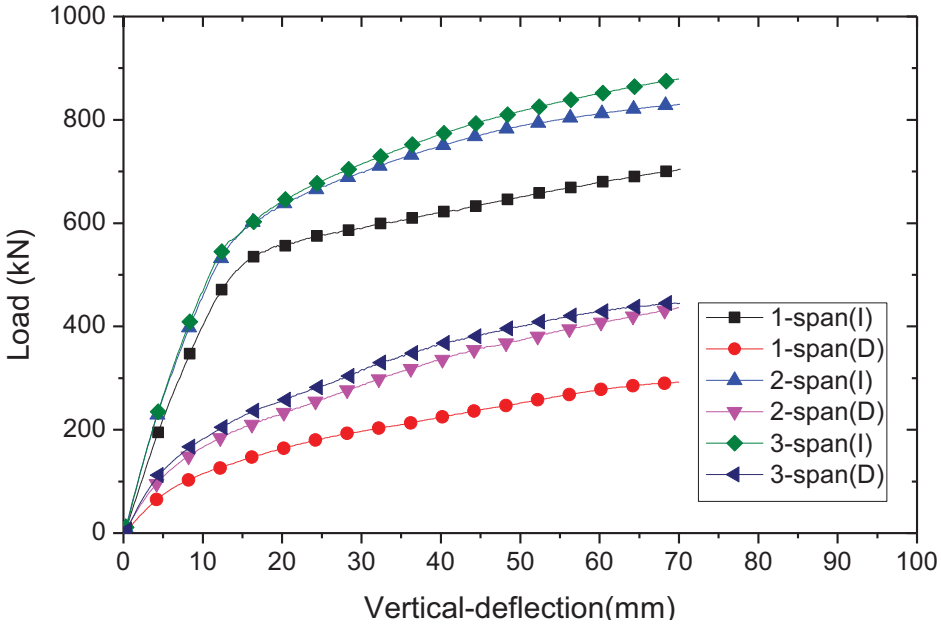

Fig.4.37 Load deflection curve of simple span, 2-sapn, and 3-span bridge models

4.6 Effect of Thickness of Concrete Slab and Concrete Strength

For composite twin I-girder bridge systems, the concrete slab serves as a very important element in redistributing the load from damaged girder to the intact girder and from damaged span to the intact span in continuous systems. This contribution will reduce the possibility of bridge collapse after the fracture of the main steel girder. In order to evaluate the effect of the concrete slab on the safety of the bridge, numerical analyses were carried out for the bridge models at different slab thicknesses (100 mm, 120 mm, and 150 mm) and concrete strengths (25 MPa, 33 MPa, and 40 MPa). Different combinations of the concrete slab thickness and concrete strength are shown in **Table.4.7**. For each case of strength and thickness, numerical analyses were performed on both the one-span (simply supported) and two-span bridge models (continuous). The increment in the self-weight owing to the increase in the thickness of the concrete slab was included in the analyses. The use of a thicker concrete slab or higher concrete strength normally increases both the yield load and the ultimate load of the intact specimen and the damaged specimen, resulting in a stronger structure, but this does not guarantee the increment of redundancy factor as the redundancy factor depends on the comparison between ultimate load and first member failure load. The results of the analyses are shown in **Table.4.7** and the effect of the concrete slab on each system reserve ratio is shown in **Fig.4.38**, **Fig.4.39**, and **Fig.4.40**.

Table.4.7 Different cases of slab thickness and concrete strength

Strength (MPa)	Thickness		
	100mm	120mm	150mm
25	100-C25	120-C25	150-C25
33	100-C33	120-C33	150-C33
40	100-C40	120-C40	150-C40

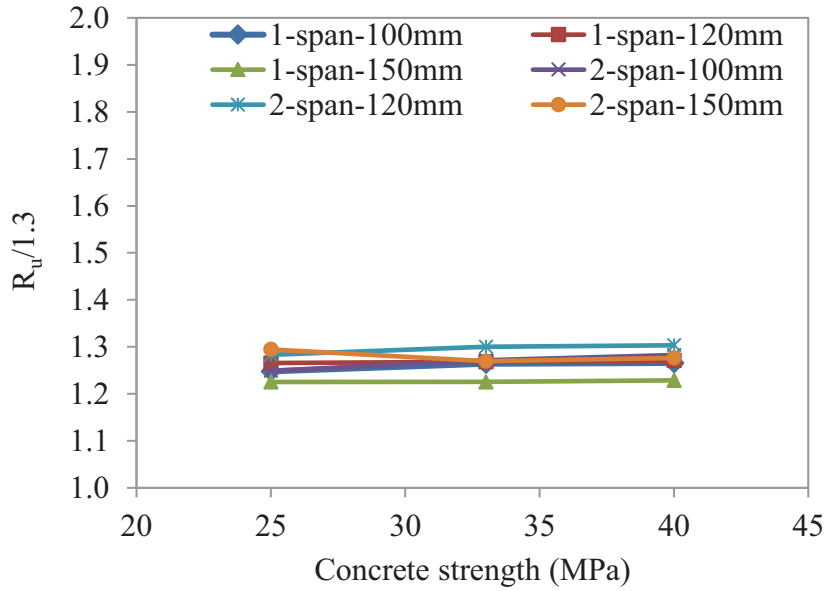

(a) Effect of concrete strength on system reserve ratio R_u

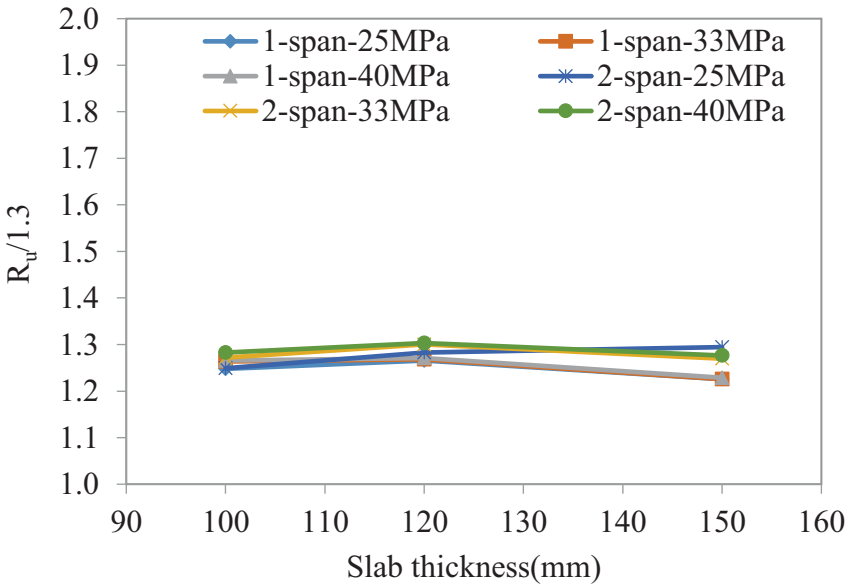

(b) Effect of slab thickness on system reserve ratio R_u

Fig.4.38 Effect of concrete strength and slab thickness on system reserve ratios R_u

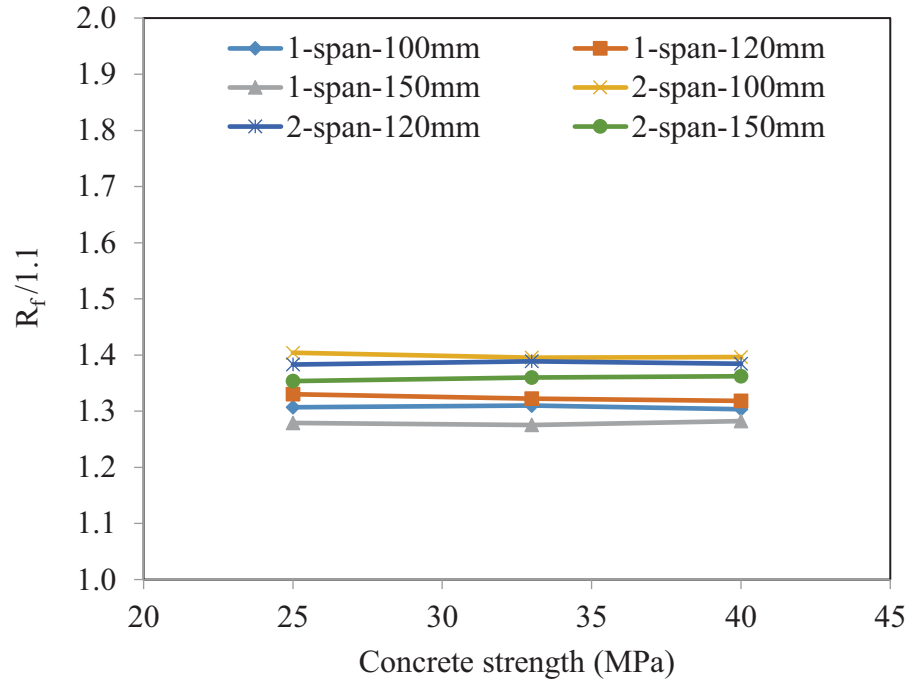

(a) Effect of concrete strength on system reserve ratio R_f

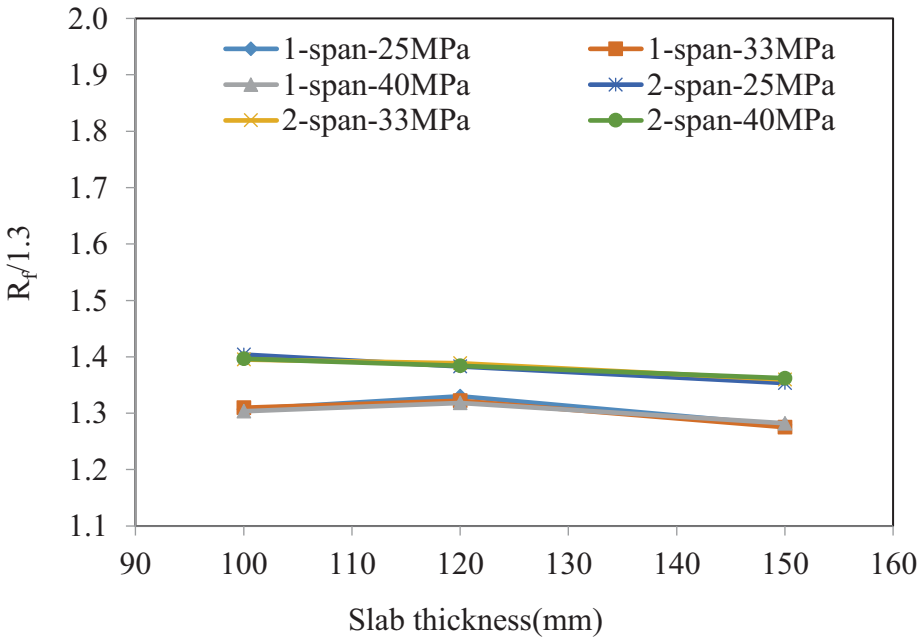

(b) Effect of slab thickness on system reserve ratio R_f

Fig.4.39 Effect of concrete strength and slab thickness on system reserve ratios R_f

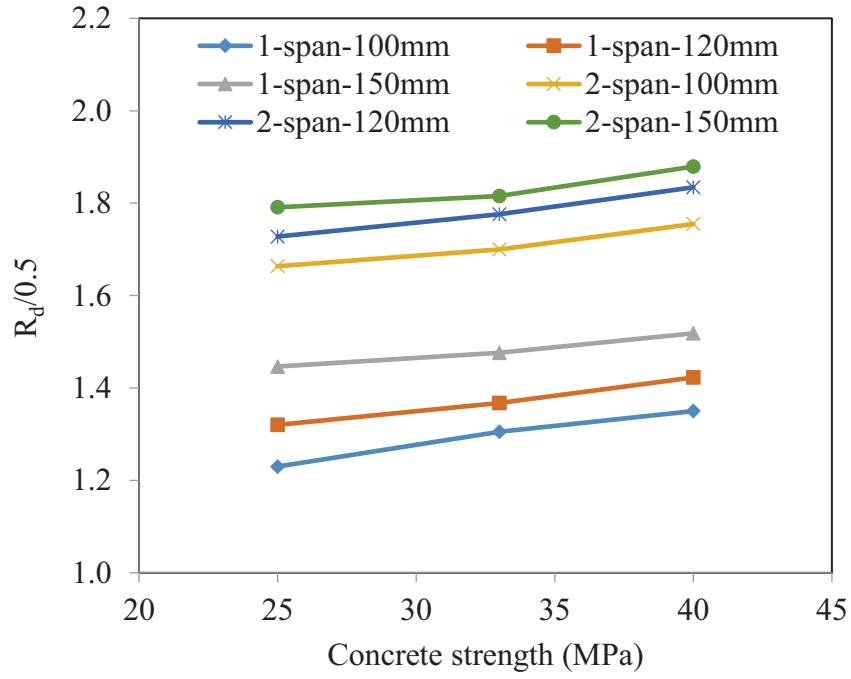

(a) Effect of concrete strength on system reserve ratio R_d

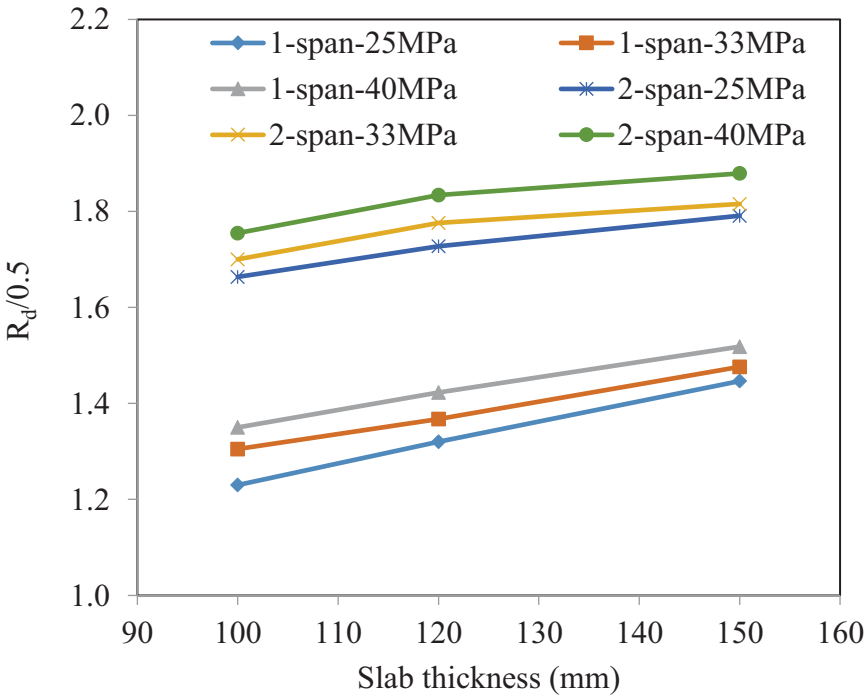

(b) Effect of slab thickness on system reserve ratio R_d

Fig.4.40 Effect of concrete strength and slab thickness on system reserve ratios R_d

Table.4.8 Redundancy factor for the bridge models with different slab thickness and concrete strength

	Model	LF_1 (kN)	LF_u (kN)	LF_f (kN)	LF_d (kN)	$\frac{R_u}{1.30}$	$\frac{R_f}{1.10}$	$\frac{R_d}{0.50}$	φ_R
Simple span	Experiment	426.00	668.00	599.00	275.00	1.21	1.28	1.29	1.21
	100-C25	368.00	597.00	529.00	227.00	1.25	1.31	1.23	1.23
	100-C33	381.00	626.00	549.00	249.00	1.26	1.31	1.31	1.26
	100-C40	392.00	645.00	562.00	265.00	1.27	1.30	1.35	1.27
	120-C25	406.00	668.00	594.00	268.00	1.27	1.33	1.32	1.27
	120-C33	427.00	704.00	621.00	292.00	1.27	1.32	1.37	1.27
	120-C40	440.00	727.00	638.00	313.00	1.27	1.32	1.42	1.27
	150-C25	477.00	760.00	671.00	345.00	1.23	1.28	1.45	1.23
	150-C33	504.00	803.00	707.00	372.00	1.23	1.28	1.48	1.23
	150-C40	519.00	829.00	732.00	394.00	1.23	1.28	1.52	1.23
Two-span	100-C25	428.00	695.00	661.00	356.00	1.25	1.40	1.66	1.25
	100-C33	447.00	739.00	686.00	380.00	1.27	1.40	1.70	1.27
	100-C40	457.00	762.00	702.00	401.00	1.28	1.40	1.75	1.28
	120-C25	470.00	784.00	715.00	406.00	1.28	1.38	1.73	1.28
	120-C33	491.00	830.00	750.00	436.00	1.30	1.39	1.78	1.30
	120-C40	507.00	859.00	772.00	465.00	1.30	1.38	1.83	1.30
	150-C25	536.00	902.00	798.00	480.00	1.29	1.35	1.79	1.29
	150-C33	575.00	949.00	860.00	522.00	1.27	1.36	1.82	1.27
	150-C40	596.00	989.00	893.00	560.00	1.28	1.36	1.88	1.28

Fig.4.38, Fig.4.39, and **Fig.4.40** show the effect of concrete thickness and concrete strength on the system reserve ratio R_u, R_f , and R_d of the composite twin I-girder bridge, respectively. The numerical results indicate that the system reserve ratio for ultimate limit state R_u (as shown in **Fig.4.38(a)** and **Fig.4.38(b)**) and system reserve ratio for service limit state R_f (as shown in **Fig.4.39(a)** and **Fig.4.39(b)**) are less likely to be affected by the changing of concrete strength or the slab thickness. Employing stronger concrete strength or thicker concrete slab cannot directly increase or decrease these two system reserve ratios and vice versa. For the system reserve ratio for the damage limit state, as shown in **Fig.4.40(a)** and **Fig.4.40(b)**, numerical results show that the use of stronger concrete strength and thicker concrete slab can directly increase the redundancy factor R_d for both simply supported and continuous 2-span bridge systems. The results clearly indicated that concrete slab is very effective for load redistribution when damage occurs on the bridge systems. It also clearly indicates the significant redundancy factor increment for damage limit state between simply supported model and two spans continuous models. Given the fact that redundancy level of the bridge system is generally considered as the capability of the bridge to survive and carry some traffic load in damaged condition, a more redundant and safer bridge design of composite twin I-girder bridge can be achieved by employing a stronger and thicker concrete slab.

4.7 Conclusions

Numerical study was carried out to understand the redundancy rating level and also the mechanical behavior of the composite twin I-girder bridge under extreme loading conditions and fracture conditions. Experimental studies and numerical analyses were carried out for both intact system and damage system on simply supported composite twin I-girder bridges. A significant reduction in system stiffness and load-carrying capacity was confirmed in post-fracture condition. Meanwhile, the failure mode of both the test specimens used in this study was governed by the crushing of the concrete slab. The validation of the numerical model is based on comparison with the experimental results including the load-strain curves, load deflection curves, failure modes, and redundancy factor. By introducing the finite element method with nonlinear analyses, numerical analyses were performed to determine the effectiveness of the concrete slab and degree of indeterminacy on redundancy level of the current bridge models. The findings from this study can be summarized as described below:

- Depending on the fracture locations, two types of failure modes were confirmed in this study: bending failure mode and shear failure mode. While the bending failure mode is found to be the most critical in terms of the load-carrying capacity, the shear failure mode is found to be brittle, which can result in the sudden collapse of the bridge.

- The concrete slab is the key element for load redistribution in the fracture condition for composite twin I-girder bridge systems. While increasing both concrete strength and thickness is found to be effective against the fatigue crack condition, increasing the concrete strength is a viable choice in terms of safety and cost. Furthermore, increasing the thickness of the slab can improve the durability of the structure as well as the performance in the fracture condition; in particular, it increases the shear capacity of the concrete slab against shear failure, which is brittle and dangerous.

- The use of a continuous span instead of a simple span for the composite twin I-girder bridge system can significantly increase the load ratio between the damaged and intact structures. Thus, the effect of the fracture of whole web and bottom flange on the performance and safety of the bridge system can be largely reduced by using the continuous system. A continuous span is highly recommended for use in composite twin I-girder bridges.

- Based on the experimental and numerical results, composite twin I-girder bridges in this study have an adequate level of redundancy and can be classified as non-fracture critical bridge system.

All in all, in the design of a composite twin I-girder bridge, it is recommended to employ a continuous girder bridge with strong and thick concrete slab in order to achieve a high level of redundancy. Meanwhile, a continuous span is highly recommended for use in composite twin I-girder bridges. Moreover, it is suggested that both fractures near the support and mid-span section should be considered in evaluating the performance and safety of the bridge in fracture condition for composite twin I-girder bridge system.

Reference

AASHTO (American Association of State Highway and Transportation Officials). (2012). "AASHTO LRFD Bridge Design Specification." 6th edition, Washington, DC.

CEN (European Committee for Standardization). (1992). "Design of Concrete Structures." Eurocode 2, Brussels.

Connor, R.J., Dexter R., and Mahmoud H. (2005). "Inspection and Management of Bridges with Fracture Critical Details." NCHRP Synthesis 354, National Cooperative Highway Research Program, Washington, DC.

Daniels, J. H., Kim, W., and Wilson J.L. (1988). "Recommended Guidelines for Redundancy Design and Rating of Two-Girder Steel Bridges." NCHRP Report 319, National Cooperative Highway Research Program, Washington, DC.

Deng, L., Wang, W., and Yu, Y. (2016). "State-of-the-Art Review on the Causes and Mechanisms of Bridge Collapse." Journal of Performance Construction Facility, ASCE, Vol. 30, No. 2, 04015005.

Diana User's manual- Release 9.4.4 (2012), TNO Building and Construction Research, Delft, Netherlands.

DÖRR, K. (1980). "Ein Beitrag zur Berechnung von Stahlbetonscheiben unter besonderer Berücksichtigung des Verbundverhaltens." Ph.D. thesis, University of Darmstadt (in German)

FHWA (Federal Highway Administration) (2012). Steel Bridge Design Handbook: Redundancy, Vol. 9, No. FHWA-IF-12-052, Washington, D.C.

Ghosn, M. and Moses, F. (1998). "Redundancy in Highway Bridge Superstructure." NCHRP Report 406, National Cooperative Highway Research Program, Washington, DC.

Ghosn, M., Moses, F., and Frangopol, D.M. (2010). "Redundancy and Robustness of Highway Bridge Superstructures and Substructures." Structures and Infrastructure Engineering, Vol 6, No 1-2, pp. 257-278.

Ghosn, M. and Yang, J. (2014). "Bridge System Safety and Redundancy." NCHRP Report 776, National Cooperative Highway Research Program, Washington, DC.

Hendawi, S. and Frangopol, D.M. (1994). "System Reliability and Redundancy in Structural Design and Evaluation." Journal of Structural Safety, Vol. 16, No.1-2, pp. 47-71.

Hunley, T.C., and Harik, I.E. (2011) "Structural redundancy evaluation of steel tub girder bridges." J. bridge eng., ASCE, Vol. 17, pp.481-489.

Idriss, R. L., White, K. R., Woodward, C. B., and Jauregui, D. V. (1995). “After-fracture redundancy of two-girder bridge: Testing I-40 bridges over Rio Grande.” Proc. 4th International Bridge Engineering Conference, pp. 316-326.

JRA (Japan Road Association). (2012). "Specifications for Highway Bridges." Part I Common, English edition, Tokyo.

JRA (Japan Road Association). (2002). "Specifications for Highway Bridges." Part II Common, English edition, Tokyo.

JSCE (Japanese Society of Civil Engineers). (2002). "Standard Specification for Concrete Structures." Tokyo.

JSCE (Japanese Society of Civil Engineers). (2007)."Standard Specifications for Steel and Composite Structures." Tokyo.

Lam, H., Lin, W., and Yoda, T. (2014). “Effect of Bracing Systems on Redundancy of Three-span Composite Twin I-girder Bridge.” JSCE Journal of Structural Engineering, Vol. 60A, pp. 59-69.

Lin, W., and Yoda, T. (2013a). “Experimental and Numerical Study on Mechanical Behavior of Composite Girders under Hogging Moment.” International Journal of Advanced Steel Construction, Vol. 9, No. 4, pp. 309-333.

Lin, W., Yoda, T., Kumagai, Y., Saigyo, T. (2013b). “Numerical Study on Post-Fracture Redundancy of the Two-girder Steel-Concrete Composite Highway Bridges.” International Journal of Steel Structures, Vol. 13, No. 4, pp. 671-681.

Liu, W.D., Ghosn, M., Moses, F., and Neuenhoffer, A. (2001). “Redundancy in Highway Bridge Substructures.” NCHRP Report 458, National Cooperative Highway Research Program, Washington, DC.

Nakasu, M., and Iwatate, J. (1996). “Fatigue experiment on bond between concrete and reinforcement.” Transaction of JSCE, Vol. 426, pp. 852-853.

Neuman, B. J. (2009). “Evaluating the Redundancy of Steel Bridges: Full-scale Destructive Testing of a Fracture Critical Twin Box-girder Steel Bridge.” M.S. Thesis, The Univ. of Texas at Austin, Austin, TX.

Okada, J., Yoda, T., and Lebet, J.P. (2006). “A Study of the Grouped Arrangement of Stud Connectors on the Shear Strength.” JSCE Journal of Structural Engineering/Earthquake Engineering, Vol. 23, No. 1, pp. 75-89.

Ollgaard, J.G., Slutter, R.G., and Fisher, J.W. (1971). “Shear Strength of Stud Connectors in Lightweight and Normal Weight Concrete.” Engineering Journal of AISC, Vol. 8, No. 2, pp. 55-64.

Samaras, V.A., Sutton, J.P., Williamson, E.B., and Frank, K.H. (2012). “Simplified Method for Evaluating the Redundancy of Twin Steel Box-Girder Bridges.” J. Bridge Eng., Vol. 17, No. 3, pp. 470-480.

Selby, R.G., Vecchio, F.J. (1993). “Three-dimensional Constitutive Relations for Reinforced Concrete.” Tech. Rep. 93-02, Univ. Toronto, Toronto, Canada.

Tamakoshi, T., Yoshida, Y., Sakai, Y., and Fukunaga, S. (2006). “Analysis of Damage Occurring in Steel Plate Girder Bridges on National Roads in Japan.” Public Work Research Institute of Japan.

Vecchio, F.J., and Collins, M.P. (1986). “The modified compression field theory for reinforced concrete elements subjected to shear.” ACI Journal, Vol. 83, No. 2, pp. 219-231.

Veggeberg, K. (2011). “Data Acquisition for a Bridge Collapse Test.” Proceeding of Structural Dynamics, Society for Experimental Mechanics, Springer, Vol. 3, pp. 1313-1324.

Yamada, Y., Pengphon, S., Miki, C., Ichikawa, A., and Irube, T. (2001). “Shear Strength of Slab-anchor and Adhesion Fixing a Non-Composite Girder Bridge's Slab.” JSCE Journal of Structural Engineering, Vol. 47A, pp. 1161-1168. (in Japanese).

5. Effects of Bracing Systems on Redundancy of Continuous Composite Twin I-Girder Bridge

5.1 Introduction

Recent studies show that many bridges in Japan will reach their design service life (50 years) within less than 10 years; therefore, the safety consideration for old bridges is becoming more and more important for current bridge infrastructures in Japan. The behavior and response of the bridge after losing or damaging some part of the structural elements are getting more and more attention after several bridge collapse disasters happened around the world. The most recent well-known incident took place in United States while one span of I-5 Skagit River Truss Bridge collapsed due to the insufficiency level of redundancy after the top frame had been hit by a truck (NTSB, 2013). Other recent incident was the collapse of I-35W over Mississippi River Bridge in 2007 (NTSB, 2007). Redundancy is one of the most important factors to evaluate the safety of a bridge since it guarantees the safety of the bridge to survive after an incident initiated by partial or full damage on the critical member of the bridge. In current highway bridge designs, continuous composite twin I-girder bridge is being frequently used due to its low cost in comparison with other types of bridge. However, there is no redundancy criterion or requirements can be found in current Japanese standard specifications. Meanwhile, in the United States, all types of two girder bridges including three-span continuous composite twin I-girder bridges are considered as non-redundant bridges (AASHTO, 2012). This judgement is based on the simple assumption that after damage of one girder, the other girder will not be able to sustain the applied load that transfer from the damaged girder. Some researchers argued about this assumption that this classification is based on unrealistic concepts widely held by bridge engineers, resulting from the oversimplified assumptions normally used in design, and not on the realistic behavior of the as-built three-dimensional structures (Daniels et al., 1988; Idriss et al., 1995; Connor et al., 2005). However, in the actual situation, the damaged girder wouldn't lose completely its capacity of supporting the load due to its continuous system of the girder, deck and the bracing

systems that can somehow effectively transfer the load and distribute to other parts of elements of the structure which we call the alternate load path. This present chapter is focusing on the mechanical behavior of the continuous composite twin I-girder bridges in the intact system (bridge without damage) and damaged system (bridge initially have one damaged member) after yielding of main girder. The first part of this chapter is focusing on the experimental model of a three-span continuous composite twin I-girder bridge performed by Park et al. (Park et al., 2012). It is believed that the bracing systems act as a very important role in establishing the alternate load paths that can guarantee the safety of the bridge and fulfill the redundancy criteria of the bridge. For this reason, analyses on the failure modes and the effectiveness of bracing systems were carried out by performing parametric study on the effect of the secondary members including transverse beams at bottom lateral cross bracing system. The secondary member is believed to be able to increase the load-carrying capacity of the bridge system in both intact and damaged conditions despite the ignorance of its effect in current civil engineering design and practice. To verify and validate the effect of the bracing system on the actual bridge system, numerical study focusing on a full scale five span continuous bridge model is carried out in the later part of this chapter.

5.2 Redundancy Evaluation Method

Research on redundancy rating and evaluation method has been interested in early 1970s as many bridges were shown to have alternate load path, but is hard to identify (Csagoly and Jaegar, 1979). In the later years, research focuses on the effect of damage and redundancy on the reliability of structural system based on a definition of structural redundancy including both system reliability and damaged assessment concepts (Frangopol, 1987). A simple truss system was being introduced and a clear effect of damage on load carrying capacity of the structure was defined. Even though the redundancy rating method or the sufficient redundancy level remains in question, the research led to the new concept that the redundancy should depend on the system behavior rather than the failure of a single member. Although computer analysis software was already available during 1990s, the redundancy rating on real bridge is still a difficult task because the real bridge response is very complicate after damaged or failure of members. Further effort is needed to collect data on bridge loading and behavior, to consistently

deal with insufficient knowledge on bridge response, and to implement system reliability-based factors in bridge design and evaluation specifications (Frangopol, 1992). Referring to The National Bridge Inspection Standards (NBIS) and AASHTO Manual for Bridge Evaluation, identifying Fracture Critical Member (FCM) is needed to study the redundancy rating and evaluation of bridge structure. The FCMs are defined in AASHTO as Steel tension members or steel components of members whose failure would be expected to result in collapse of the bridge (AASHTO, 2012). NBIS defines FCM as a steel member in tension, or with a tension element, whose failure would probably cause a portion of or the entire bridge to collapse (NBIS, 2012). With multiple interpretations for "failure," "probably," "expected" and "collapse," just as for redundancy, a good, universally accepted definition does not exist for fracture-critical members or bridges (FHWA, 2012).

Up to now, the redundancy rating method has never been clearly defined and worldwide accepted in civil engineering practice. A good, concise, universally accepted definition of redundancy does not currently exist in the bridge design or evaluation specifications (FHWA, 2012). Work is under way within the steel bridge industry, AASHTO and the Federal Highway Administration to better define redundancy and fracture-critical member requirements (FHWA, 2012). Currently, redundancy can be classified into three categories according to the redundancy concept including load path redundancy, structural redundancy, and internal redundancy. However, the understanding of these three types of redundancy is not enabling civil engineers to clearly define or justify the redundancy level of the bridges at all. In fact, understanding these three types of redundancy classifications will only allow researchers to understand the possibility of alternate load path. Several studies have been performed to understand and to rate the redundancy of a bridge. In order to determine the redundancy rating method, the most commonly used method is the method developed in NCHRP Report 406 (Ghosn and Moses, 1998). This method is based on reliability analyses which provide quantitative limit of redundancy of bridge structure (Hunley and Harik, 2011). In the report, an attempt to quantify the level of redundancy was made based on the system reliability principles and the widely-accepted idea among other researchers that all simply supported four girder bridges can be classified as redundant. A parametric study based on finite element method includes several bridges types, different span length and different number of

girders and its spacing was presented with the recommendation for civil engineering to determine and judge the redundancy of bridge. According to this method, to satisfy the redundancy criteria and calculate the redundancy factor, four loading factors are needed to determine by using three-dimensional models with non-linear analyses. **Fig.5.1** shows the typical behavior of bridge system (Ghosn et al., 2010). The graph shows the load-displacement curve of typical bridge behavior under vertical load. The curve labeled with "Intact System" represents the bridge system without any structural or elemental damage. The load that makes the first member failed or reaches yielding limit is defined as LF_1. LF_u is the ultimate load carrying capacity of the intact bridge system. Before bridge reaches ultimate state, large displacements may occur at certain load level, which makes the bridge unfit for used and is define as LF_f. For the damaged bridge, only the ultimate failure load is concerned and defined as LF_d. Three system reserve ratio for each limit states were proposed for quantify the redundancy of the bridge systems and are defined as follows (Ghosn and Moses, 1998):

$$R_u = \frac{LF_u}{LF_1} \tag{5.1}$$

$$R_f = \frac{LF_f}{LF_1} \tag{5.2}$$

$$R_d = \frac{LF_d}{LF_1} \tag{5.3}$$

where:

- R_u : system reserve ratio for the ultimate limit state (Ghosn and Moses, 1998)
- R_f : system reserve ratio for the functionality limit state (Ghosn and Moses, 1998)
- R_d : system reserve ratio for the damaged condition (Ghosn and Moses, 1998)

These reserve ratios are deterministic and can explain the level of redundancy by its value. For example, the bigger value of R_u means the higher level of redundancy as the ultimate capacity LF_u of bridge is higher compared to the first member failure load LF_1. However, minimum acceptable values of R_u, R_f and R_d need to be established according to the bridge that are clearly redundant in current engineering practice. As mentioned earlier, four girders simply supported bridge which are generally considered as redundant

bridges are considered as the target to determine the minimum acceptable values of R_u, R_f and R_d. According to the results provided by NCHRP Report 406, the average values of R_u, R_f and R_d for four girders simply supported steel bridge and pre-stressed bridge is found as 1.3, 1.1, and 0.5, respectively. To this point, the redundancy factor φ_s was proposed and can be calculated by using the following equation:

$$\varphi_s = min\ \left(\frac{R_u}{1.3}; \frac{R_f}{1.1}; \frac{R_d}{0.5}\right) \tag{5.4}$$

If the value of φ_s is larger than one, then the bridge can be considered as redundant and safety factor can be reduced according to the value of φ_s that exceeds 1.0. Otherwise, it should be considered as non-redundant and the safety factor must be increased to achieve a uniform level of safety.

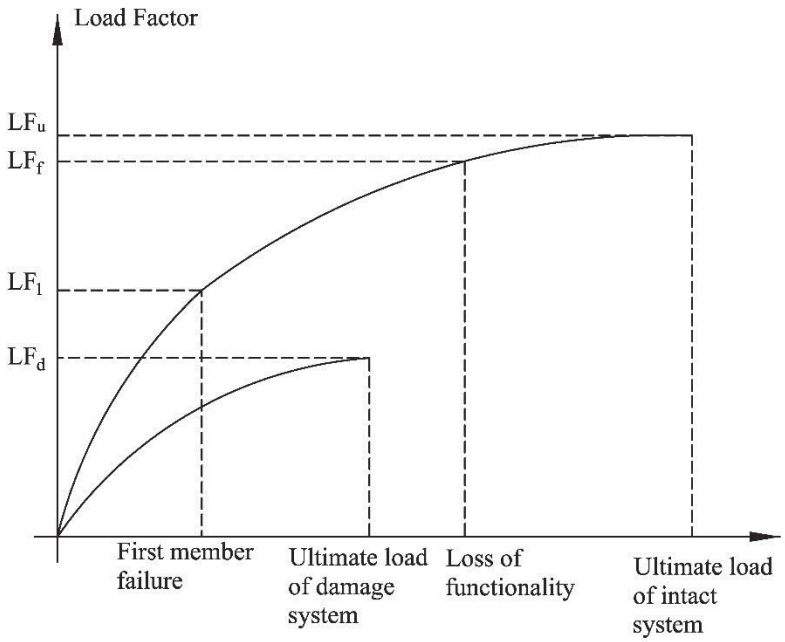

Fig.5.1 Typical behavior of bridge system (Ghosn and Moses, 1998)

5.3 Model Description and Analyses Method

5.3.1 Bridge model validation

Computer Software TNO Diana 9.4.4 was used to simulate and analyze the bridge models (Diana User's Manual, 2012). Finite Element Method with non-linear analysis and load increment method is used to study the behavior and collapse mechanism of the bridge. The detail of numerical model can be found in the following. To validate the numerical model, comparison with the experimental data is made on a half model of three span continuous twin I-girder bridge. The half models of three span continuous bridges with span length 8m+4.5m (shown in **Fig.5.2**) were tested under point loads with the severely damaged condition (through crack) of web and bottom flanges below the loading location shown in **Fig.5.3** (Park et al., 2012). Two specimens were tested including one with and another one without X-type bottom lateral bracing. L-50×50×6 angles were selected to comprise X-type lateral bracings in the second specimen. Results show that the bottom X-type lateral bracing is effective in increasing the load carrying capacity of the system in the damaged condition. The damaged condition of tested bridge is as shown in **Fig.5.3**. The experimental result is valuable for further research into the effectiveness of the secondary member of composite twin I-girder bridge in the following study. **Fig.5.4** shows the experimental result and the numerical result of the load-displacement curve of tested bridge. The stiffness of the structural system in the numerical result has a good agreement with the experimental result. Both the yielding load and the ultimate load were found to be in good agreement between numerical and experimental results. Same failure mode was obtained at the ultimate state. The numerical model is proved to be able to accurately estimate the performance of the damaged bridge in both pre- and post- elastic behaviors. This model is used to make further investigations on the effect of bracing systems on the redundancy behavior of three-span composite twin I-girder bridges.

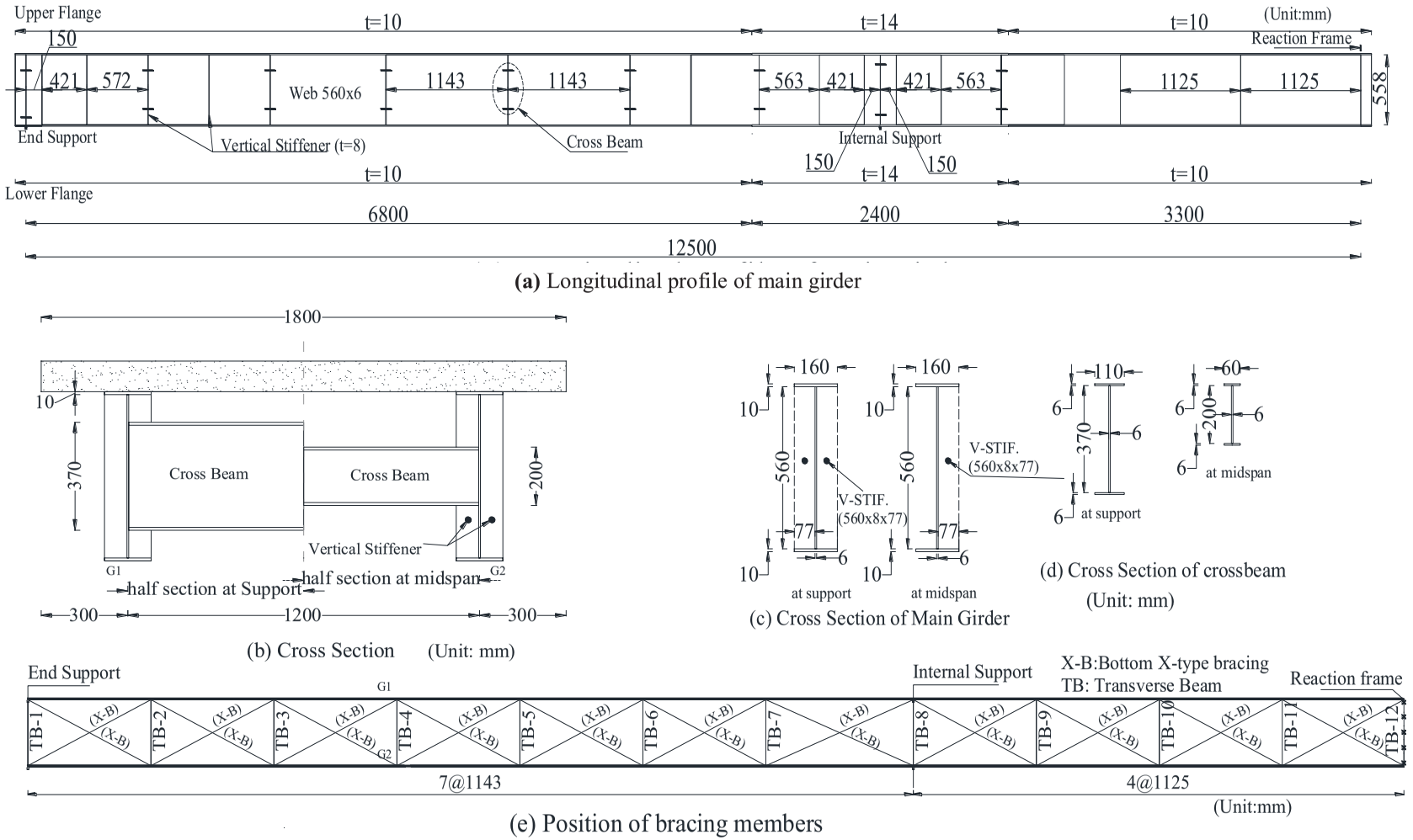

Fig.5.2 Configuration of the bridge model (Park et al., 2012)

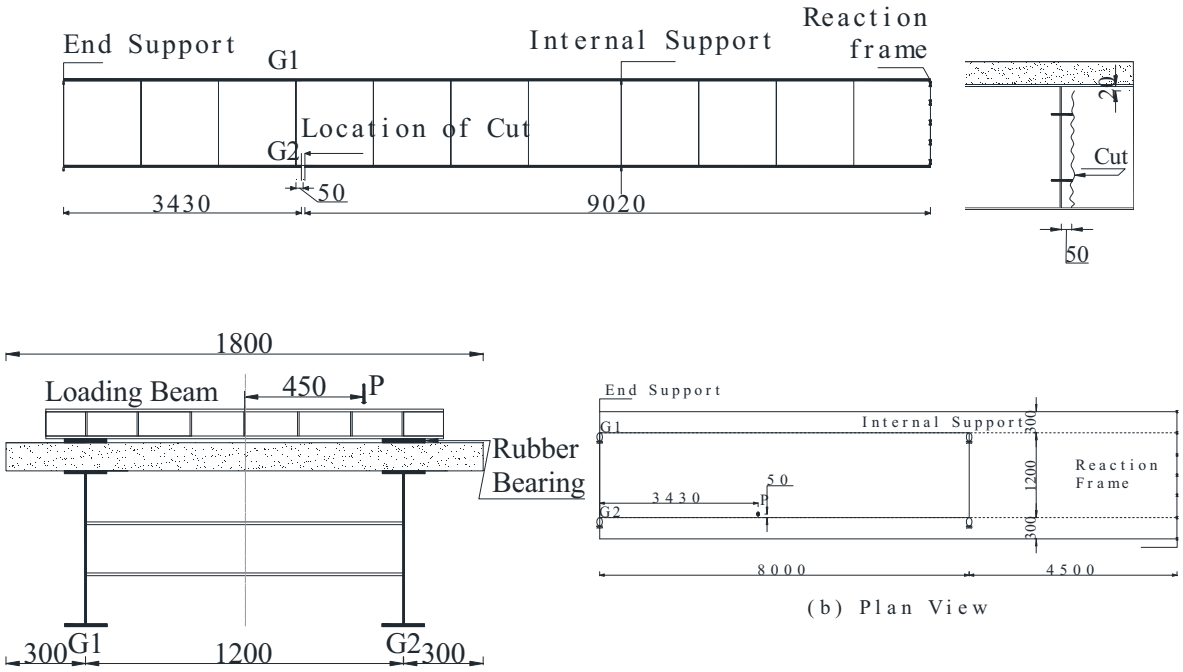

(a) Section View

Fig.5.3 Damaged location and loading condition (Park et al., 2012)

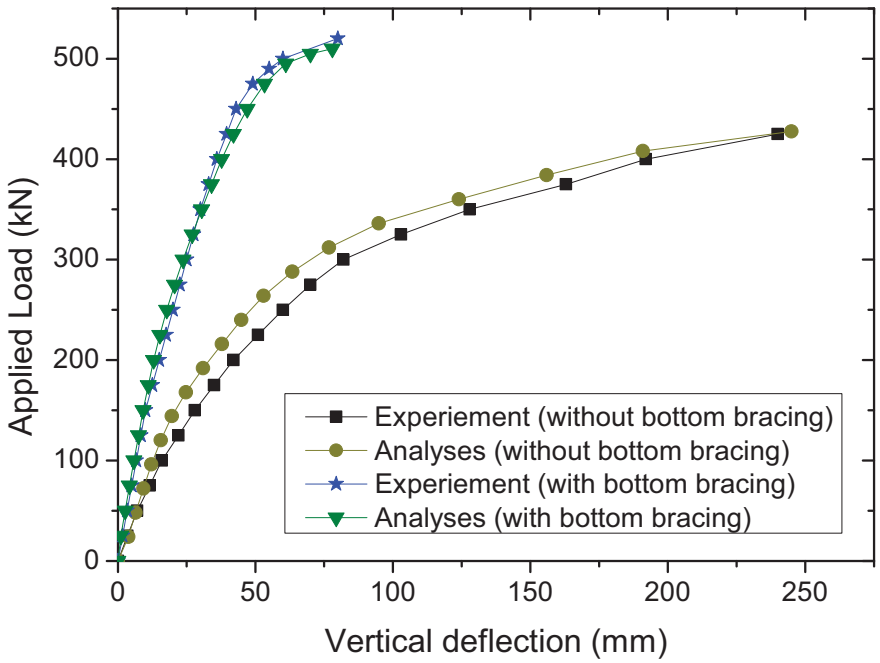

Fig.5.4 Load-deflection relationship of experimental and numerical results at the mid-span section

5.3.2 Numerical analyses

The post-elastic behavior of the structural system is not symmetric due to the effect of large displacements; a full model with span length (8 m + 9 m + 8 m) was built to simulate the response of the three-span bridge system. As shown in **Fig.5.5** and **Fig.5.6**, solid elements, grid elements, and beam elements were used to simulate the concrete slab, reinforcement bars, and bottom lateral X-type bracings, respectively. Shell elements, on the other hand, were used to simulate the main girders and transverse beams. Because the full connection is employed, perfect bond was assumed for the interface between the top flange and the bottom of the concrete slab. The model is considered as fine mesh with the length to width ratio less than three for shell element and length to thickness ratio less than six for the solid element. In this model, a total number of 14942 elements and 17750 nodes were constructed. The size of shell elements varies gradually from (30 mm x 30 mm) to (270 mm x 200 mm). In the analyses, non-linear analyses including both material and geometry nonlinearity are employed. Two phases are used in the analyses; the dead load was applied in the phase 1, and the live load was applied in the phase 2. For the live load, one-point load was applied on a node on the top surface of the slab on top of the damaged girder. Then the load was gradually increased until the failure of the system. To prevent the effect of local stress concentration, a steel plate with dimension (0.45 m x 0.45 m x 0.05 m) was built around the loading node. The load which causes the failure or yield point of a member is defined as LF_1. The nonlinear analysis is then continued until a member reaches its maximum strain which is considered as failure of the whole system. Since the maximum strain for each element of the structure is different; the failure strain for concrete is defined when compression strain reaches 0.0035. Steel rupture or reinforcement bar breaking is defined when their maximum strain reaches 20%. These cases are considered as the ultimate limit state and the failure load is defined as LF_u. Before reaching the ultimate load, the serviceability of the structure may fail when the maximum deflection reaches 1% of span length which is believed to be the maximum visible displacement that a bridge user or an observer can tolerate (Ghosn and Moses, 1998). The load that makes this deflection to reach this level is defines as LF_f. For the damaged system, the failure load LF_d is defined by the same way as LF_u in the intact system.

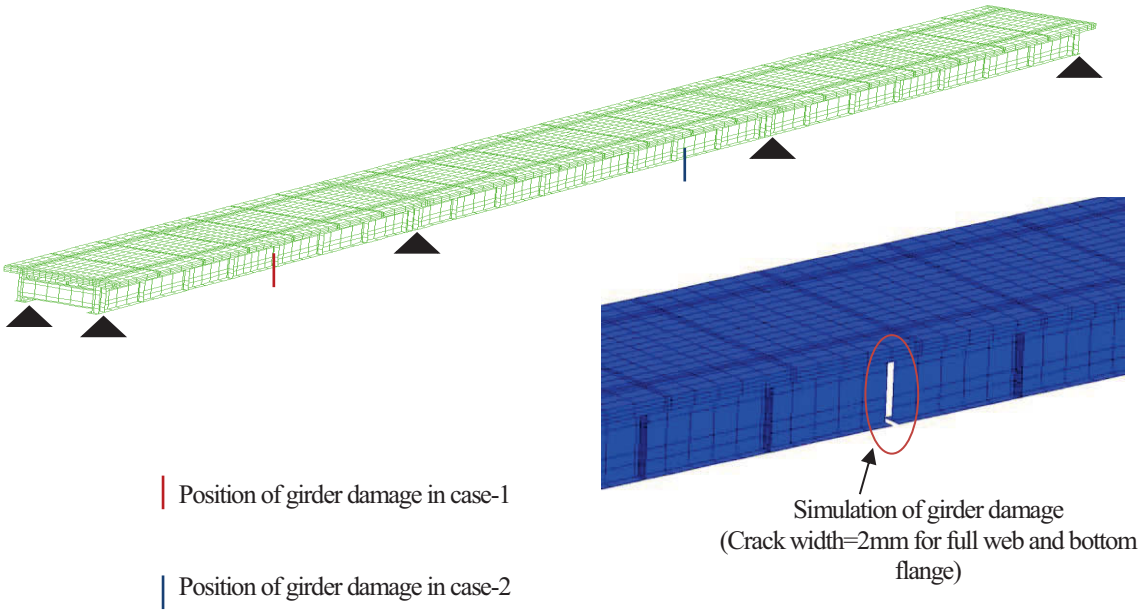

Fig.5.5 Numerical model and damaged condition

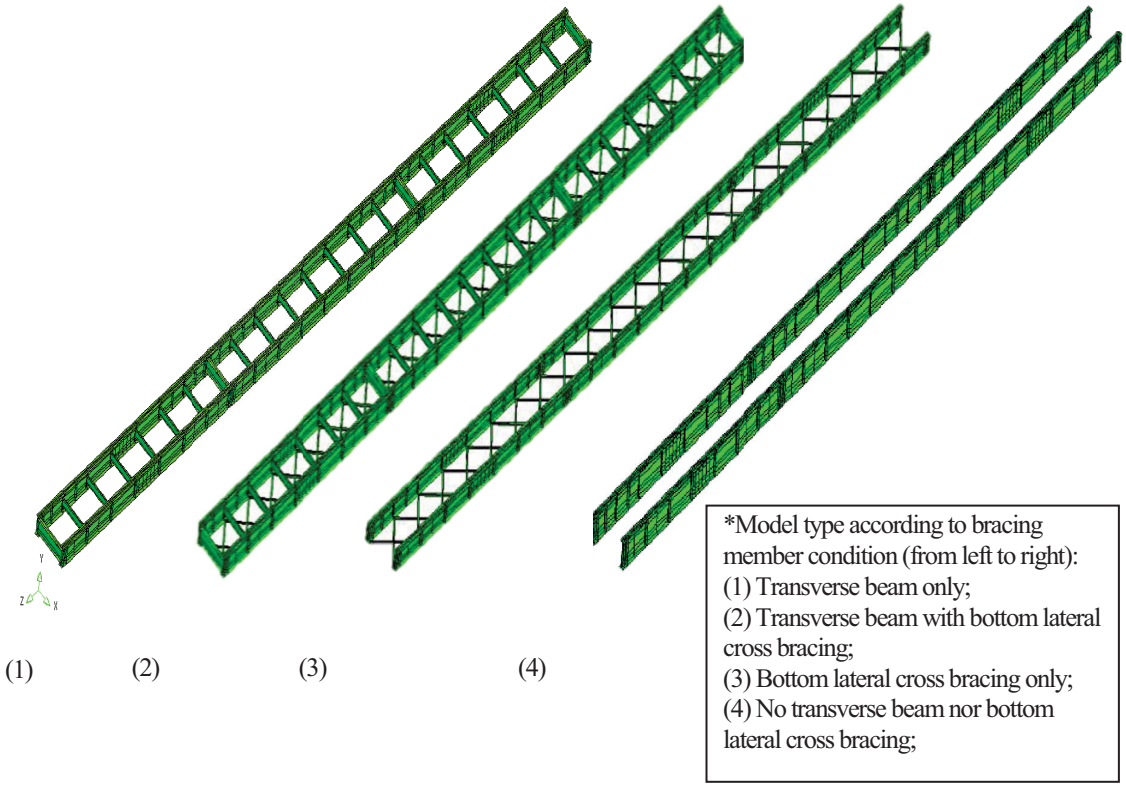

Fig.5.6 Numerical simulation for different type of bracing members

5.3.3 Loading and damaged conditions

Determining the Fracture Critical Members is essential in redundancy evaluation. The Fracture Critical Members (FCMs) are tension members whose failure would be expected to result in the collapse of the bridge (AASHTO, 2011). Since the fracture critical members are related with tension members, full crack of bottom flange and web is considered at the mid-span where the bending moment is at maximum value. This type of fracture is considered in the side span as case-1 and middle span as case-2. Bracing systems are believed to be the essential elements that enable the two I-girder bridge to establish the alternate load path after the failure of critical members (full crack of web and bottom flange in this study). Existing studies show that the after-fracture behavior of the structure is primarily dependent on the strength and stiffness of the redundant bracing system and its connections to the girder flanges (Daniel et al., 1988). For composite bridges, the effectiveness of the bracing systems remains in question. To study the effectiveness of these members, 4 types of models, 2 cases of damaged conditions are proposed as shown in **Fig.5.7** and **Table.5.1**. The result of analysis from these 4 types of models can show the effectiveness of different types of bracing systems to the behavior and redundancy level of the composite twin I-girder bridge.

For loading condition, concentration load is critical in this study and match with the experiment protocol. Unsymmetrical loading condition is used (Hendawi and Frangopol, 1994) and one-point load is applied on the top of the main girder with the fracture. The point load was applied on the top of the slab at the fracture location in all cases as shown in **Fig.5.7**. Steel plates (450mm x 450mm x 50mm) were employed at the loading point to avoid the stress concentration effect due to the point load. Including the intact and damaged models, 16 numerical models were built to study the effectiveness of bracing systems (transverse beams and bottom X-type bracings) on the redundancy rating of the bridge by using the method proposed in NCHRP (Ghosn and Moses, 1998; Liu et al., 2001; Ghosn et al., 2008; Ghosn and Yang, 2014).

Table.5.1 Bridge model description

Types of models	Damaged cases	
	Mid span of one side span	Mid span of middle span
1.Transverse Beams without bottom lateral cross bracing	I11/D11	I12/D12
2.Transverse Beams with bottom lateral cross bracing	I21/D21	I22/D22
3.Bottom lateral X-type bracings without transverse beams	I31/D31	I32/D32
4.No transverse beams nor bottom lateral cross bracings	I41/D41	I42/D42

*D=Damaged; I=Intact;

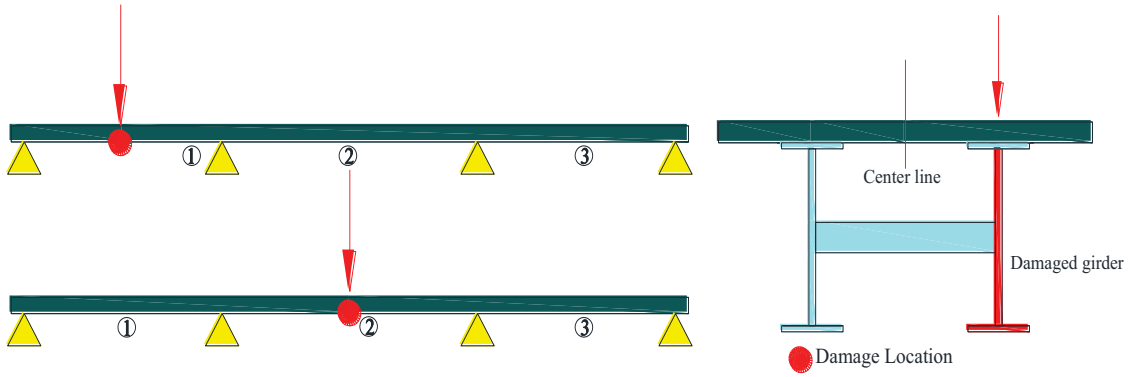

Fig.5.7 Loading conditions

5.3.4 Material properties

In this study, same material strengths in the experiment were applied in the numerical analysis as shown in **Table.5.2** and the stress-strain curves are shown in **Fig.5.8** for concrete and **Fig.5.9** for steel.

(a) Concrete

Similar to Chapter 4, the total strain crack model was used to simulate the three-dimensional constitutive model of concrete (Vecchio and Collins, 1986; Selby and Vecchio, 1993). The stress-strain curve shown in **Fig.5.7** was used to simulate the compression and tension behavior of concrete. The tensile strength of concrete was calculated according to **Eq.5.5** based on the JSCE specification for concrete structures (JSCE, 2002), in which f_t and f'_{ck} denote the tensile and compression strengths of concrete, respectively. The tension-stiffness curve as shown in **Fig.5.7** was used in the numerical analyses to reflect the softening

of the concrete according to **Eq.5.6** (Nakasu et al., 1996). The stress-strain relationship in compression was determined according to **Eq.5.7**. The ultimate compression strain ε'_{cu} is taken as 0.0035. This value is suggested in the Japanese specifications (JRA, 2002; JSCE, 2002) and Eurocode 2 (CEN, 1992).

$$f_t = 0.28 {f'_{ck}}^{2/3} \tag{5.5}$$

$$\sigma_t = f_t \left(\frac{\varepsilon_t}{\varepsilon}\right)^{0.4} \tag{5.6}$$

$$\sigma_c = \begin{cases} k_1 f'_{cd} . \frac{\varepsilon'_c}{0.002} . \left(2 - \frac{\varepsilon'_c}{0.002}\right); & \varepsilon'_c \le 0.002 \\ k_1 f'_{cd}; & \varepsilon'_c \ge 0.002 \end{cases} ; \quad k_1 = 1 - 0.003 f'_{ck} \tag{5.7}$$

$$\varepsilon'_{cu} = \frac{155 - f'_{ck}}{3000} ; 0.0025 \le \varepsilon'_{cu} \le 0.003 \tag{5.8}$$

where:

+ σ_c : Compression stress of concrete

+ ε'_c : Compression strain of concrete

+ f'_{cd} : design compression stress of concrete

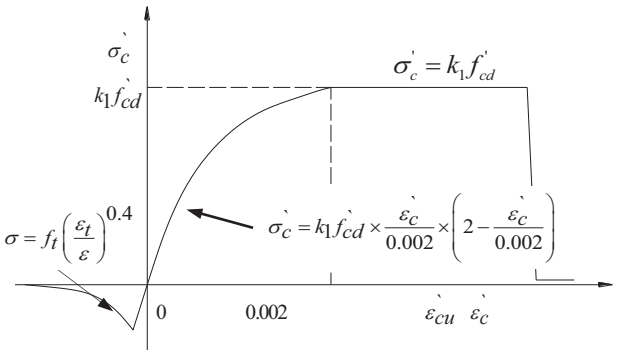

Fig.5.8 Stress-strain curve of concrete

(b) Structural steel and reinforcing bar

As shown in **Fig.5.9**, the stress-strain relationships of the structural steel and reinforcing bars proposed in Japanese Specifications was employed in the numerical models (JSCE, 2007). The stiffness in the plastic region is account for 1% of the elastic stiffness before it reaches ultimate strength to simulate the strain hardening of the structural steel and reinforcing bars suggested in Japanese Specifications (JSCE, 2007).

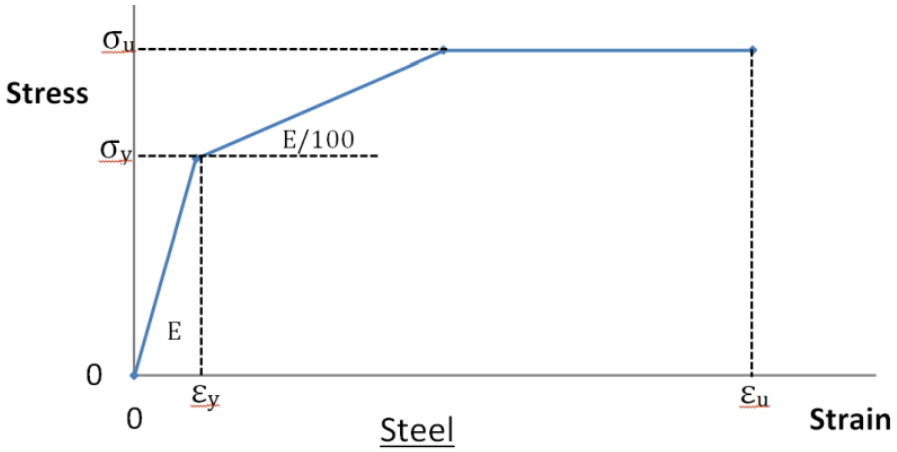

Fig.5.9 Stress-strain curve of steel and reinforcement bars

Table.5.2 Strength of materials

Materials	Thickness (mm)	Yield Strength (MPa)	Ultimate Strength (MPa)
Steel Plate	6	305.5	371.6
	8	381.8	533.5
	10	337.5	519.1
	14	315.6	504.5
Reinforcing bar (D10)		460.4	642.0

5.4. Numerical Results and Redundancy Analyses

5.4.1 Force-displacement curves and collapse mechanism

In Case-1, as mentioned in the section 5.3.3, full crack of the web and bottom flange was assumed at the midpoint of the side span in damaged condition. The point load is applied on the top of the slab at the fracture location in all cases. Instead of using the live load factor, all direct loading value is used for LF_i. In the Case-2, full crack of the web and bottom flange is assumed at the midpoint of the middle span. Same loading condition as the case one is applied on fracture section.

(a) Bridge model with only transverse beams (Type 1)

Fig.5.10 shows the load-displacement curves of Type 1 bridge model. Numerical models show that the intact system in the case-1 loading condition is less critical than case-2 while the damaged condition works in opposite way. Since redundancy is more concerned with the behavior of the bridge in damaged condition, fracture of girder in the midpoint of side span is believed to be more dangerous and less redundant. The failure mode of the intact system is determined by crush of concrete slab at the loading point. For the damaged specimen, from the deformation of the test specimen at the ultimate load, the failure of the web near the support is observed and governed by the buckling as shown in **Fig.5.11** and **Fig5.12**. This observation is also confirmed by the applied load versus out of plane displacement curve at the web buckle location as shown in **Fig.5.13**. In conclude, the failure mode of the damaged specimens are determined by web buckling near the internal support of damaged girder following by concrete crush at the loading point.

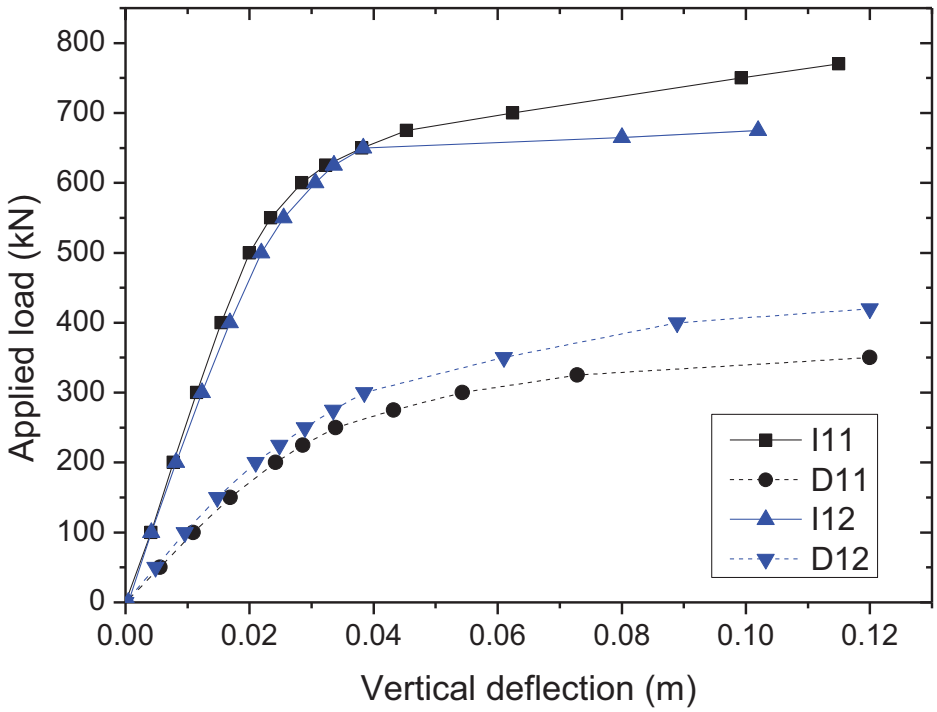

Fig.5.10 Type 1 bridge load-displacement curves

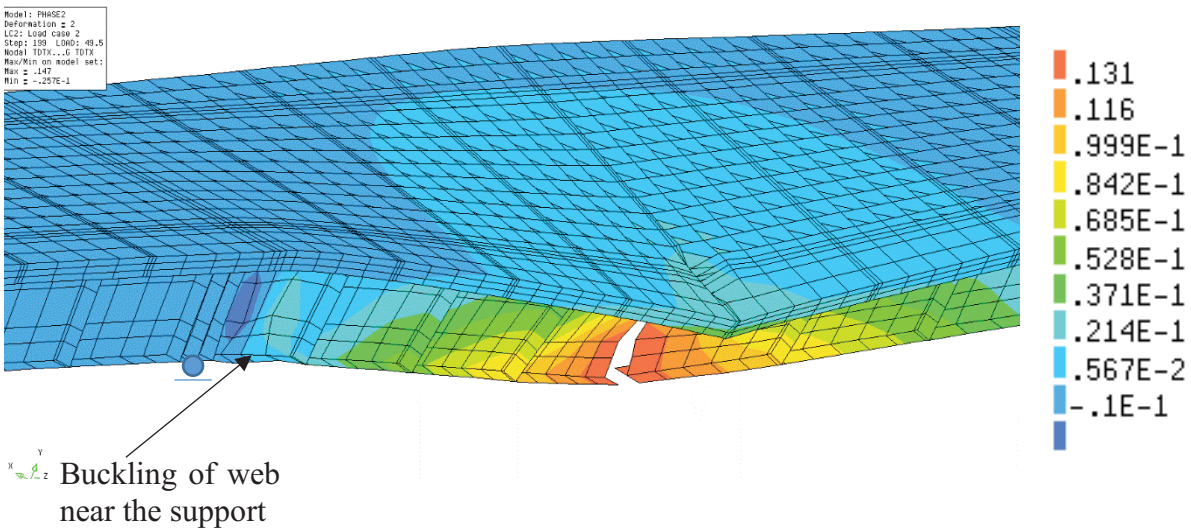

Fig.5.11 Failure mode of Type 1 bridge (D12)

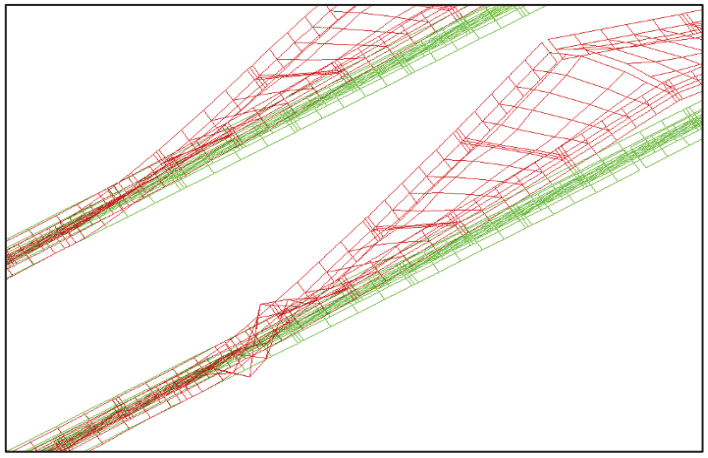

Fig.5.12 Buckling of web near the support (D12)

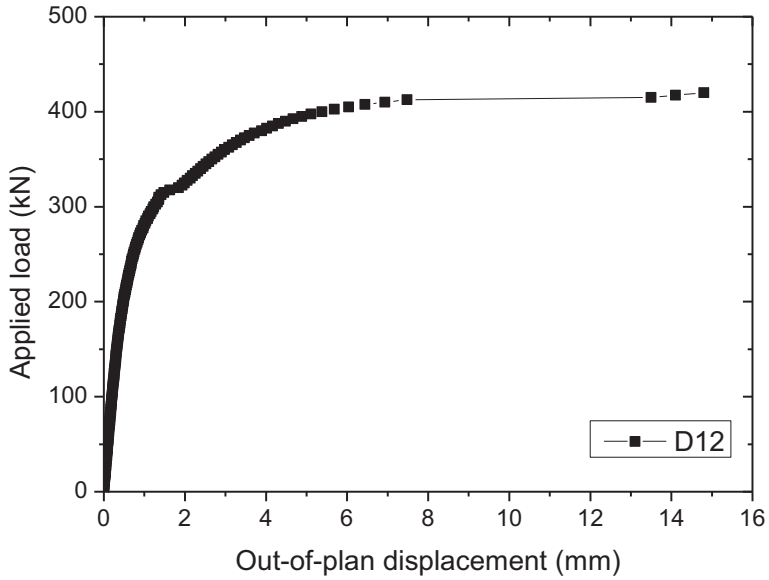

Fig.5.13 Out-of-plane displacement versus applied load curve of Type 1 bridge (D12)

(b) Bridge model with transverse beams and bottom lateral X-type bracing (Type 2)

Fig.5.14 shows the load-displacement curves of Type 2 bridge model. Both load carrying capacity and system stiffness are higher in the case one loading and damaged condition. Fracture of the girder is more critical in the middle span than in the side span. The failure mechanism of both intact and damaged systems is determined by concrete crushing at the loading point associated with rupture of the web below. The same failure mode was obtained in the experimental result performed on the half model of this type of bridge (Park et al., 2013).

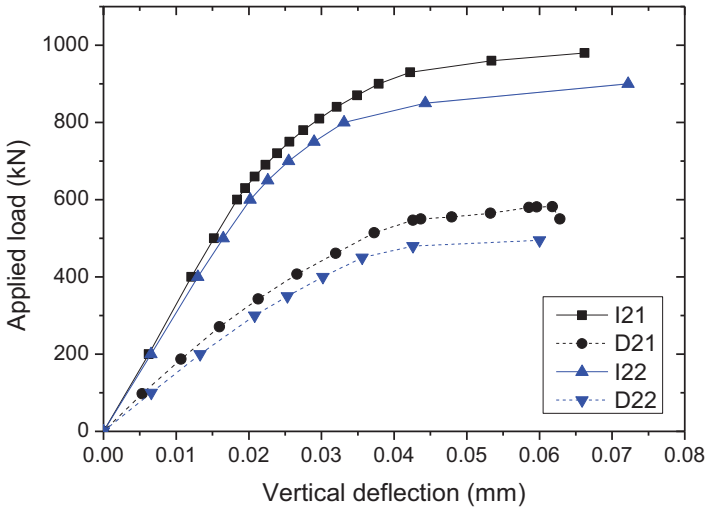

Fig.5.14 Load-displacement curves of Type 2 bridge

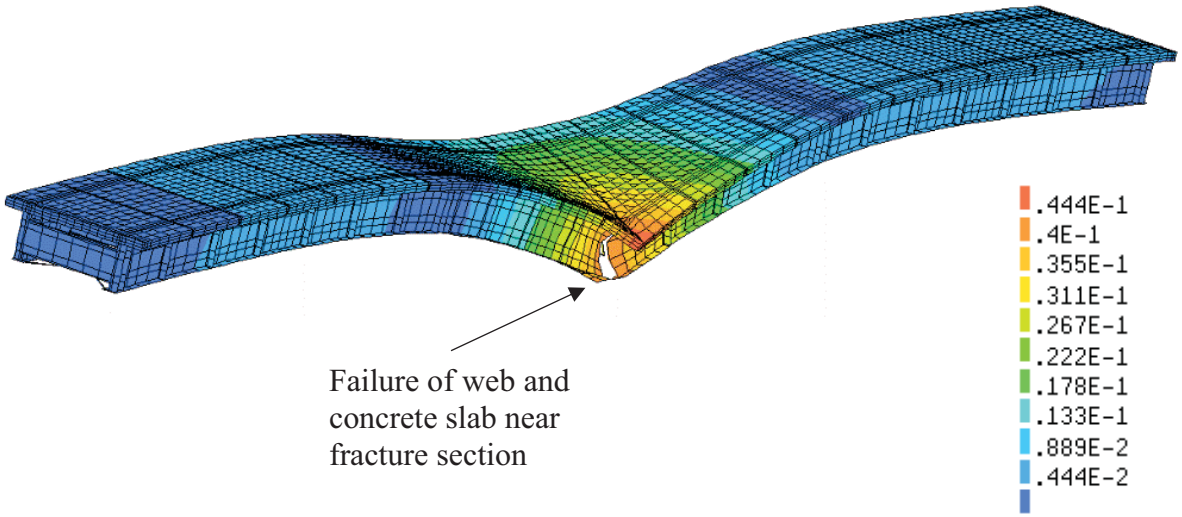

Fig.5.15 Failure mode of Type 2 bridge (D22)

(c) Bridge model with only bottom lateral X-type bracing (Type 3)

Fig.5.16 shows the load-displacement curves of Type-3 bridge model. For intact system, the ultimate load is higher for loading case on the side span than middle span. The bridge with girder fracture at middle span can be considered as more critical. The failure mechanism of the intact system is determined by concrete crush at the loading point. No buckling behavior was observed in the intact system. For damaged system, the failure mode is the same as Type-2 bridge model, resulting in concrete crush at the loading point associated with rupture of web below.

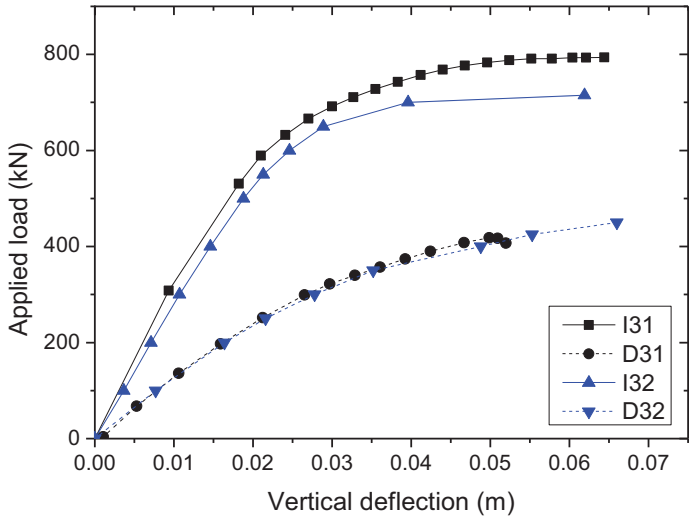

Fig.5.16 Load-displacement curves of Type 3 Bridge

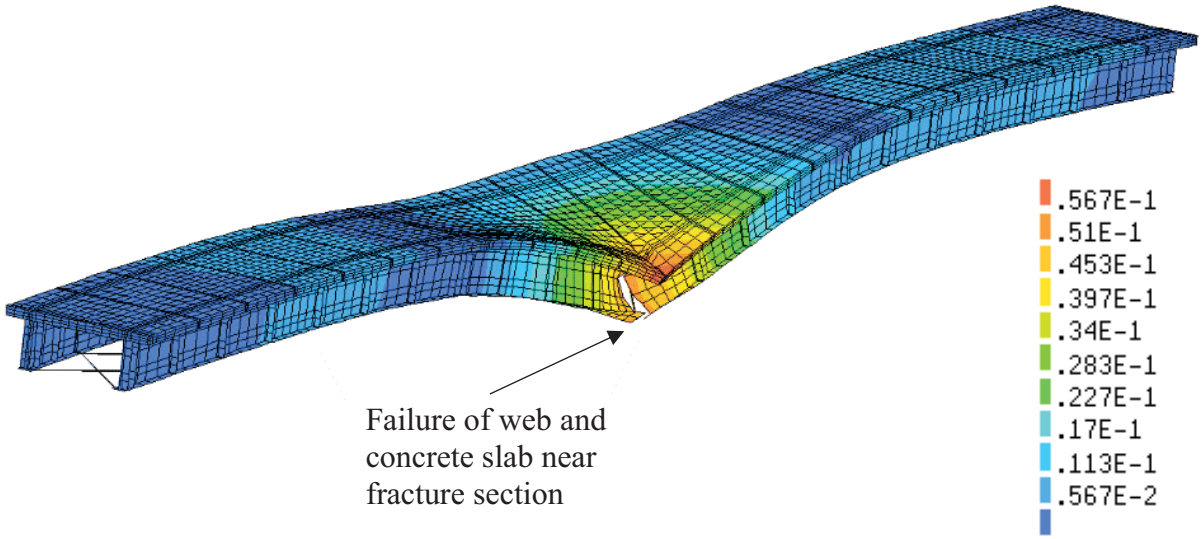

Fig.5.17 Failure mode of Type 3 bridge (D32)

(d) Bridge model without bracing systems (Type 4)

Fig.5.18 shows the load-displacement curves of Type 4 bridge model. Without transverse beams and bottom lateral bracing, the concrete slab is the only element that acts as alternate load path after the fracture of the girder. Numerical results show that the performance of the bridge is very close to the Type 1 bridge models. Damage at the side span is more critical for this type of bridge. The failure mode of the intact system is determined by concrete crush at the loading point. The failure mode of the damage system is similar to the bride Type 1 which is governed by the web buckling as shown in **Fig.5.19**.

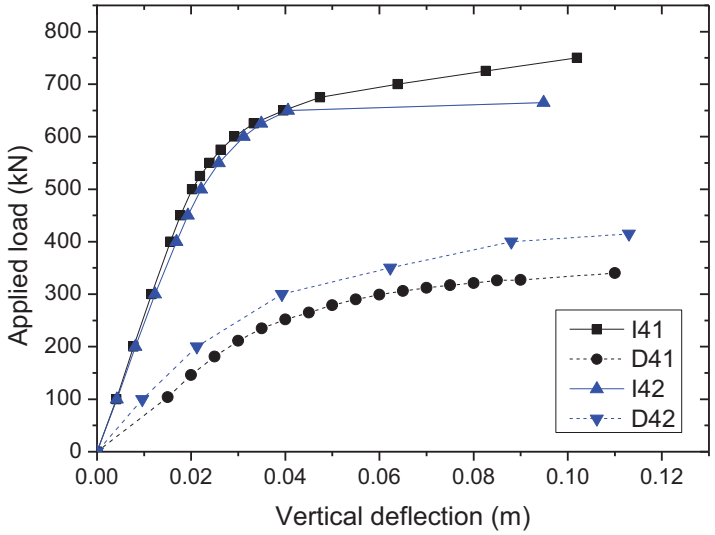

Fig.5.18 Load-displacement curves of Type 4 bridge

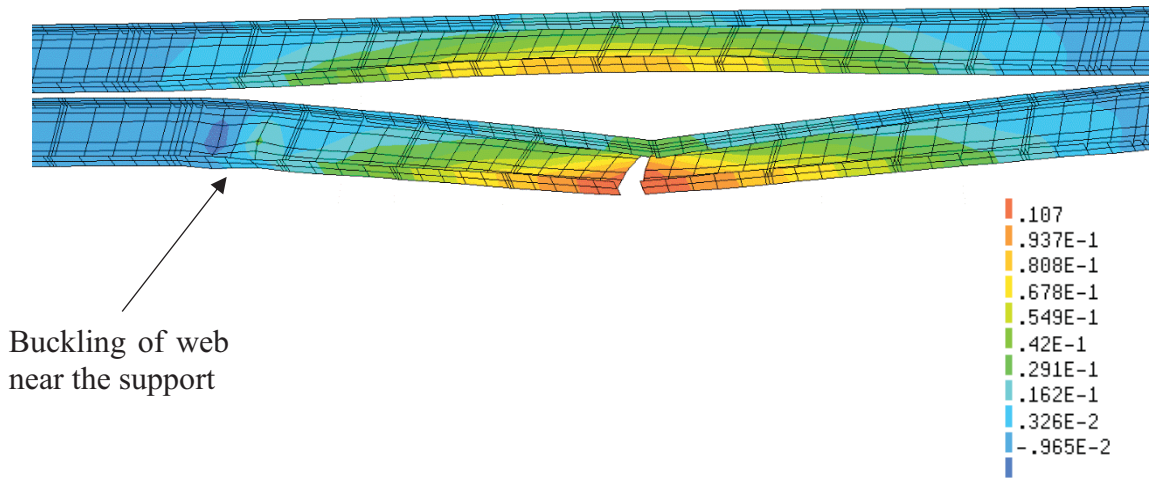

Fig.5.19 Failure mode of Type 4 bridge (D42)

5.4.2 Redundancy analyses

From the numerical model analyses, LF_1, LF_u, LF_f, LF_d could be determined. For intact system, LF_1 was obtained when the steel plate or reinforcing bar reached yielding strain. In all intact systems, the bottom flange under loading position firstly reached the yielding point, and then the stiffness of the structural system slowly approached to nearly zero. LF_u was obtained when the section failed depending on one of the following reasons: the concrete crush, steel buckling or rebar breaking. LF_f was obtained when the deflection reached 1/100 of the span length (8 cm in this case). All the bridge models with bottom X-type bracings reached the ultimate limit state before the maximum deflection reach 8 cm. Loads that make the bridge unfit from using were not observed. It means that this type of bridge doesn't have to verify the service limit state. For damaged condition, two types of failure modes could be defined; the buckling web near the internal support associated with concrete crush and the concrete crush associated with rupture of web below, and LF_d was obtained at the ultimate load of damaged system. The value of each limit state is summarized in **Table.5.3** and redundancy factors are calculated by using **Eq.5.1**, **Eq.5.2**, **Eq.5.3**, and **Eq.5.4**. The load for the service limit state could not obtain in some cases because the collapse of the bridge system was obtained before deflection reached 1/100 of the span length. **Table.5.3** shows the results of redundancy factor in each type of bridge. According to the numerical results, the same redundancy factor was obtained for bridge without bracing system and bridge model with I-shape transverse beams. A bridge with only bottom L-shape X-type lateral bracing has a higher level of redundancy factor comparing with a bridge with or without transverse beams. A bridge with both transverse beams and bottom lateral bracing has the highest level of redundancy factor among other 4 types of models. It shows that the bracing members are effective in increasing the redundancy factor of the three-span composite twin I-girder bridge. The bridge itself can be classified as redundant even the bracing system does not exist. This bridge is proved to have the alternate load paths and moreover concrete slab is believed to be the main member in redistributing the load after fracture or failure of a member.

Table.5.3 Redundancy Factors

Model		LF_1 (kN)	LF_u (kN)	LF_f (kN)	LF_d (kN)	R_u /1.3	R_f /1.1	R_d /0.5	$\varphi_{R,i}$	φ_R
Type 1	(I+D)11	510	770	725	350	1.16	1.29	1.37	1.16	1.10
	(I+D)12	470	670	665	420	1.10	1.29	1.79	1.10	
Type 2	(I+D)21	620	980	-	550	1.22	-	1.77	1.22	1.21
	(I+D)22	570	900	-	582	1.21	-	2.04	1.21	
Type 3	(I+D)31	520	794	-	407	1.17	-	1.57	1.17	1.15
	(I+D)32	480	715	-	450	1.15	-	1.88	1.15	
Type 4	(I+D)41	505	755	720	340	1.15	1.30	1.35	1.15	1.10
	(I+D)42	465	665	660	415	1.10	1.29	1.78	1.10	

5.4.3 Effectiveness of bracing systems

(a) Effect of transverse beams

Fig.5.20 shows the load-displacement curves of bridge model with and without transverse beams. Bottom lateral bracing systems does not involve in these models. From the load-displacement curve in both intact and damaged systems, the transverse beams do not have any effect on the stiffness nor load-carrying capacity of the bridge at all. It is found that the transverse beams alone are useless in increasing the load carrying capacity, reducing the deflection or modifying the bridge response in damaged condition. The transverse beams alone can be considered as a non-effective element in response to the vertical loading condition, yet the result is different with the present of the x-type lateral bracing and is explained in the later section.

Fig.5.21 shows the load-displacement curves of the bridge with and without I-shape transverse beams. With the existing of the bottom X-type bracing system, the transverse beams are found to be effective in increasing the stiffness and load carrying capacity of the bridge. It can explain that the transverse beam alone is not effective because of the weak torsional stiffness of the main girder. However, with the presence of bottom lateral bracing, the torsional stiffness is increased as this bottom bracing act as a limitation of the distance between two bottom flanges and thus enables the transverse beam to help distributing the load between the two main girders. The load-carrying capacity of the bridge increases more than 23% for the intact system and around 30% for damaged condition in both case-1 and case-2. The failure mechanism and deflection level remain the same for these cases.

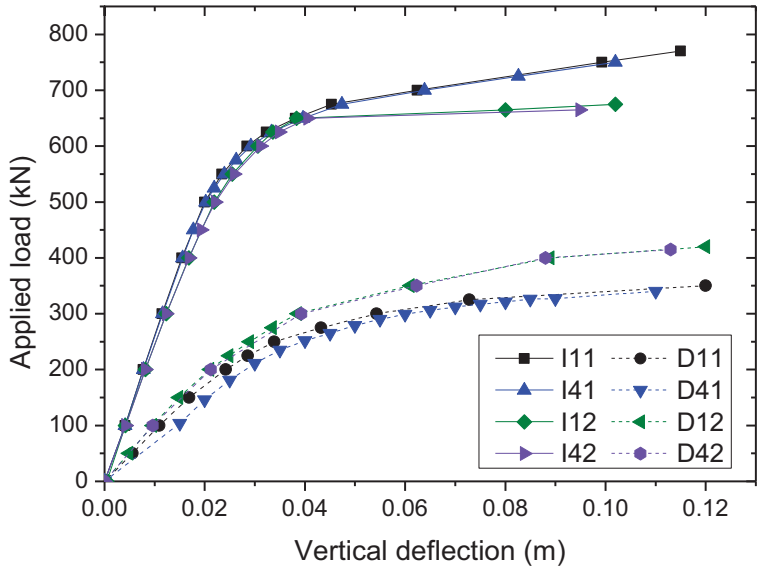

Fig.5.20 Load-displacement curves for type 1 and type 4 model

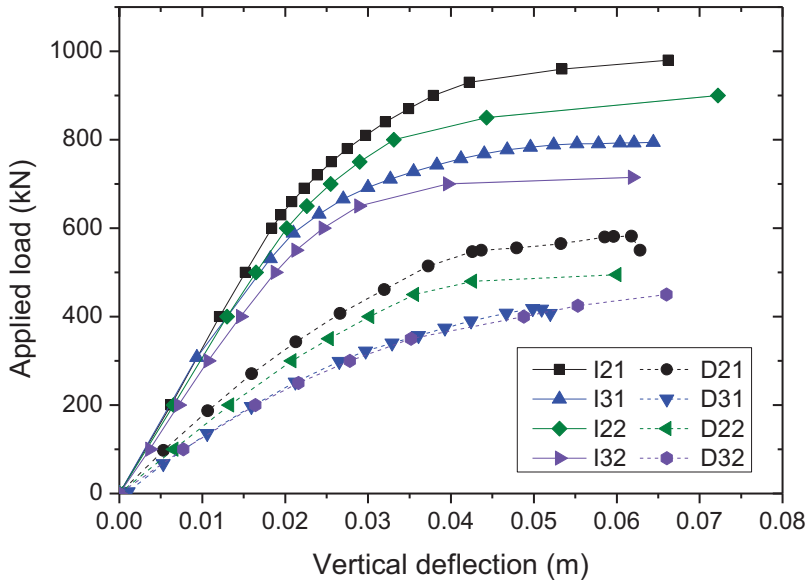

Fig.5.21 Load-displacement curves of type 2 and type 3 model

(b) Effect of bottom X-type lateral bracing

According to the numerical results, with either case of having transverse beams or not, the bottom X-type lateral bracing is found to be effective in increasing stiffness, the load carrying capacity and even the yielding load of the system. **Table.5.4** shows the different load carrying capacity ratio of the bridge with and without bottom lateral bracing systems. With the existing of transverse beams, lateral bracing systems effectively increases the load-carrying capacity of the bridge more than 25% in all cases. But without the transverse beams, the effectiveness of bottom lateral bracing is found to be as low as 5% among other cases. **Fig.5.22** shows the load-displacement curves of the bridge with and without bottom lateral bracing systems. Bridge model with the bottom lateral bracings always collapsed before the deflection reached 1/100 of the span length. This level of deflection is less than 70% of the deflection of bridge model without bottom lateral bracing systems. It can be said that the bottom lateral bracing systems increase the load carrying capacity and the redundancy factor of the bridge; however, the ductility of the structural system is reduced to some level as large as 30%.

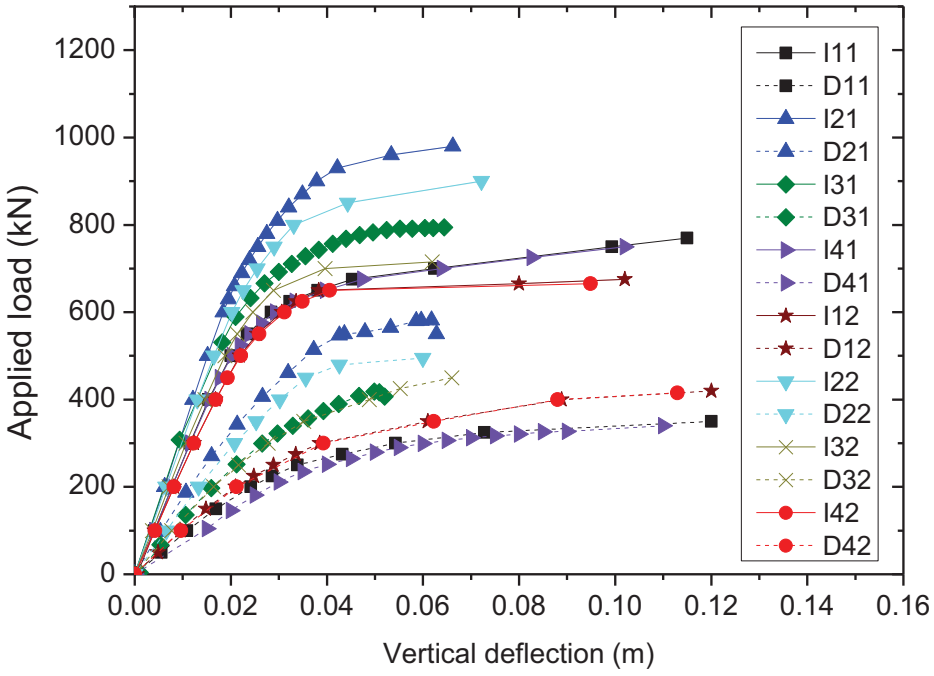

Fig.5.22 Load-displacement curves for bridge models with and without bottom X-type lateral bracings

Table.5.4 Ratio of loading carrying capacity of bridge with and without bottom X-type bracing systems

Model	Intact System	Damaged System
21:11	1.27	1.57
22:12	1.34	1.39
31:41	1.05	1.20
32:42	1.08	1.08

5.5 Numerical Analyses on the Full-Scale Bridge Model

The bottom X-type lateral bracings with the transverse beam are found to be effective in increasing the redundancy factors and the load carrying capacity of the small scale three span composite twin I-girder bridge model. To validate the application of this x-type bracing in the design of the actual bridge, a full scale five spans composite twin I-girder highway bridge model is analysed in this section. The location of the Fracture Critical Members is first determined. Then, bridge models with different types of X-type cross bracing are studied based on nonlinear analyses.

5.5.1 Bridge model description

A five span full-scale composite twin I-girder highway bridge model with the span length of (34.6+38.3+38.3+38.3+34.6) m was selected as a study target. The bridge was designed according to Japanese design code (JRA, 2002). The side view and plan view of the bridge were shown in **Fig.5.23** and **Fig.5.24**, respectively. The cross sections of this bridge were shown in **Fig.5.25**. Live load condition according to Japanese design code (JRA, 2002) was used in this study. Nonlinear analysis including material nonlinearity and geometrical nonlinearity was included in the analysis. **Fig.5.26** shows the numerical model of the five-span composite twin I-girder bridge. The same modeling method to the three span bridge model in this study is used to simulate the five-span bridge model. Solid elements, grid elements, and beam elements were used to simulate the concrete slab, reinforcement bars, and bottom lateral cross bracing, respectively. Shell elements, on the other hand, were used to simulate the main girders and transverse beams. Phase analysis and load increment method were employed in order to determine the load-carrying capacity of the bridge model.

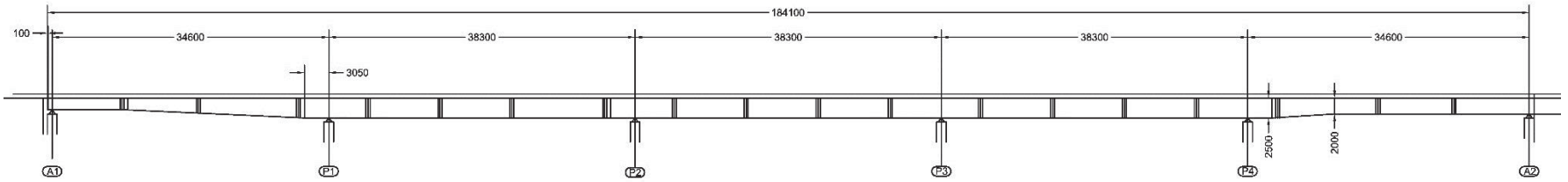

Fig.5.23 side view of the bridge model

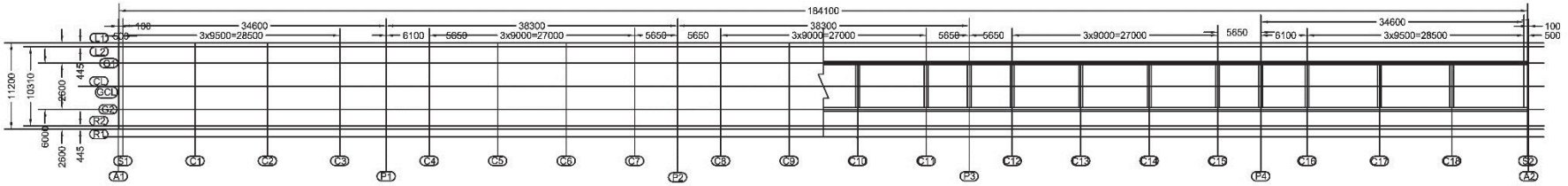

Fig.5.24 Plan view of the bridge model

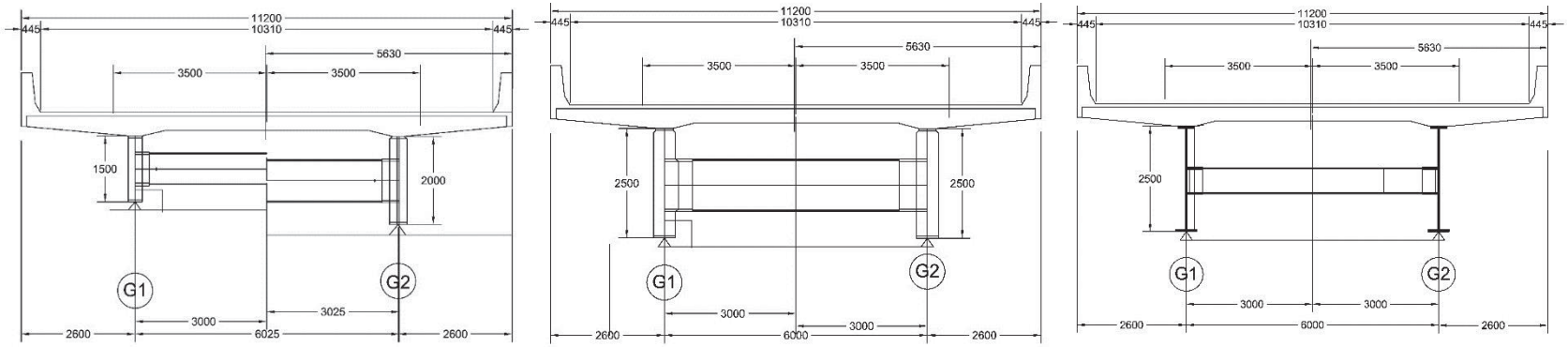

(a) End support sections A1 and A2 **(b)** Other support sections **(c)** Other sections

Fig.5.25 Configuration of bridge models

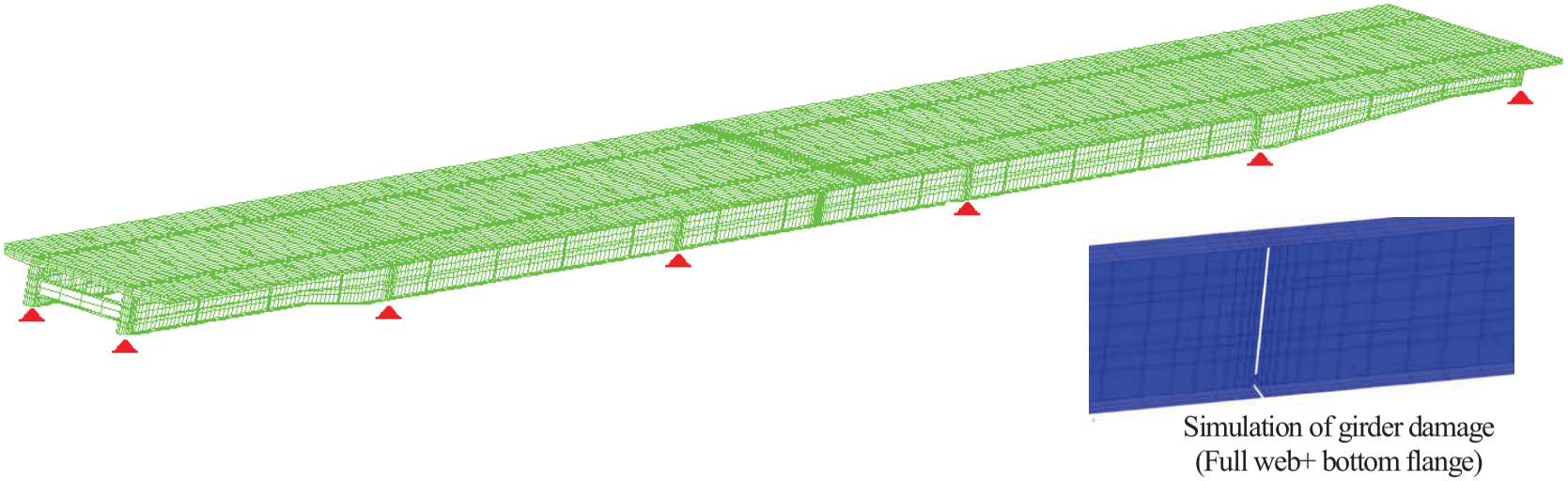

Fig.5.26 Numerical Model Simulation

5.5.2 Live load conditions

The bridge was designed using the type B live load condition in Japan (JRA, 2002). Live load condition (P1+P2) according to Japan standard was used and is shown in **Fig.5.27**. Uneven loading condition was applied on the bridge system to produce the most critical loading condition in reliability and redundancy analysis (Hendawi et al., 1994). **Fig.5.28** shows the live load distribution in the transverse direction. The loading condition is selected to produce the most critical loading effect on the damaged girder.

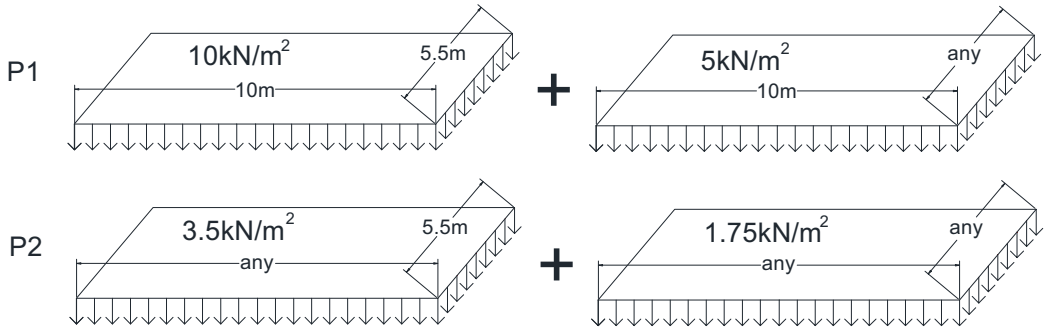

Fig.5.27 P1 and P2 loading conditions

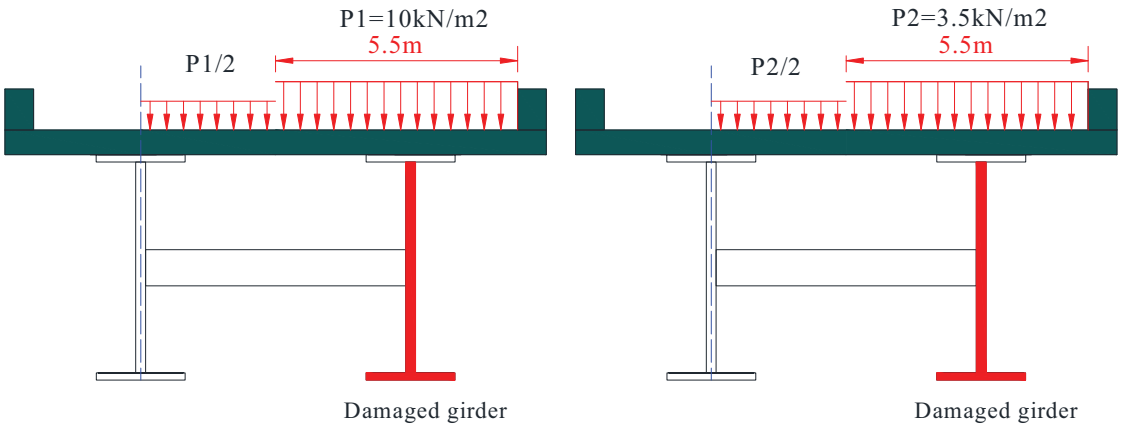

Fig.5.28 Distribution of live load in transverse direction

5.5.3 Fracture critical members

(a) Damaged cases and its loading condition

For composite twin I-girder bridges, fracture at the mid-span section is normally considered as the most severe cases in comparison with other locations along the span length. Based on the survey report published by Public Work Research Institute of Japan about girder bridge damage in Japanese national road, the fracture of the girder happens randomly along the main girders. The report points out that the rate of severe crack is low at the end of the girders, and tended to grow gradually higher nearer the center of the span. The fracture section could happen at random positions along the span. For this reason, a series of random damaged cases from the locations near the support to mid-span were assumed in this section on the full-scale bridge model. The damaged condition is set as the fracture of whole web and bottom flange as suggested in the guidelines for redundancy design and rating of two-girder steel bridges (Daniel et al., 1988). Any damage assumed to make the bridge collapse under dead load are Fracture Critical Members and the bridge system can be concluded as non-redundant. In the case the bridge survives under dead load; the possible FCM is taken as the case that has the lowest remaining load carrying capacity corresponding to the different type of failure mode. **Fig.5.29** shows the damaged locations assumed in this study. In each case, only one fracture is assumed to occur at one girder, and only one girder is assumed to fracture. For each damaged case, influence line analysis was employed to determine the most dangerous loading condition and is shown in **Fig.5.30**.

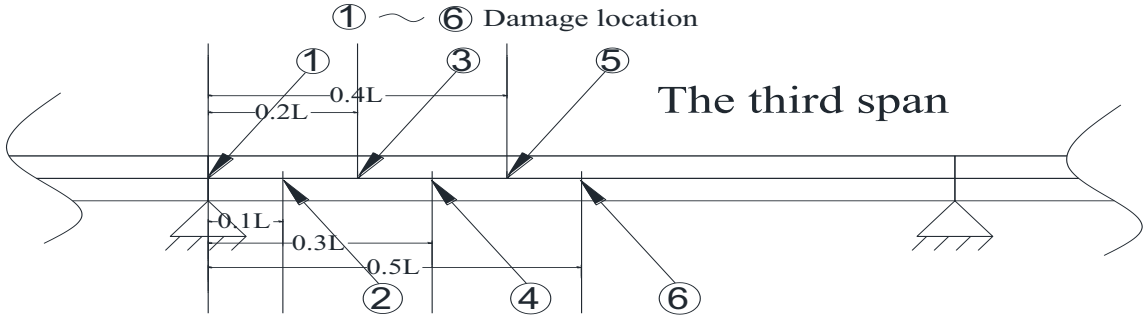

Fig.5.29 Fracture locations associated with each damaged case

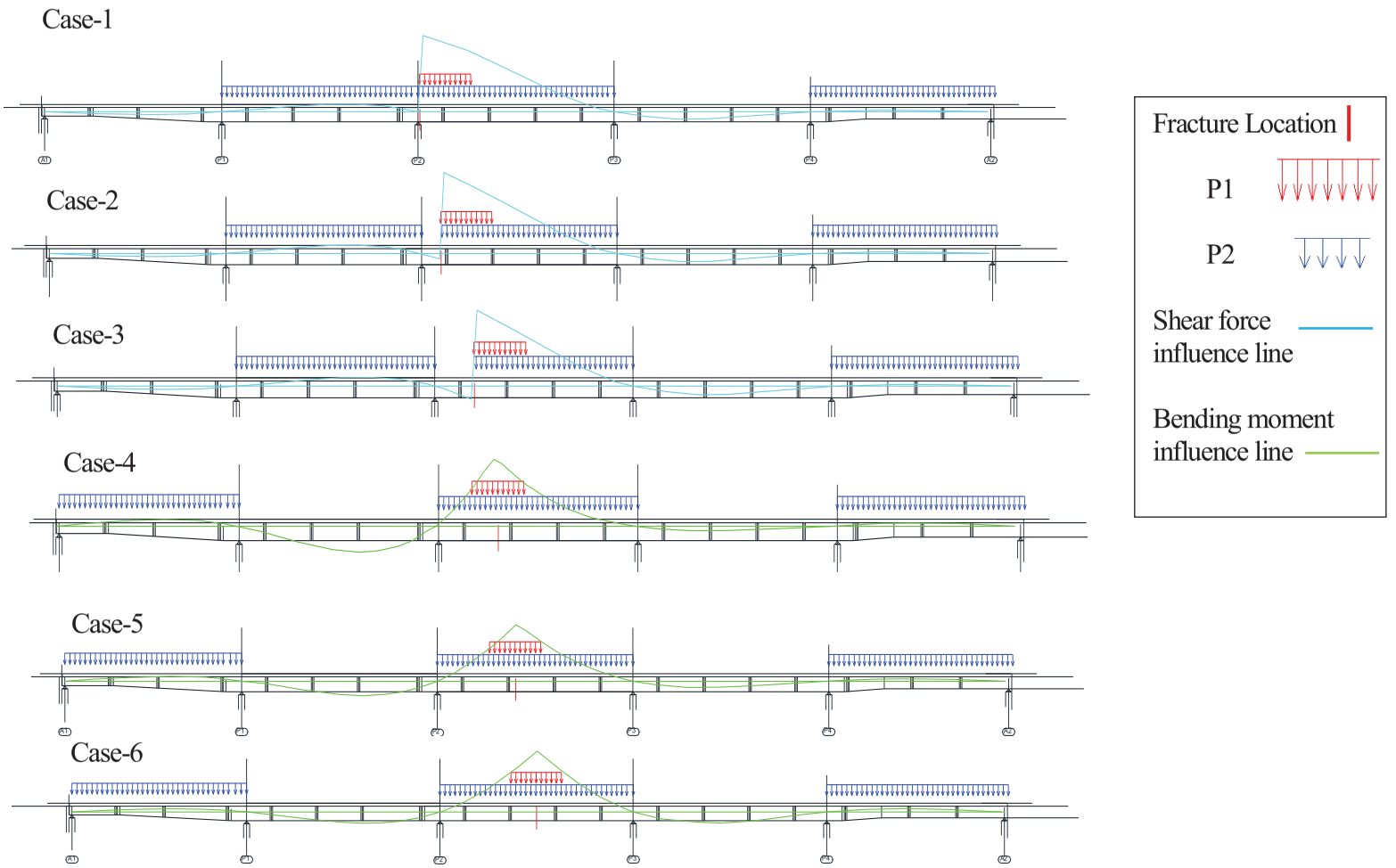

Fig.5.30 Loading condition corresponding to each damaged case

(b) Numerical results

The load-displacement curves corresponding to each damaged case obtained from numerical analyses are shown in **Fig.5.31**. Load carrying capacity of each damaged case and also the failure modes are summarized in **Table.5.5**. According to the numerical results, two different failure modes can be classified: shear failure of the concrete slab and rebar breaking at fracture location as type-1 and concrete crush at fracture location following by steel web buckling near the support location as type-2. For Case-1, Case-2 and Case-3, fracture locations are near the support region, the failure beginning with concrete crack above damaged girder. As the live load increases, the cracks on the slab spread across the section and the rebar strain slowly increases until break and the final failure is observed. An example of failure mode is shown in **Fig.5.32**. It has been noticed that shear buckling of the web near the fracture girder appears in Case-3 (**Fig.5.33**) and the rebar strain greatly increases and reaches the failure state of the bridge. For Case-4, Case-5, and Case-6, the failure mode is progressing by firstly the crush of the concrete at the fracture location, and soon after, the buckling appears at the web near the support due to the increasing in negative bending moment transferring from positive bending moment region (**Fig.5.34**). Among three damaged cases at support region, Case-3 has the lowest load carrying capacity. This is due to shear buckling caused by lower sectional capacity from the design at the region where both shear force and bending moment are considered as lowest. Because two types of different failure modes were obtained, two cases of the possible fracture critical members are suggested corresponding to each failure mode. To conclude, it is suggested that the damaged Case-3 (fracture at 0.2L from support) should be considered as the possible FCM which corresponds to type-1 failure mode, and the damaged Case-6 (fracture at the mid-span) should be considered as possible FCM which corresponds to the Type-2 failure mode. These two damaged cases will be carried on for redundancy analysis in the next section.

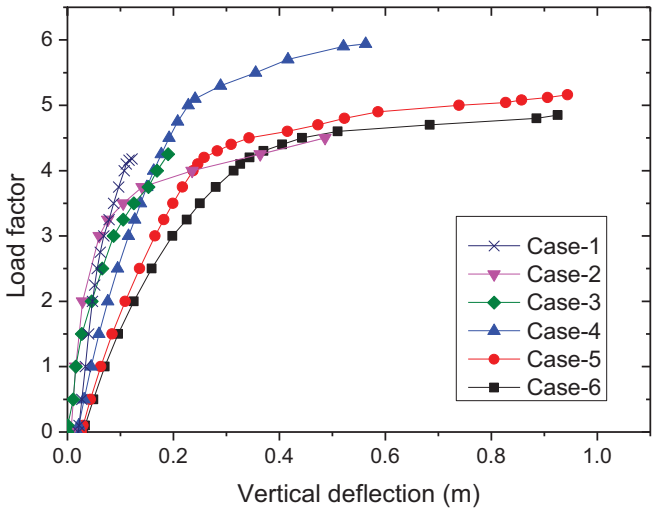

Fig.5.31 Load-displacement curves corresponding to each damage case

Table.5.5 Load carrying capacity of bridge associated with different damaged locations

Damage Case	Damage location	LF_d	Failure Mode
Case-1	0.01L	4.18	Type-1
Case-2	0.1L	4.25	Type-1
Case-3	0.2L	4.15	Type-1
Case-4	0.3L	5.70	Type-2
Case-5	0.4L	4.70	Type-2
Case-6	0.5L	4.40	Type-2

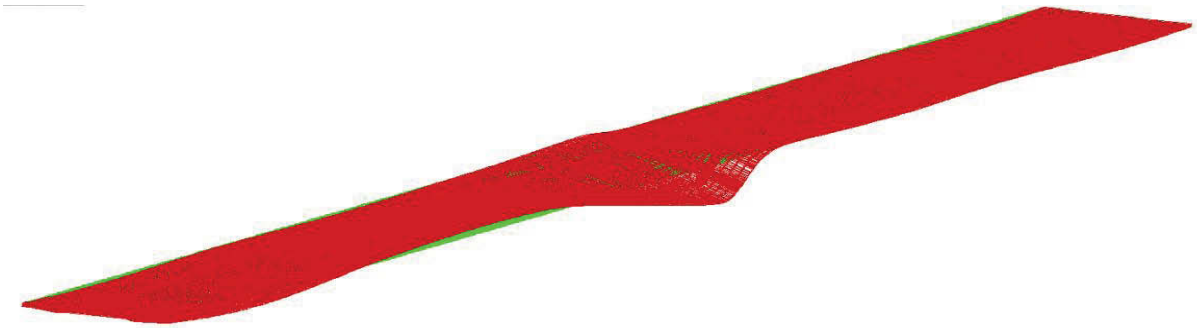

Fig.5.32 Shear failure of concrete slab (type-1)

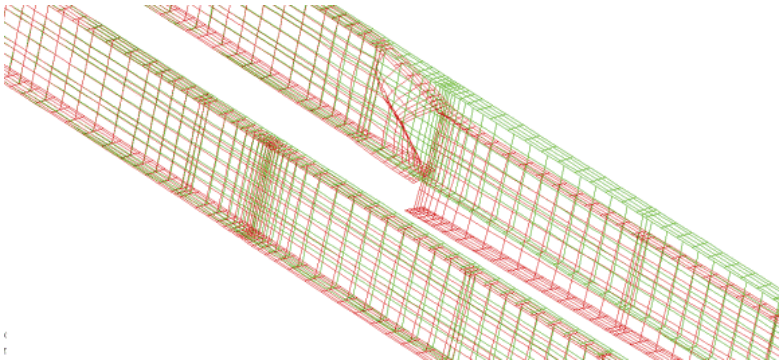

Fig.5.33 shear failure due to web buckling (type-1)

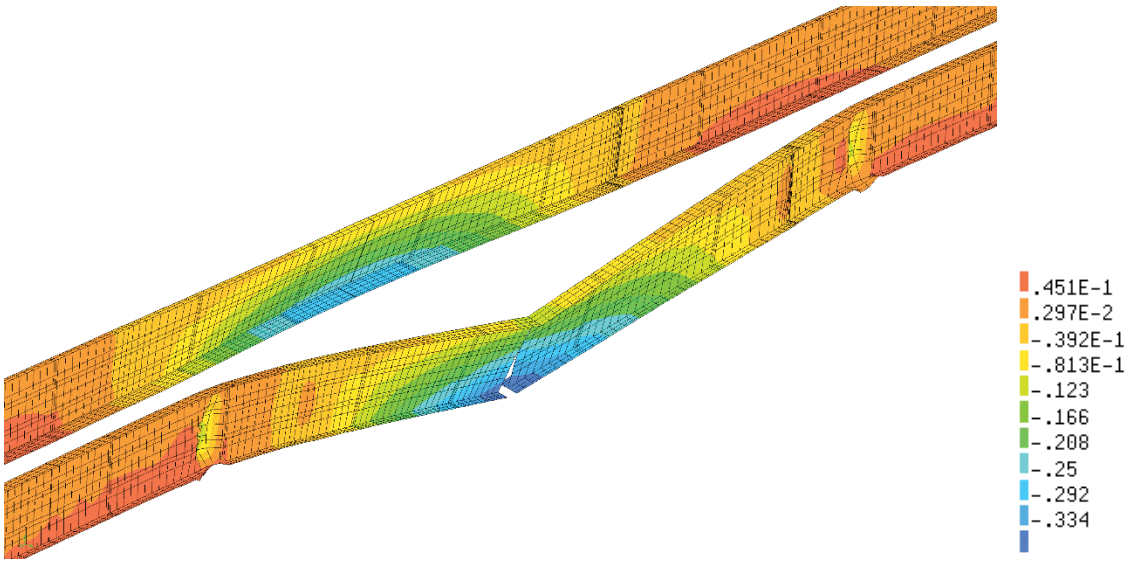

Fig.5.34 Web buckling near the support (type-2)

(c) Case study on other spans

Determination of possible FCMs was presented in the previous section. Damage Case-3 and Case-6 are the two most dangerous cases among other cases. To evaluate the redundancy of the entire bridge, the damaged condition in Case-3 and Case-6 were carried out for all others spans. A total of 15 damage cases were identified for evaluating the redundancy of the five-span bridge model. The damaged conditions are shown in **Fig.5.35**. The red line indicates that the damage is at 0.2L (L: Span length) from support while the blue line indicates that the damage is at mid span section. In each span, three damage cases are assumed separately (one at mid-span, two at 0.2L from left and right supports). **Table.5.6** summarizes the intact cases and damaged cases used for evaluating the redundancy level of the bridge model. **Fig.5.36**

shows the loading conditions associate with each intact case and damaged case. The load-displacement curves were presented in **Fig.5.37**. LF_1, LF_u, LF_f and LF_d in each case can be obtained from the numerical results. LF_1 was obtained when the steel plate or reinforcing bar reached yielding strain. LF_u was obtained when the bridge system reach its ultimate state (failure). LF_f was obtained when the deflection reaches 1% of the span length (346 mm for side spans and 384 mm for other spans). The details results of LF_1, LF_u, LF_f and LF_d corresponding to each case were presented in **Table.5.7**. The failure modes of intact system in all load cases were governed by the crush of concrete slab and the web buckling near the support which is the same as the previous description of Type-2 failure for the damage at the mid-span region (**Fig.5.34**). When the fracture is assumed at a distance 0.2L from the support, the failure mode is governed by rebar breaking and shear buckling of web near fracture locations as shown in **Fig.5.33**.

Table.5.6 Summary of 5 intact and 15 damaged cases

Damage Span	Intact bridge	Mid span	0.2L from left support	0.2L from right support
Span-1	1I	1D1	1D2	1D3
Span-2	2I	2D1	2D2	2D3
Span-3	3I	3D1	3D2	3D3
Span-4	4I	4D1	4D2	4D3
Span-5	5I	5D1	5D2	5D3

Table.5.7 Numerical Result of LF_1, LF_u, LF_f and LF_d

Damage Span	LF_1	LF_u	LF_f	LF_{d-1}	LF_{d-2}	LF_{d-3}
Span-1	5.80	8.32	8.30	4.50	4.60	5.14
Span-2	5.04	8.20	8.18	4.70	4.50	4.20
Span-3	5.02	8.21	8.20	4.40	4.15	4.15
Span-4	5.04	8.20	8.18	4.60	4.20	4.50
Span-5	5.80	8.22	8.22	4.50	4.90	4.26

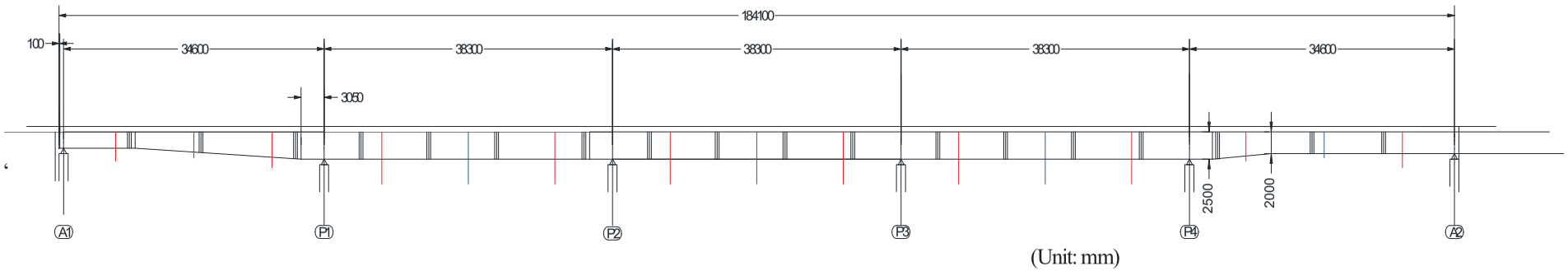

Fig.5.35 Fracture locations

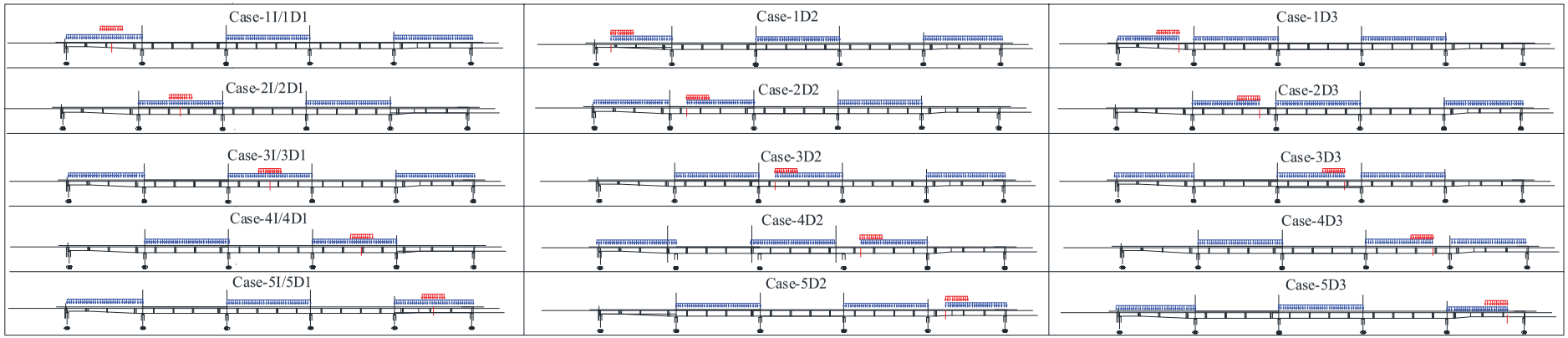

Fig.5.36 Loading conditions associate with each damage case

Table.5.8 Redundancy factors of bridge system

Damage span	LF_1	LF_u	LF_f	LF_d	$R_u/1.30$	$R_f/1.10$	$R_d/0.5$	φ_R
Span-1	5.02	8.32	8.30	4.50	1.27	1.50	1.80	1.27
Span-2		8.20	8.18	4.20	1.26	1.48	1.68	1.26
Span-3		8.21	8.20	4.15	1.26	1.48	1.65	1.26
Span-4		8.20	8.18	4.20	1.26	1.48	1.68	1.26
Span-5		8.22	8.22	4.26	1.26	1.49	1.70	1.26

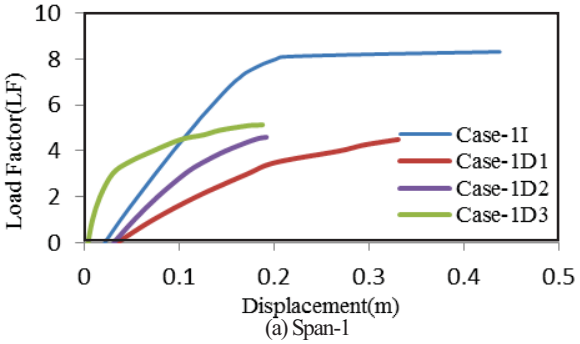

(a) Span-1

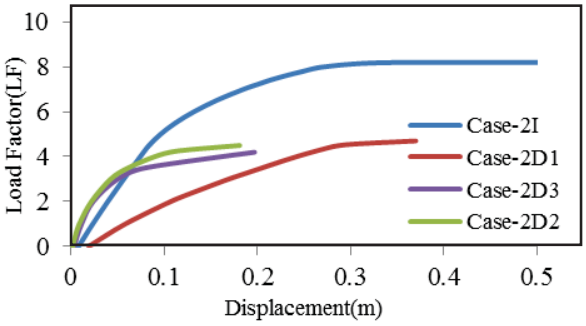

(b) Span-2

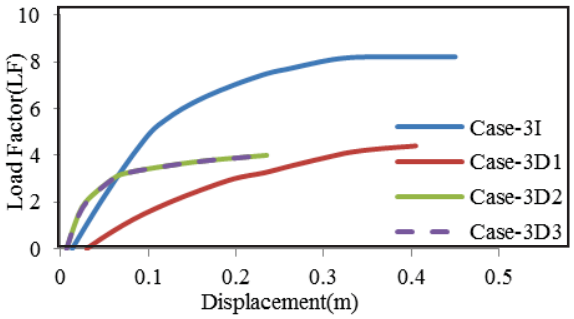

(c) Span-3

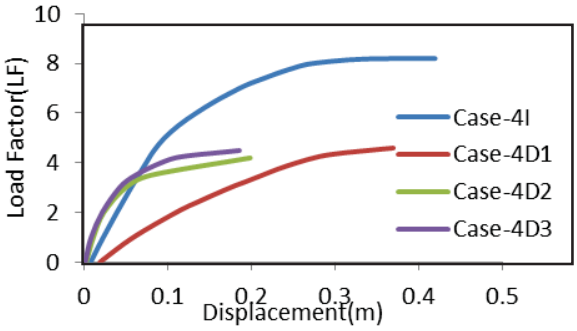

(d) Span-4

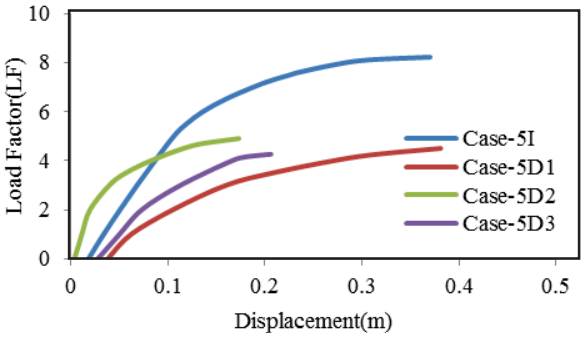

(e) Span-5

Fig.5.37 Load displacement curve of intact and damaged bridge models

5.5.4 Effect of secondary members

Bracing in steel bridges serves the dual purposes of providing overall stability of the girders as well as directly increasing the stiffness and strength of the system. Transverse beam is normally required during the construction stage of twin I-girder bridge to provide lateral stability, especially during the concrete casting period, and is used for the studied bridge model. It has been proved that the transverse beam alone is not usefull in increasing the redundancy level of composite twin I-girder bridge. Meanwhile, the bottom X-type cross bracing is found to be useful in increasing system stiffness and load carrying capacity of twin I-girder bridge in damaged condition (fracture) both experimentally and numerically. To evaluate the effect of bottom bracing on the redundancy level of the bridge, Span-3, which has the lowest redundancy level, was selected as a study target, and bottom X-type cross bracings were added to the bridge model. Five L-shape sections were selected to study the effect of bottom X-type cross bracing as shown in **Fig.5.38**. **Table.5.9** summarized the bridge models with different sections of bottom X-type cross bracings.

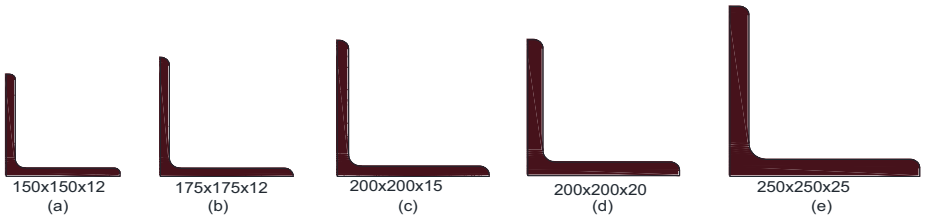

Fig.5.38 Configuration of bottom X-type bracings

Table.5.9 Summary of bridge models with bottom X-type bracing

Bottom X-type bracing cross section	Intact	Damage at mid-span	Damage at 0.2L from support
No X-type bracing	3I	3D1	3D2
150x150x12x12	3Ia	3D1a	3D2a
175x175x12x12	3Ib	3D1b	3D2b
200x200x15x15	3Ic	3D1c	3D2c
200x200x20x20	3Id	3D1d	3D2d
250x250x25x25	3Ie	3D1e	3D2e

(a) Effect of bracing on the intact system

Fig.5.39 shows the load-displacement curve of intact bridge attached with different section of X-type bottom bracing as mentioned in **Table.5.9**. Numerical results show that the bottom X-type bracings do increase the strength and the stiffness of the system. At the same time, the cross section has little influence on the overall performance of the bridge system.

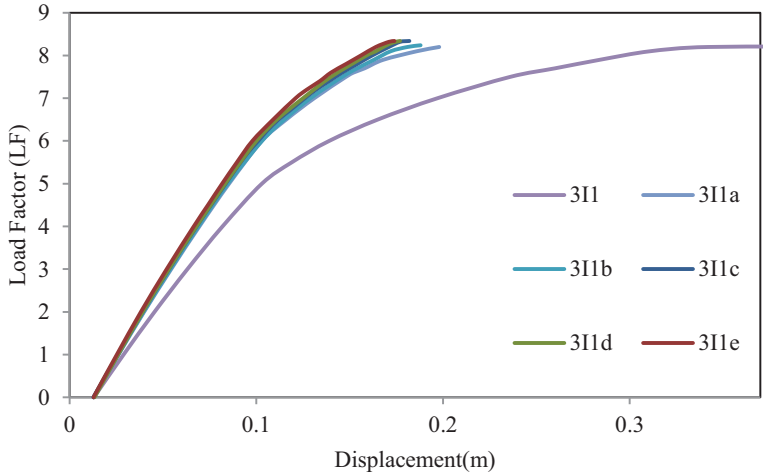

Fig.5.39 Load displacement curve of intact bridge (I)

(b) Effect of bracing on the damaged system

Fig.5.40 shows the load-displacement curve of mid-span fracture bridge model with and without bottom X-type cross bracing. Unlike intact system, the load carrying capacity of the damaged bridge increases significantly as the stronger section of bracing provided to the bridge model. However, the deflection of the bridge at the failure load is reduced as large as 30%. Since the load-carrying capacity of the bridge increases, the redundancy level of damaged structure will also increase. **Fig.5.41** shows the load-displacement curves of damaged bridge with fracture at 0.02L from support with and without bottom X-type bracing. The load carrying capacity of the damaged bridge slightly increases (around 10%).

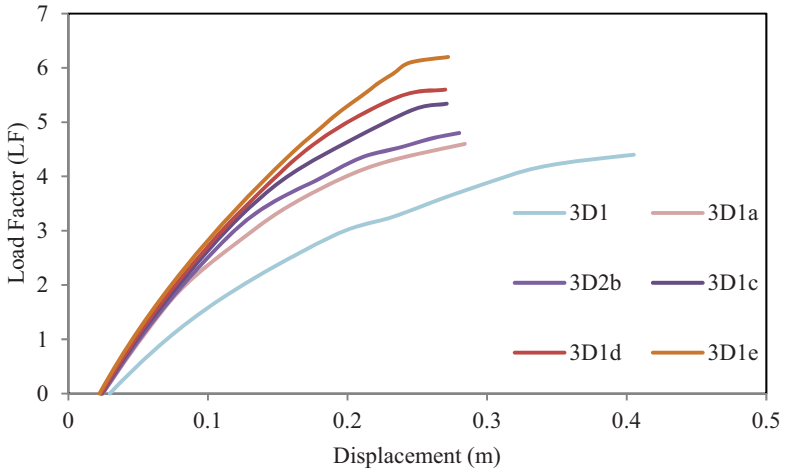

Fig.5.40 Load displacement curve of damaged bridge (D1)

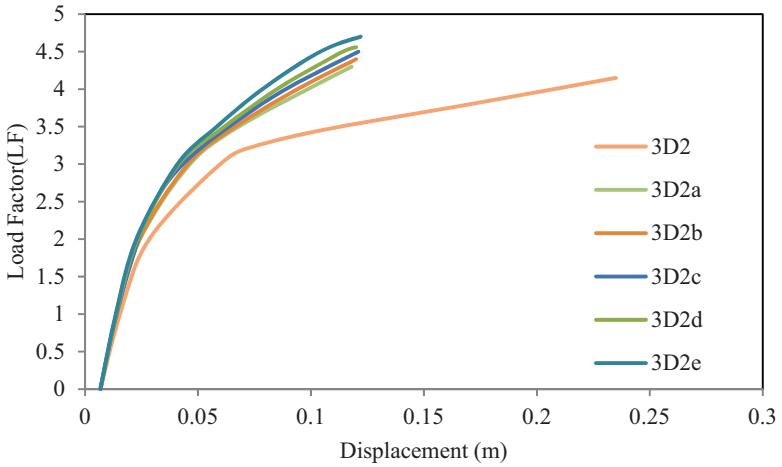

Fig.5.41 Load displacement curve of damaged bridge (D2)

(c) Effect of bracing on the redundancy level of the bridge systems

Table.5.10 summarizes the redundancy level of Span-3 when different bottom X-type bracing was attached to the bridge model. Based on the analyses resuts, it was found that the bottom X-type cross bracing is effective in increasing the load carrying capacity of the damaged structure. However, such effect is relatively low when applied on the intact system. If the redundancy level of the bridge system is governed by the damaged system ($R_d/0.5$), then the bottom X-type bracing is effective in increasing the redundancy level of the bridge. On the other hand, if the redundancy level of the bridge is governed by the intact system ($R_u/1.3$), then the bottom X-type bracing is considered as ineffective to improved the redundancy of the bridge.

Table.5.10 Redundancy factor of the bridge with and without bottom bracings

Model	$LF_{1\text{-}min}$	LF_u	$LF_{d\text{-}1}$	$LF_{d\text{-}2}$	$R_u/1.3$	$R_{d\text{-}1}/0.5$	$R_{d\text{-}2}/0.5$	φ_R
3	5.02	8.20	4.40	4.15	1.26	1.17	1.10	1.10
3a		8.20	4.60	4.30	1.26	1.22	1.14	1.14
3b		8.24	4.80	4.40	1.26	1.27	1.17	1.17
3c		8.32	5.34	4.50	1.27	1.42	1.20	1.20
3d		8.34	5.60	4.56	1.28	1.49	1.21	1.21
3e		8.34	6.20	4.70	1.28	1.65	1.25	1.25

5.6 Conclusions

This chapter describes the mechanical behavior and redundancy analyses of the continuous composite twin I-girder bridge model in the intact system and damaged system. For the three spans continuous bridge system, sixteen models were used in this study to understand the effectiveness of two different types of bracing systems and to define the alternate load path in the three-span composite twin steel I-girder bridge. Nonlinear analyses were performed to investigate the redundancy level of bridge models. The bottom X-type lateral bracings with the transverse beam are found to be effective in increasing the redundancy factors and the load carrying capacity of the small scale three span composite twin I-girder bridge model. To generalize the application of this X-type bracing in the design of the actual bridge, parametric study were performed on a full-scale five spans composite twin I-girder highway bridge. The finding of this research can be summarized as follows:

- The continuous composite twin-I girder bridges, which is classified as non-redundant according to AASHTO Specifications, is proved to have enough redundancy level, and can be considered as non-fracture critical bridge system.

- The I-section transverse beams of the continuous composite twin I-girder bridge are found to be effective in increasing the load carrying capacity with the existence of bottom lateral bracings.

- The concrete slab is found to be effective in distributing the load after fracture of the steel girder. With the existence of concrete slab, alternate load path in the three-span composite twin I-girder bridge can be confirmed to have sufficient level of load redistribution capability.

- The bottom X-type lateral bracings are generally found to be effective in increasing the redundancy factors and the load carrying capacity of the studied models. With the existence of transverse beams, this effect can be largely increased. At the same time, it can somehow decrease the deflection of the bridge at the ultimate load.

- The transverse beams are found useful in increasing the efficiency of the bottom lateral bracing systems to distribute the load and creating the alternate load path.

- Mid-span section is found not always the most critical section for composite twin I-girder bridge system. Fracture critical member or critical section is dependent on both load effects and the variation of sectional capacity of the bridge along the span length.

Reference

AASHTO (American Association of State Highway and Transportation Officials). (2012). AASHTO LRFD Bridge Design Specification." 6th edition, Washington, DC.

CEN (European Committee for Standardization). (1992). "Design of Concrete Structures." Eurocode 2, Brussels.

Csagoly, P. F., and Jaeger, L. G., (1979). "Multi-Load-Path Structures for Highway Bridges." Transportation Research Record 711, National Academy of Sciences, Washington, D.C.

Connor, R.J., Dexter R., and Mahmoud H. (2005). "Inspection and Management of Bridges with Fracture Critical Details." NCHRP Synthesis 354, National Cooperative Highway Research Program, Washington, DC.

Daniels, J. H., Kim, W., and Wilson J.L. (1988). "Recommended Guidelines for Redundancy Design and Rating of Two-Girder Steel Bridges." NCHRP Report 319, National Cooperative Highway Research Program, Washington, DC.

FHWA (Federal Highway Administration) (2012). Steel Bridge Design Handbook: Redundancy, Vol. 9, No. FHWA-IF-12-052, Washington, D.C.

Frangopol, D.M. (1992). "Bridge loading, reliability and redundancy: concepts and applications." International Federation for Information Processing, Geneva, Switzerland.

Frangopol, D.M. and James Curley, P. (1987). "Effects of damage and redundancy of structural reliability." J. Struct. Eng., ASCE, Vol. 113, pp. 1533-1549.

Ghosn, M. and Moses, F. (1998). "Redundancy in Highway Bridge Superstructure." NCHRP Report 406, National Cooperative Highway Research Program, Washington, DC.

Ghosn, M., Moses, F., and Frangopol, D.M. (2010). "Redundancy and Robustness of Highway Bridge Superstructures and Substructures." Structures and Infrastructure Engineering, Vol 6, No 1-2, pp. 257-278.

Ghosn, M. and Yang, J. (2014). "Bridge System Safety and Redundancy." NCHRP Report 776, National Cooperative Highway Research Program, Washington, DC.

Hendawi, S. and Frangopol, D.M. (1994). "System Reliability and Redundancy in Structural Design and Evaluation." Journal of Structural Safety, Vol. 16, No.1-2, pp. 47-71.

Hunley, T.C., and Harik, I.E. (2011) "Structural redundancy evaluation of steel tub girder bridges." J. bridge Eng., ASCE, Vol. 17, pp.481-489.

Idriss, R. L., White, K. R., Woodward, C. B., and Jauregui, D. V. (1995). “After-fracture redundancy of two-girder bridge: Testing I-40 bridges over Rio Grande.” Proc. 4th International Bridge Engineering Conference, pp. 316-326.

JRA (Japan Road Association). (2012). "Specifications for Highway Bridges." Part I Common, English edition, Tokyo.

JSCE (Japan Society of Civil Engineers). (2002). "Standard Specification for Concrete Structures." Tokyo.

JSCE (Japan Society of Civil Engineers). (2007)."Standard Specifications for Steel and Composite Structures." Tokyo.

Lam, H., Lin, W., and Yoda, T. (2014). “Effect of Bracing Systems on Redundancy of Three-span Composite Twin I-girder Bridge.” JSCE Journal of Structural Engineering, Vol. 60A, pp. 59-69.

Lin, W., and Yoda, T. (2013a). “Experimental and Numerical Study on Mechanical Behavior of Composite Girders under Hogging Moment.” International Journal of Advanced Steel Construction, Vol. 9, No. 4, pp. 309-333.

Lin, W., Yoda, T., Kumagai, Y., Saigyo, T. (2013b). “Numerical Study on Post-Fracture Redundancy of the Two-girder Steel-Concrete Composite Highway Bridges.” International Journal of Steel Structures, Vol. 13, No. 4, pp. 671-681.

Liu, W.D., Ghosn, M., Moses, F., and Neuenhoffer, A. (2001). “Redundancy in Highway Bridge Substructures.” NCHRP Report 458, National Cooperative Highway Research Program, Washington, DC.

Nakasu, M., and Iwatate, J. (1996). “Fatigue experiment on bond between concrete and reinforcement.” Transaction of JSCE, Vol. 426, pp. 852-853.

NBIS (National Bridge Inspection Standard) (2012). “Bridge Inspector’s Reference Manual.”, Federal Highway Administration, Washington D.C.

NTSB (National Transportation Safety Board). (2007). “Collapse of I-35W Highway Bridge”, Accident report PB2008-916203, Washington D.C.

NTSB (National Transportation Safety Board). (2013). “Collapse of the Interstate 5 Skagit River Bridge Following a Strike by an Oversize Combination Vehicle”, Accident report PB2014-106399, Washington D.C.

Okada, J., Yoda, T., and Lebet, J.P. (2006). “A Study of the Grouped Arrangement of Stud Connectors on the Shear Strength.” JSCE Journal of Structural Engineering/Earthquake Engineering, Vol. 23, No. 1, pp. 75-89.

Ollgaard, J.G., Slutter, R.G., and Fisher, J.W. (1971). “Shear Strength of Stud Connectors in Lightweight and Normal Weight Concrete.” Engineering Journal of AISC, Vol. 8, No. 2, pp. 55-64.

Park Y., Joe, W., Park, J., Hwang, M., Choi, B.H. (2012). ”An experimental study on after-fracture redundancy of continuous span two-girder bridges.” Int. J. Steel Struct., vol. 12, No. 1, pp. 1-13.

Vecchio, F.J., and Collins, M.P. (1986). “The modified compression field theory for reinforced concrete elements subjected to shear.” ACI Journal, Vol. 83, No. 2, pp. 219-231.

6. Summary and Conclusions

6.1 Summary

The main objective of the present study is to investigate the redundancy of the steel-concrete composite twin I-girder bridge system. The experimental program was carried out to study the post-fracture performance of the composite twin I-girder bridge under vertical loading condition. The behavior of the bridge subject to horizontal loading condition such as earthquake and strong wind (typhoon or hurricane) is not in the scope of this study. Three-dimensional numerical model based on Finite Element Method (FEM) was built to simulate the behavior of the bridge models based on nonlinear analyses. The validity of the numerical model was verified by the experimental results. Parametric studies were performed to investigate the effects of the structural indeterminacy and the effect of concrete slab on the safety of the composite twin I-girder bridge in the fracture condition. In addition, the effect of the secondary members was investigated and the effectiveness on the redundancy of the composite twin I-girder bridge system was confirmed in the study.

To provide detailed results and knowledge concerning the redundancy analyses and mechanical behavior of the steel-concrete composite twin I-girder bridge system in critical damage condition, the research program based on the extensive literature review, experimental results, and numerical analyses were carried out in this study. The investigation can be divided into three principal stages. Firstly, literature review concerning the redundancy analyses including the historical events, which highlight the importance of the redundancy on bridge safety, the philosophy of the redundancy criteria, the development of the evaluation process, and the existing guidelines in the design specifications were reported. Secondly, an experimental program was carried out on two test specimens including an intact specimen and a damaged specimen to investigate the redundancy and mechanical behavior of the composite twin I-girder bridges in the post-fracture condition. Lastly, by using the verified numerical models, counter measures to improve the redundancy of the composite twin I-girder bridge were proposed including the effect of degree of indeterminacy, the effect of the concrete slab, and the effect of the secondary members. The principal findings of this study can be summarized as follows:

- It has been widely recognized by structural engineering community that redundancy is an important criterion that can guarantee the survival of the bridge in the critical damage condition. However, in current design specifications, only general prescriptions and very limited guidelines are provided for the bridge designers to account for the redundancy during the design stage. A uniform redundancy evaluation method is required to prevent bridge collapse from the non-redundant problem.

- Based on the existing concepts of redundancy, a uniform redundancy evaluation should consist of two important aspects: 1. Providing a uniform level of reliability with an objective measure which is independent to design specifications, and 2. Do not require nonlinear analyses and applicable to most of the bridge designers.

- In the event of fatigue crack occurrence and its propagation to the entire bottom flange and the web in one main girder of a composite twin I-girder bridge, a significant reduction in system stiffness and load-carrying capacity was confirmed for simply supported composite twin I-girder bridge system.

- Based on the experimental results, fracture of the whole web and bottom flange at the mid-span section of the composite twin I-girder bridge system can result in a considerable increase in the shear strain on the studs near the middle section, thus reducing the strength and lifespan of the shear studs against fatigue failure.

- Both concrete strength and thickness are found to be effective against the fracture of the steel girder. Increasing the concrete strength is a viable choice in terms of safety and cost. Furthermore, increasing the thickness of the slab can improve the durability of the structure as well as the performance in the fracture condition; in particular, it increases the shear capacity of the concrete slab against shear failure, which is brittle and dangerous.

- The use of a continuous span instead of a simple span for the composite twin I-girder bridge system can significantly increase the load ratio between the damaged and intact structures. Thus, the fracture of whole web and bottom flange will have a smaller influence on the performance and safety of the bridge system. It is highly recommended that continuous span should be used in the design of the composite twin I-girder bridge system.

- Based on the experimental and numerical results, the composite twin I-girder bridge system used in this study has an adequate level of redundancy with enough reserve strength in overload or fracture conditions which can be classified as redundant bridge system.

- For the use of the secondary member in the composite twin I-girder bridge system, I-section transverse beams are found to be effective in increasing the load carrying capacity with the existence of bottom lateral bracings.

- The bottom X-type lateral bracings are generally found to be effective in increasing the redundancy factors and the load carrying capacity of the composite twin I-girder bridge system. With the existence of transverse beams, this effect can be largely increased.

- Transverse beams can be used to increase the efficiency of the bottom lateral bracing systems to distribute the load and to establish the alternate load path.

- The concrete slab is found to be the key element for load redistribution in the fracture condition for the composite twin I-girder bridge systems. With the existence of concrete slab, alternate load path in the composite twin I-girder bridge can be confirmed to have sufficient level of load redistribution capability.

- In general, the composite twin I-girder bridge with a fracture of whole web and bottom flange at any location can sustain the damage without significant deformation under self-weight and manage to carry some imposed live load which can be classified as non-fracture critical bridge system.

Despite these findings, the outcomes of this research are based on a very limited number of experimental models and numerical models. More researches are required to develop a unified redundancy evaluation for composite twin I-girder bridge structure as well as for general bridge systems before a general method can be developed and implemented in the design of bridge structures.

6.2 Potential Impact

The potential availability of the composite twin I-girder bridge system for highway bridge design is highlighted in this study. Despite providing enough residual strength in damaged conditions, such a bridge is currently still classified as fracture critical due to the oversimplified design procedures and assumptions in engineering practice. This dissertation provides more concrete evidence concerning the redundancy evaluation of the composite twin I-girder bridge system in the purpose of having a more accurate bridge classification based on the safety level. The contribution of the current study toward the safety of the composite twin I-girder bridge can be highlighted as follow:

- Existing design practice considered all two girder bridge system as non-redundant and fracture critical including steel-concrete composite type based on the simplified assumption in the design. This study, which is based on experimental program and nonlinear analyses of three-dimensional model of steel concrete composite bridge, proved that the steel-concrete composite twin I-girder bridge systems generally have adequate level of redundancy and should be classified as non-fracture critical bridge systems which encourage the use of such bridges in the design practice that can guarantee the performance of the bridge with both safety and economic perspectives.

- The current practice of maintenance and retrofit of the steel-concrete composite girder lacks the detailed analyses of the performance of the shear connectors in the damage condition. However, based on the finding in this study, girder fracture can result in a considerable increase in the shear strain on the studs near the middle section, thus reducing the strength and lifespan of the shear studs against the fatigue failure. It is recommended that in the assessment of fatigue damage in a composite twin I-girder bridge, the behavior and condition of the shear studs near the fracture location should be verified.

- Comparing to the existing methods to strengthen the existing aged composite twin I-girder bridges, installing of the additional bottom X-type bracings can be used as a more economical and practical measure that can increase the load carrying capacity as well as redundancy level of the bridge structure.

- Shear failure can result in a brittle failure which leads to catastrophic collapse without precaution. Additional safety measures should be considered to avoid such failure. Among all the existing measures, increasing the design strength and thickness of concrete slab in the design stage is found as an effective way to improve the performance of the composite twin I-girder bridge system against such catastrophic failure.

- Though a unified redundancy evaluation method for bridge structure is not proposed in this study and currently does not exist in the design practice, general aspects of redundancy providing uniform level of reliability with an objective measure and engineering practice which do not require nonlinear analyses can be used as key concept in the research of uniforming redundancy evaluation for bridge systems.

6.3 Future Works

This dissertation discusses the redundancy of the composite twin I-girder bridge in the fracture critical condition. The fracture of the web or bottom flange on the main girders is typically detected for the existing steel girders during their service life. Although considered as not critical as the fracture of whole web and bottom flange assumed in this study, there are several other damage types that should be considered in the redundancy evaluation for the composite twin I-girder Bridge. Those damage scenarios suggested for future study including the loss of the bearing or one support (typically happens during an earthquake, tsunami, and strong wind), corrosion of the main steel girders and other secondary members which can result in member failure, partial failure of the concrete slab, and corrosion of the rebar. Among them, the corrosion of the main girder near the support location should be carefully treated as it may trigger the shear failure which is considered as critical as fracture case.

Concerning the modeling of the bridge model with the finite element method, it is true that the current modeling technique can be used to predict the mechanical behavior of the bridge system in both intact and damaged specimen. However, some details are not available by using the current modeling technique. For example, the current modeling technique unable to simulate the actual behavior of the shear connectors which were considered critical for damage specimen in the experimental program. Improving the modeling details of the interface element and shear connectors for future study is essential to observe the local behavior of the interface properties which are necessary to ensure the composite action between steel girders and concrete slab.

Concerning the current redundancy evaluation method, it is necessary to perform the nonlinear analyses which require complicated analyses and very time-consuming. The future direction of the redundancy evaluation of the bridge structures is to propose a method for redundancy evaluation that is based on theoretical approach and linear analyses which do not require any complicated analyses.

List of Published Papers

Journal Papers:

Heang Lam, Weiwei Lin, Teruhiko Yoda (2017). "Performance of Composite Twin I-Girder Bridges with Fatigue Induced Crack." *Journal of Bridge Engineering*, American Society of Civil Engineering, Vol. 22, Issue. 9.

Weiwei Lin, Heang Lam, Teruhiko Yoda, Haijie Ge, Ying Xu, Hideyuki Kasano, Kuinei Nogami, and Jun Murakoshi. (2017). "After-Fracture Redundancy analysis of an aged truss bridge in Japan." *Structure and Infrastructure Engineering*, Taylor and Francis, Vol. 13, No. 1, pp. 107-117.

Heang Lam, Weiwei Lin, Teruhiko Yoda (2014). "Effect of Bracings Systems on Redundancy of Three-span Composite Twin I-girder Bridge." *Journal of Structural Engineering*, Japan Society of Civil Engineering, Vol. 69A, pp. 59-69.

Conference Papers:

Heang Lam, Weiwei Lin, and Teruhiko Yoda (2016). "Redundancy Evaluation of Simply Supported Composite Twin I-Girder Bridge" *Proceeding of Eighth International Conference on Steel and Aluminum Structures*, Hong Kong, China.

Weiwei Lin, Heang Lam, Teruhiko Yoda, Campbell R. Middleton (2016). "Steel-Concrete Composite Beams Subjected to Combined Hogging Bending and Torsion." *Proceeding of Eighth International Conference on Steel and Aluminum Structures*, Hong Kong, China.

Heang Lam, Weiwei Lin, Teruhiko Yoda (2016). "Fracture Critical Member and Redundancy Evaluation of Simply Supported Composite Twin I-Girder Bridge." *Proceeding of 11th German-Japanese Bridge Symposium*, Osaka, Japan.

Weiwei Lin, Heang Lam, Teruhiko Yoda (2016). "Elastic Behavior of Steel-Concrete Composite Beams under Negative Bending Moment." *Proceeding of 11th German-Japanese Bridge Symposium*, Osaka, Japan.

Weiwei Lin, Teruhiko Yoda, Nozomu Taniguchi, Heang Lam, Kazuki Nakabayashi (2016). "Post-Fracture Redundancy Evaluation of a Twin Box-Girder Shinkansen Bridge in Japan*." Proceeding of IABSE Conference Guangzhou*, China.

Heang Lam, Teruhiko Yoda, Weiwei Lin, Hideyuki Kasano (2015). "Fracture Critical Members and Redundancy Analysis of Continuous Composite Twin I-Girder Bridges" *Proceeding of the 8th International Conference on Advances in Steel Structures*, Lisbon, Portugal.

Weiwei Lin, Teruhiko Yoda, Haijie Ge, Ying Xu, Hideyuki Kasano, Heang Lam (2015). "Post-Fracture Redundancy Analysis of an Aged Steel Truss Bridge in Japan: Field Test and Numerical Analysis." *Proceeding of the 8th International Conference on Advances in Steel Structures*, Lisbon, Portugal.

Weiwei Lin, Teruhiko Yoda, Heang Lam. (2015). "Corrosion Damage Assessment for Simply Supported Steel-Concrete Composite Bridges." *Proceeding of IABSE Conference Nara*, Japan.

Heang Lam, Teruhiko Yoda, Weiwei Lin, Hideyuki Kasano (2014). "Numerical Analysis on Redundancy of Continuous Twin I-Girder Steel Concrete Composite Bridges." *Proceeding of the 4th International Symposium on Life Cycle Engineering*, Tokyo, Japan.

Heang Lam, Teruhiko Yoda, Weiwei Lin, Hideyuki Kasano (2014). "Fracture Critical Members of Continuous Composite Twin I-girder Bridge." *Proceeding of 15th International summer symposium*, JSCE annual conference, Osaka, Japan.

Weiwei Lin, Teruhiko Yoda, Heang Lam.(2014). "Reliability and Redundancy of Two-Girder Steel-Concrete Composite Bridges under Uncertainty." *Proceeding of The Second International Conference on Vulnerability and Risk Analysis*, Liverpool, England.

Teruhiko Yoda, Weiwei Lin, Nozomu Taniguchi, Hideyuki Kasano, Heang Lam, Haijie Ge. (2013) "Comparative Study on Continuous Steel-Concrete Composite Beams with Normal and Steel Fiber Reinforced Concrete Slab." *Proceeding of The Thirteenth East Asia-Pacific Conference on Structural Engineering and Construction*, Hokkaido, Japan.

Heang Lam, Weiwei Lin, Teruhiko Yoda (2013). "Numerical Study on Damage of Bearing in Continuous Composite Twin I-girder Bridge*." Proceeding of 14th International summer symposium*, JSCE annual conference, Tokyo, Japan.

Hideyuki Kasano, Teruhiko Yoda, Kuniei Nogami, Jun Murakoshi, Mamoru Sawada, Weiwei Lin, Heang Lam, Haijie Ge.(2013). "Ultimate Behavior of Steel Truss Bridge Gusset Plates Subjected to Compressive Force." *Proceeding of the Twelfth Japan-Korea Joint Seminar on Steel Bridges*, Okinawa, Japan.

Heang Lam, Haijie Ge, Weiwei Lin, Hideyuki Kasano, Teruhiko Yoda (2013). "Study of M-N Interaction Curve on a Pier of PLS flyover Bridge Project." *Proceeding of the 40th JSCE Kanto Branch Conference*, Utsunomiya, Japan.

Haijie Ge, Heang Lam, Weiwei Lin, Hideyuki Kasano, Teruhiko Yoda (2013). "A numerical simulation on multi-functional mild steel damper." *Proceeding of the 40th JSCE Kanto Branch Conference*, Utsunomiya, Japan.

Poster Presentation:

Heang Lam, Teruhiko Yoda, Weiwei Lin (2015). "Resilience Evaluation of Girder Bridges in Japan." *World Engineering Conference and Convention*, Kyoto, Japan.